Role of DOT1L in epigenetic regulation of the *HOXA9* gene expression in mixed lineage leukemia

By

Hedieh Sattarifard

A Thesis submitted to the Faculty of Graduate Studies of The University of Manitoba in partial fulfillment of the requirements of the degree of

Master of Science

Department of Biochemistry and Medical Genetics

University of Manitoba

Winnipeg

Abstract

Mixed lineage leukemia (MLL) is often characterized by chromosomal translocations involving the lysine methyltransferase 2A *(KMT2A)* gene with various partner genes, creating fusion proteins that can mistarget DOT1L to the homeobox A9 (*HOXA9*) gene, leading to *HOXA9* expression. Among the possible translocations with *KMT2A*, the fusion of *KMT2A* with myeloid/lymphoid or mixed-lineage leukemia; translocated to 3 *(MLLT3)*, also known as *KMT2A-MLLT3*, is particularly significant because it has been reported in more than 50% of pediatric and 25% of adult acute myeloid leukemia cases. The *KMT2A-MLLT3* translocation creates the fusion protein that aberrantly recruits DOT1L (disruptor of telomeric silencing 1-like) and other chromatin-modifying enzymes to the *HOXA9* locus, resulting in increased *HOXA9* gene expression. *HOXA9* expression disrupts normal hematopoietic differentiation and contributes to the development of mixed lineage leukemia by promoting the proliferation and survival of leukemic cells. My research focuses on unraveling the mechanisms that drive heightened DOT1L activity and its specific targeting to *HOXA9*, which are pivotal for the robust transcription observed in MLL.

Our results showed that the *HOXA* cluster is marked by several active marks and chromatin-modifying enzymes including H3K27ac, H3K4me3, H3K36me3, and H3K79me2, as well as DOT1L and DNase I. The heavy decoration by these active marks and proteins indicates that *HOXA9* has an unstable chromatin structure, which reflects higher nucleosome turnover over the *HOXA9* region. Higher turnover makes the chromatin more accessible to the transcriptional machinery, thereby increasing *HOXA9* expression. Histone H3 has three forms: H3.1 and H3.2 as canonical, and H3.3 as a variant. The H3.3 variant can be more incorporated into nucleosomes with higher turnover, which can further enhance the transcription of the *HOXA9* gene in MOLM-13 cells.

Our results showed that the H3K79me2 level, which indicates DOT1L enzyme activity, is higher in MOLM-13 cells with the *KMT2A-MLLT3* translocation. Several studies have shown that DOT1L activity depends on Histone H2B monoubiquitination at Lys 120 (H2BK120ub), a key modification in transcription elongation. Our results also revealed that the level of H2BK120ub is higher in MOLM-13 cells, which have increased DOT1L activity, suggesting a direct relationship between H2BK120ub and DOT1L activity in these cells.

Bortezomib, an FDA-approved drug commonly used in clinical practice for multiple myeloma, was employed to investigate its effect on epigenetic marks involved in transcription elongation including the H3K79me2, H3K36me3, and H2BK120ub in MOLM-13 cells. Treatment with 5 nM bortezomib demonstrated significant reductions in H2BK120ub levels, H3K79me2, and *HOXA9* gene expression in MLL. My findings underscore the critical role of H2BK120ub in regulating DOT1L methyltransferase activity as well as *HOXA9* expression in MOLM-13 cells. These compelling results position bortezomib as a promising therapeutic avenue for treating MLL, offering new hope for patients affected by this challenging disease.

Acknowledgments

I would like to express my sincere gratitude to my supervisor and mentor, Dr. Jim Davie. His expertise and profound knowledge in the field of epigenetics are recognized globally, and his reputation was instrumental in my decision to pursue further education in Canada under his guidance. I vividly remember the day I discovered his profile on LinkedIn; I immediately recognized him as the ideal mentor whose research aligns perfectly with my interests. Throughout my journey, Dr. Davie's unwavering guidance and consistent support have been invaluable. He has always made himself available whenever I needed assistance, whether it was discussing research ideas or navigating challenges in academia. I am profoundly grateful to Dr. Davie for his enduring mentorship, which has not only enriched my scientific knowledge but also shaped me into the researcher I am today. His mentorship goes beyond academia; it extends to fostering critical thinking, and a deep passion for scientific inquiry. I am privileged to have had the opportunity to learn from Dr. Davie and am truly thankful to him for his mentorship and unwavering support.

I would also like to extend my heartfelt gratitude to my advisory committee members, Dr. Ted Lakowski and Dr. Etienne Leygue, for their generous support, invaluable feedback, and guidance during my graduate program.

I would like to express my deepest gratitude to the present past and members of Dr. Davie's lab: Sadhana R.N. Sudhakar, Dhanvi Prajapati, Camila Lopez, Ishdeep Muker, Madeline Lee, Kari Green, Milan Lukes, Enzhe Khazeeva, and Narges Fatemiyan. During our time together, we formed strong relationships and supported each other like a family, striving to create a positive and nurturing environment. I cherish the memories we've shared and am deeply grateful to have had you all in my life. You will always hold a special place in my heart.

I would also like to extend my heartfelt thanks to Fadumo Osman, academic programs & human resources assistant at the BMG office, for her invaluable help and guidance during this time. Her patience in answering my questions and her unwavering support have been deeply appreciated.

Dedication

Firstly, I want to dedicate this thesis to myself because I have put my heart and soul into this project. I've always prioritized my scientific work and dedicated over two years to this research. It was not an easy journey, but I helped myself whenever I was down and motivated myself when I was in the deepest darkness.

Secondly, I want to dedicate this research to my mother, whom I lost when I was only a child. I have always wanted to make her proud, and I will continue to try my best to do so. She was a great scientist in her field, and I always looked up to her. She was a remarkable woman, a great leader, and a mentor. Rest in peace, Mommy.

Thirdly, I would like to dedicate this research to Dr. Mohammad Hashemi, who was my mentor and supervisor during my master's studies in Iran. He was a great scientist who not only guided me but also helped me find my path and create my scholarly foundation. He was instrumental in shaping my passion for science and influencing my journey to where I am today. Rest in peace, Dr. Hashemi.

Finally, I would like to dedicate this research to all the women around the world who are fighting for their rights, especially Iranian women who have faced violence and oppression in their pursuit of freedom. In the name of life, women, and freedom

Table of contents

Abbreviations

Acetic acid-urea-Triton X-100 polyacrylamide gel electrophoresis	AUT
Acute lymphoid leukemia	ALL
Anti-silencing factor 1	Asf1
Calcineurin-binding protein 1	CABIN1
Chromatin assembly factor 1	CAF-1
Chromatin Immunoprecipitation Sequencing	ChIP-seq
Chromodomain	CHD
Chronic myeloid leukemia	CML
C-terminal domain	CTD
DOT1L	Disruptor of Telomeric Silencing 1-Like
Deubiquitinates	DUBs
Dimethylation on lysine 79 of histone H3	H3K79me2
DNA methyltransferases	DNMTs
Electrophoretic Mobility Shift Assay	EMSA
Embryonic stem cells	ESCs
Facilitates Chromatin Transcription	FACT
Fetal bovine serum	FBS
hematopoietic stem	HSC
Hematopoietic stem and progenitor cells	HSPC
Heterochromatin Protein 1	HP1
Histone Coimmunoprecipitation	Co-IP
Histone deacetylases	HDACs
Histone demethylases	HDMs
Homeobox A9	HOXA9
Immunodepleted	ID
Immunoprecipitated	IP
Lysine acetyltransferases	KATs

Lysine methyltransferases	KMTs
Lysine Methyltransferase 2A	KMT2A
Lysine Demethylase 5C	KDM5C
Messenger RNAs	mRNAs
Myeloid/Lymphoid or Mixed-Lineage Leukemia; Translocated to 3	MLLT3
Mixed lineage leukemia	MLL
Mono-methylation on lysine 4 of histone H3	H3K4me1
Monoubiquitination of H2B at lysine 120	H2BK120ub
Monoubiquitination of H2B at lysine 34	H2BK34ub
Monoubiquitination of H2B at lysine 120	H2BK120ub
Monoubiquitination of H2B at lysine 34	H2BK34ub
Monoubiquitination of histone H2A at lysine 119	H2AK119ub
Phenylmethylsulfonyl fluoride	PMSF
Polycomb Repressive Complex 1	PRC1
Polycomb Repressive Complex 2	PRC2
Post-translational modifications	PTMs
Protein arginine methyltransferases	PRMTs
Regulation of Ty1 transposition	Rtt106
Replication and cell cycle-dependent	RD
Replication and cell cycle-independent	RI
RNA polymerase II-associated factor 1	PAF1
RNA sequencing	RNA-Seq
S-adenosyl-L-methionine	SAM
Sodium dodecyl sulfate-polyacrylamide gel electrophoresis	SDS-PAGE
Super Elongation Complex	SEC
Suppressor of Ty 16	SPT16
Transcription start site	TSS
Trimethylation of lysine 27 on histone H3	H3K27me3
Trimethylation on lysine 36 of histone H3	H3K36me3
Zeste Homolog 2	EZH2

Figures

Tables

List of copyrighted material for which permission was obtained

Figure 2: The distribution of various histone modifications across different regions of the genome in active and silent genes

Figure 5: Schematic representation of different types of histones PTMs crosstalk

Figure 6: The role of H2BK120 ubiquitination in stabilizing DOT1L and enhancing its methylation activity on H3K79

Figure 8: Subunit composition and inhibitors targeting constitutive and immunoproteasomes.

Chapter I

1. Introduction

This chapter contains materials from the following publication: **Bioinformatic Analyses of Broad H3K79me2 Domains in Different Leukemia Cell Line Data Sets** P. Sharma, H. Sattarifard, N. Fatemiyan, T. M. Lakowski and J. R. Davie/ Cells 2022 Vol. 11 Issue 18 Pages 2830/ Accession Number: doi:10.3390/cells11182830

Preface

Leukemia is a group of blood cancers that typically begin in the bone marrow and result in the production of high numbers of abnormal, immature blood cells. Leukemia can be classified as acute or chronic based on the rate of proliferation, and as myeloid or lymphoid depending on the cell of origin. The predominant subtypes include acute myeloid leukemia (AML), chronic myeloid leukemia (CML), and acute lymphoblastic leukemia (ALL). Mixed lineage leukemia (MLL) is a distinct subtype that encompasses both AML and ALL, characterized by chromosomal rearrangements involving the *KMT2A* gene on chromosome 11q23. These rearrangements lead to the production of fusion proteins that disrupt normal gene regulation, resulting in aggressive leukemias with features of both myeloid and lymphoid lineages, contributing to a more complex and challenging clinical presentation. A hallmark of MLL is the chromosomal translocations that fuse the *KMT2A* gene with various partner genes, leading to the formation of fusion proteins that dysregulate gene expression and drive leukemogenesis.

Among the dysregulated genes, *HOXA9* plays a critical role in the development and progression of MLL. The fusion protein continuously recruits DOT1L to the *HOXA9* gene, sustaining its expression and establishing an aberrant epigenetic landscape that contributes to the pathogenesis of MLL. Consequently, DOT1L is a key target for therapeutic intervention. While DOT1L inhibitors like EPZ5676 have shown promise in early trials, challenges remain due to off-target effects and toxicity concerns. Therefore, there is a continuing need to identify an effective and low-risk method to target the *HOXA9* gene and DOT1L enzyme activity.

My project primarily focuses on investigating the role of DOT1L in the epigenetic dysregulation of the *HOXA9* gene in mixed-lineage leukemia. In addition, I explored the involvement of histone epigenetic marks, such as H3K36me3 and H2BK120ub, in the transcriptional elongation of the *HOXA9* gene, which may significantly impact *HOXA9* gene expression in leukemic cells. The next phase of my research involved using bortezomib, a proteasome inhibitor, to assess its effects on H3K79me2 and other histone marks associated with *HOXA9* gene expression. Bortezomib, an FDA-approved drug widely used in clinical practice for treating multiple myeloma, has shown promising results with minimal side effects in these patients. While bortezomib's role as a cytotoxic agent against leukemia cells has been explored, its potential to influence epigenetic marks and

DOT1L remains largely unexplored. This study aims to address this knowledge gap and uncover novel therapeutic insights.

In addition to my primary focus on DOT1L and *HOXA9* gene expression, I investigated the levels of histone H3s, including H3.1, H3.2, and H3.3 in leukemic cells, along with the K79me2 modifications level associated with H3s. Understanding these levels will provide critical insights into the distribution and modification of H3 isoforms. Several studies have demonstrated that the incorporation of histone variants, particularly H3.3, into nucleosomes can destabilize chromatin structure. This destabilization may have significant implications for regulating *HOXA9* expression in leukemia, further elucidating the complex epigenetic mechanisms driving leukemogenesis.

1.1 Introduction to epigenetics and chromatin organization

1.1.1 Definition of epigenetics

The epigenetics field has a rich history, developing considerably throughout the ages. The modern concept of epigenetics was first introduced by Conrad Waddington, a British developmental scientist, in the 1940s. He used the term "epigenetics" to describe the study of heritable changes in gene expression that do not involve alterations to the underlying DNA sequence (Waddington, 1942). In the early 1950s, researchers discovered the molecular mechanisms of epigenetic regulation, such as DNA methylation and histone modification, which showed how gene expression could be controlled without altering the DNA sequence. By the 1980s, the understanding of epigenetic mechanisms was expanded more by studying the role of DNA methylation in gene silencing and X-chromosome inactivation (Riggs, 1975). In the late 1990s, scientists began paying close attention to genomic imprinting. This idea sheds light on how specific genes are expressed differently based on whether they come from the mother or the father. This finding significantly advanced our understanding of how genes are regulated during development (McGrath & Solter, 1984). While there is still debate about epigenetics terminology, the best-described definition of epigenetics is provided by the Canadian Institutes of Health Research (CIHR), which defines epigenetics as the study of changes in gene activity and expression that are not dependent on alterations in the DNA sequences.

1.1.2 Chromatin organization

The genome of eukaryotes is significantly large, and efficient packaging within the cell nucleus is needed. This packaging is accomplished through the formation of chromatin, a complex of DNA and protein. The fundamental unit of chromatin is the nucleosome, which consists of approximately 147 bp of DNA wrapped around a set of eight proteins called octamer histones (H2A, H2B, H3, and H4). This facilitates the compact organization of DNA, allowing it to fit within the nucleus while also playing a crucial role in regulating gene expression and maintaining genomic integrity. Chromatin is primarily categorized into two distinguishable categories: euchromatin and heterochromatin. Heterochromatin is highly compact and has silenced and not actively transcribed genes, while euchromatin is less compact, and contains a high number of genes which actively transcribed (Huisinga et al., 2006; Tamaru, 2010).

1.1.3 Epigenetics and chromatin structure

Chromatin structure and function are controlled through various epigenetic modifications, most notably histone post-translational modifications (PTMs) and DNA methylation. The histone PTMs include acetylation, methylation, ubiquitylation, SUMOylation, glycosylation, ADP-ribosylation, and many others. These histone PTMs play a crucial role in controlling the accessibility of chromatin and also DNA by targeting the N-terminal tails, globular domains, and C-terminal domains of histones, thereby affecting the regulation of gene expression (Strahl & Allis, 2000).

1.1.4 Epigenetic tools for histone PTMs

Histone PTMs are introduced by specific enzymes known as writers, removed by erasers, and interpreted by readers**.** The schematic representation of epigenetics tools for histone PTMs is shown in **Figure 1.**

1.1.4.1 Writers

Histone writers are enzymatic complexes responsible for catalyzing the addition of specific PTMs onto histones, thereby modulating chromatin structure and gene expression. These writers include various classes of enzymes, such as lysine acetyltransferases (KATs), lysine methyltransferases (KMTs), histone ubiquitin ligases, and many others. For instance, KATs add acetyl groups to lysine residues on histone, promoting an open chromatin state and activating gene transcription.

KMTs and protein arginine methyltransferases (PRMTs) can methylate histone lysine or arginine residues, leading to diverse transcriptional outcomes depending on the specific methylation residue and location. Together, histone writers dynamically regulate chromatin accessibility and gene activity through the precise addition of PTMs, contributing to cellular identity and response to environmental factors (Gillette & Hill, 2015).

1.1.4.2 Erasers

Erasers are enzymatic complexes that play a crucial role in the dynamic regulation of chromatin structure by removing specific PTMs from histones. These erasers include various classes of enzymes, such as histone deacetylases (HDACs), lysine demethylases (KDMs), deubiquitinases (DUBs; also named USPs), and phosphatases. For example, HDACs catalyze the removal of acetyl groups from lysine residues on histone, leading to a more compact chromatin structure that often correlates with transcriptional repression. Similarly, KDMs can remove methyl groups from histone lysine residues, influencing gene expression patterns.

1.1.4.3 Readers

Histone PTMs are regulated by writer and eraser enzymes, while their functional impact on DNA transcription is facilitated by proteins referred to as "readers." These reader proteins were initially identified by experiments involving modified histone peptides aimed at pinpointing proteins capable of selectively recognizing and interacting with specific histone PTMs. Readers are classified into many types, including bromodomain, chromodomain, PHD Finger, SH2 domains, and many others (Yun et al., 2011).

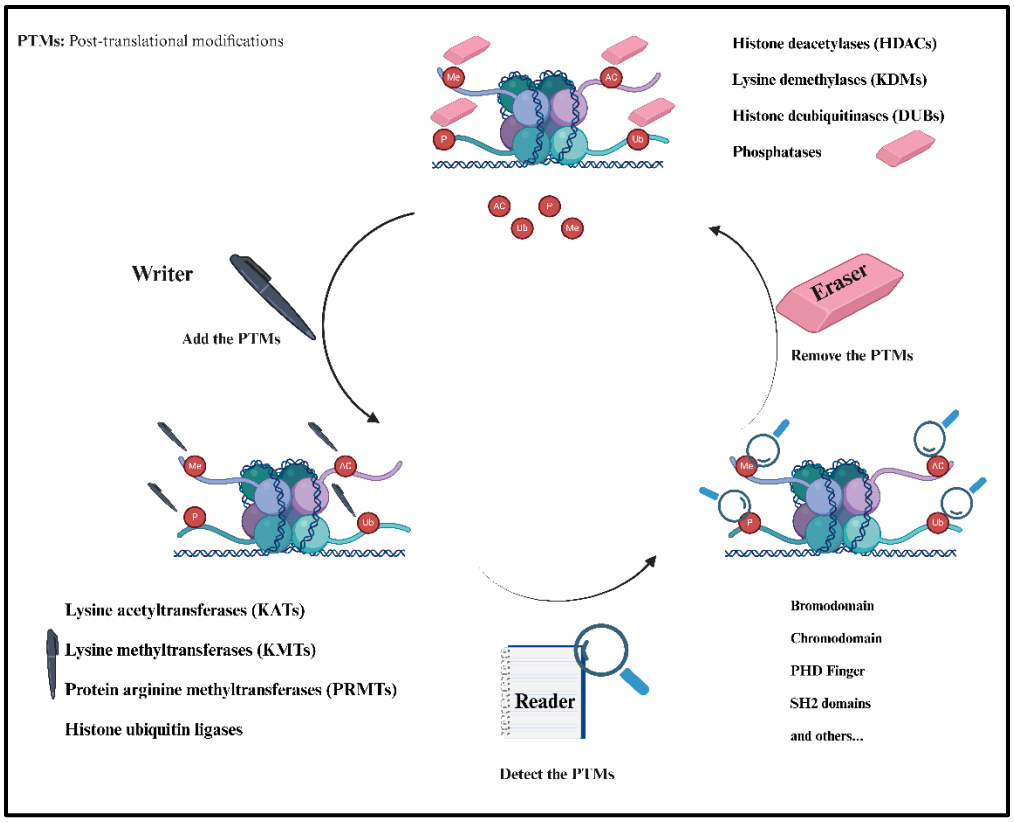

Figure 1: Schematic representation of the role of epigenetic writers, erasers, and readers in regulating histone post-translational modifications (PTMs). Writers add PTMs to histones. Erasers remove these modifications. Readers detect and interpret the PTMs, influencing gene expression and chromatin structure. Created with BioRender.com.

1.2 DNA methylation

DNA methylation is a fundamental epigenetic mechanism that plays a crucial role in regulating gene expression and maintaining genomic stability. DNA methylation involves the addition of a methyl group to the cytosine base of DNA by DNA methyltransferases (DNMTs) (writer). Once methylated, DNA can be recognized and bound by proteins called methyl-CpG binding domain proteins, serving as "readers" of DNA methylation. DNA methylation typically can happen on promoter and gene bodies which has distinct effects. Methylation of promoter regions is usually associated with gene repression (Swigut & Wysocka, 2007). When promoters are heavily methylated, transcription factors and the RNA polymerase complex have difficulty binding to the DNA, leading to silence in the gene expression. However, gene body methylation is often associated with active transcription (Newell-Price et al., 2000).

1.3 Histone methylation

Histone methylation is a fundamental biological process involving adding methyl groups to lysine and arginine within histones. Histone lysine methyltransferases (KMTs) and protein arginine methyltransferases (PRMTs) use S-adenosyl-L-methionine (SAM) as the methyl group donor, respectively, to mediate histone methylation on lysine and arginine. Lysine can undergo mono-, di-, and trimethylation, while arginine can be monomethylated, symmetrically methylated, or asymmetrically methylated. Histone methylation can have both activating and repressive effects on transcription, depending on the specific methylated lysine or arginine residue and the number of methyl groups added (Bedford & Clarke, 2009).

1.3.1 Role of histone methylation in gene expression regulation

Certain methylations on lysines and arginines are often associated with active transcription. These post-translational modifications (PTMs) are crucial in attracting or repelling specific protein readers that influence chromatin dynamics. Examples of such histone methylations include but are not limited to, mono-methylation on lysine 4 of histone H3 (H3K4me1) (Santos-Rosa et al., 2002), trimethylation on lysine 36 of histone H3 (H3K36me3) (Wagner & Carpenter, 2012), and dimethylation on lysine 79 of histone H3 (H3K79me2) (Schübeler et al., 2004). In contrast, certain histone methylations, such as trimethylation of lysine 27 on histone H3 (H3K27me3) and H3K9me3, are associated with transcriptional repression. These modifications inhibit access to the transcriptional machinery, effectively silencing gene expression (Li et al., 2007)**.** Therefore, multiple histone methylations are associated with both gene activation and repression. Understanding how these histone methylations collaborate to control transcriptional activity has been challenging due to the intricate interplay and complex layering of combinatorial histone post-translational modifications and their crosstalk.

The modification of lysine residues by histone lysine methyltransferases (KMTs) serves a diverse function in controlling gene expression. This epigenetic process significantly impacts gene regulation by altering the structure of chromatin.

Some histone methylations can play a vital role in both the establishment and maintenance of heterochromatin:

1. SUV39H family and EZH2 are essential in silencing gene expression, constitutive heterochromatin formation, and genome stability.

H3K9me3, which, as a repressive mark, binds to the chromodomain of Heterochromatin Protein 1 (HP1). This binding event triggers chromatin condensation and effectively restricts access to DNA (Campos & Reinberg, 2009)**.** The interaction between HP1 and H3K9me3 can be disrupted by certain histone PTMs. For instance, phosphorylation at serine 10 on histone H3 blocks the binding of HP1 to H3K9me3. This disruption can lead to alterations in chromatin structure and, consequently, impact gene expression patterns. In summary, these findings highlight the dynamic nature of epigenetic regulation, where modifications of histones can influence the formation and stability of heterochromatin, ultimately shaping gene expression outcomes (Fischle et al., 2005). The H3K9me3 mark is removed by histone demethylases, such as Lysine Demethylase 4A (KDM4A) and Lysine Demethylase 4B (KDM4B) (Fodor et al., 2006).

Another example is H3K27me3, which is involved in silencing gene expression. H3K27me3 is primarily catalyzed by the histone methyltransferase known as Enhancer of Zeste Homolog 2 (EZH2). EZH2 is a critical component of the Polycomb Repressive Complex 2 (PRC2), a protein complex that adds methyl groups to specific histone residues. H3K27me3 is a well-known epigenetic mark associated with gene silencing and the formation of repressive chromatin structures. It plays a central role in regulating gene expression and maintaining cellular identity during various biological processes (Cao et al., 2002). JMJD3, a histone demethylase, catalyzes the removal of the H3K27me3 mark (Malinczak et al., 2020).

On the other hand, several histone lysine methyltransferases are engaged in transcription activation and have been found in transcriptionally active regions and genes.

2. SET1(KMT2), SET2 (KMT3A), and DOT1L (KMT4) significantly contribute to activating gene expression pathways.

One prominent example of histone methylation that plays a crucial role in gene expression activation is the H3K4me3. H3K4me3 is catalyzed by SET1/COMPASS complexes, and the removal of tri-methyl groups from H3K4 is carried out by lysine demethylases, specifically the Lysine Demethylase 5C (KDM5C) family enzymes (Outchkourov et al., 2013). This modification is often found near promoters of actively transcribed genes and serves as an epigenetic mark

associated with gene activation. H3K4me3 helps recruit transcriptional machinery and other regulatory proteins to the gene, facilitating the transcription of genes (Shilatifard, 2008).

Another example is DOT1L / or KMT4 (Lysine Methyltransferase 4), the sole lysine methyltransferase responsible for catalyzing mono-, di-, and tri-methylation of histone H3 at lysine 79 (K79me1, me2, or me3). H3K79me2 is decorated in the gene body of actively transcribed genes and plays a crucial role in transcription elongation (Li et al., 2014). The enzyme that specifically targets and removes methyl groups from histone H3 at lysine is the histone demethylase KDM2B (Kang et al., 2018). Research studies have shown that DOT1L plays an important role in leukemogenesis involving KMT2A fusion proteins. A comprehensive discussion of DOT1L will be provided later in this chapter.

Methylation of H3K36 is facilitated by SETD2 (KMT3A), NSD1 (KMT3B) , NSD2 (KMT3G), NDS3 (KMT3F), and ASH1L (KMT2H) . In mammalian cells, SETD2 is the only enzyme that can catalyze H3K36 tri-methylation (H3K36me3). NSD1, NSD2, NDS3, and ASH1L are responsible for catalyzing H3K36 mono- and di-methylations. H3K36me3 modification is prominently localized within the gene body of actively transcribed genes and plays a pivotal role in facilitating transcriptional elongation (Edmunds et al., 2008; Venkatesh & Workman, 2013). H3K36me3 is removed by specific histone demethylases named KDM2A (Verrier et al., 2011). A comprehensive discussion of SET2 will be provided later in this chapter.

Histone methylation not only plays a crucial role in regulating gene expression but also contributes to other biological processes, including X chromosome inactivation (Heard et al., 2001) and spatiotemporal patterning of *Hox* genes in mice (Heard et al., 2001; Minard et al., 2009). The **Figure 2** shows the PMTs including, H3K4me3, H3K79m1/2/3, H3K36me3, H3K9me2/3, H3K27me3, and others distribution along the active genes and silent gene (Lim et al., 2010).

The dynamics of PTMs are crucial for the precise regulation of gene expression. By adding or removing PTMs dynamically, cells can adjust gene expression levels in response to developmental cues, stressors, or external stimuli. Proteins that interpret these modifications play essential roles in translating PTMs into specific changes in chromatin structure and transcriptional activity. The intricate interplay between different PTMs and their modifying enzymes forms a complex regulatory network that ensures proper gene expression profiles necessary for cellular function.

Understanding the dynamic nature of PTMs is crucial for deciphering how cells maintain precise gene expression patterns under different conditions.

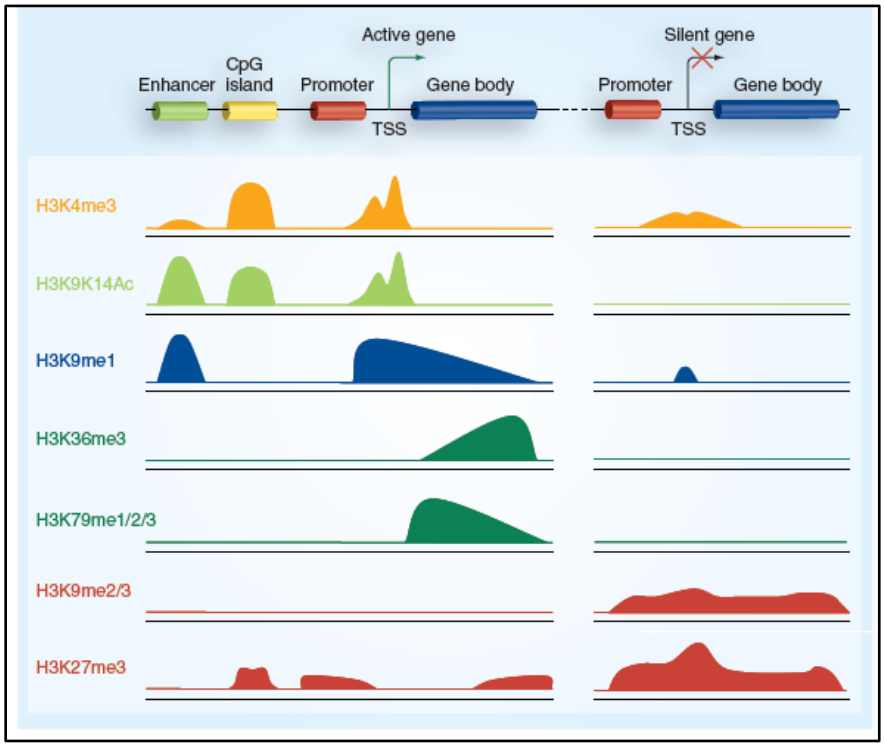

Figure 2: Distribution of various histone modifications across different regions of the genome in active and silent genes. The genomic features shown include enhancers, CpG islands, promoters, transcription start sites (TSS), and gene bodies. The figure was adopted with permission from (Lim et al., 2010) .

1.4 *HOXA* gene family

The homeobox gene family was initially identified by genetic analysis of active genes involved in the development of *Drosophila* (McGinnis et al., 1984). The *HOX* gene family plays a vital role among the homeobox genes that code for transcription factors. These transcription factors are proteins that attach to specific DNA sequences to control the activity of different genes. The *HOX* gene family members all possess a shared characteristic that is highly conserved: a 61-amino-acid section referred to as the homeodomain (Kessel et al., 1988; Wright et al., 1989). This homeodomain contains a unique design known as a helix-turn-helix, allowing the proteins to attach

to DNA and carry out their controlling roles. Mammals have a total of 39 *HOX* genes divided into four clusters: *HOXA* on chromosome 7, *HOXB* on chromosome 17, *HOXC* on chromosome 12, and *HOXD* on chromosome 2. In each group, 13 paralog genes were identified based on both their sequence similarity and position. Each *HOX* gene contains two exons and one intron, with a conserved homeobox domain encoded by a 120-nucleotide sequence in exon 2 (Aryal et al., 2023; Holland et al., 2007).

1.4.1 *HOXA9* gene regulation in normal hematopoiesis

In normal hematopoiesis, the majority of *HOX* genes that are expressed belong to *HOXA*, *HOXB*, and *HOXC* clusters. These *HOX* genes are expressed at various stages during hematopoietic development. *HOXA9* expression is high in hematopoietic stem and progenitor cells (HSPC), which are immature progenitor cells, whereas it is downregulated during differentiation. Different *HOX* clusters are expressed in specific lineage-restricted patterns. For example, *HOXA* cluster genes are normally expressed in myeloid cells, *HOXB* cluster genes in erythroid cells, and *HOXC* cluster genes in lymphoid cells. *HOXA5, HOXA6, HOXA7, HOXA8, HOXA9*, and *HOXA10* genes are highly expressed in hematopoietic stem (HSC) and progenitor cells (HSPCs) and are crucial for maintaining HSPCs (Argiropoulos & Humphries, 2007). The *HOXA5-10* genes are downregulated and epigenetically silenced as they differentiate and become fully mature by the PRC1/PRC2 complex enzyme. *HOXA9* is tightly regulated by the interplay of two master regulators, KMT2A (MLL1) and Polycomb Repressive Complex 1 (PRC1) and Polycomb Repressive Complex 2 (PRC2). KMT2A functions as a transcriptional activator by methylating histone H3 at lysine 4 (H3K4), a modification that promotes the recruitment of transcriptional machinery to the *HOXA9* promoter, thereby enhancing its expression (Collins & Hess, 2016). In contrast, PRC2 and PRC1 serve as transcriptional repressors by catalyzing H3K27me3 and H2AK119 ubiquitination, leading to chromatin compaction and gene silencing (Rugo et al., 2020). Moreover, HSC differentiation can also lead to the accumulation of DNA methylation at *HOXA* 5-10 cluster, mediated by de novo methyltransferases DNMT3A and DNMT3B, further ensuing gene silencing and protecting aberrant *HOX* gene activation in more mature hematopoietic cells (Bock et al., 2012). This dynamic regulation by KMT2A and PRC1/PRC2 ensures that *HOXA9* expression is precisely controlled, facilitating proper cellular functions such as hematopoiesis and differentiation while preventing aberrant gene activity (**Figure 3).** *HOXA9* plays an important role

in normal hematopoiesis (Abramovich & Humphries, 2005). In mice, overexpression of *HOXA9* results in increased proliferation of HSC and myeloid progenitor cells, leading to leukemogenesis in the long run (Alharbi et al., 2013). On the other hand, eliminating *HOXA9* in mice reduces the number of myeloid progenitors and leads to cell differentiation into the erythroid lineage with maturation (Lawrence et al., 2005).

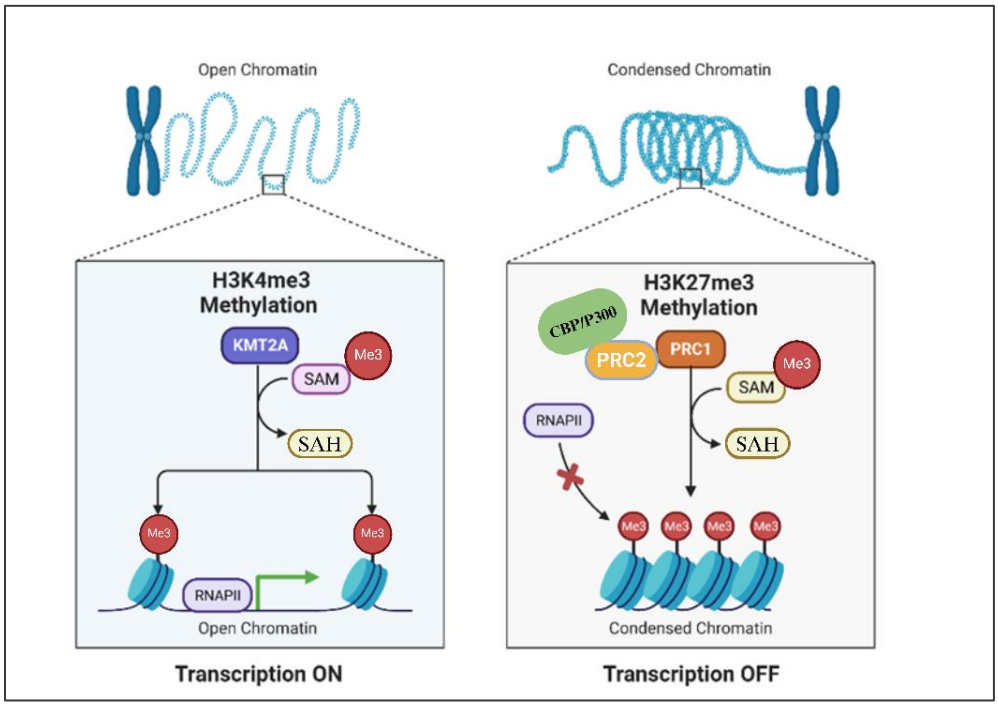

Figure 3 : Schematic representation of dynamic regulation of *HOXA9* by KMT2A and PRC1/PRC2. Created with BioRender.com

1.4.2 *HOXA9* gene in leukemia

Expression of *HOXA9* is found in about 70% of acute myeloid leukemia (AML) cases and 25% of acute lymphoid leukemia (ALL) cases. In MOLM-13 cells which is the AML-MLL cell type, the KMT2A fusion proteins continuously recruit DOT1L to *HOXA9*, leading to its expression. The oncogenic function of *HOXA9* promotes cell proliferation and alters differentiation. Studies have shown that removing *HOXA9* can lead to arrested proliferation and enhanced apoptosis, especially in MOLM-13 cells, highlighting its potential as a therapeutic target (Faber et al., 2009).

Targeting *HOXA9* directly as a transcription factor remains challenging. An alternative approach involves understanding and targeting the key factors regulating *HOXA9* transcription, such as the DOT1L enzyme and other chromatin-modifying enzymes like RNF20/40 complex, significantly enhancing transcription elongation. It may be possible to develop targeted therapies to modulate *HOXA9* expression in diseases such as leukemia by manipulating these regulatory factors. Moreover, high levels of transcription require increased nucleosome turnover. Nucleosome turnover refers to the process of disassembling and reassembling nucleosomes, which is crucial for transcriptional regulation. Studies have shown nucleosomes act as structural barriers to RNA polymerase II during transcription (Izban & Luse, 1991). For the *HOXA9* gene, high transcriptional activity necessitates frequent nucleosome remodeling to allow transcription machinery access to the DNA. This dynamic process involves constantly removing and replacing nucleosomes along the *HOXA9* gene, contributing to its instability. High nucleosome turnover is particularly pronounced at regulatory regions and is associated with active transcription. Bioinformatic analyses of Chromatin Immunoprecipitation Sequencing (ChIP-seq) data from MOLM-13 cells indicate that *HOXA9* has an unstable nucleosome structure (Sharma et al., 2022).

1.4.3 Mixed lineage leukemia and *HOXA9* expression

Mixed lineage leukemia is an aggressive blood cancer that mainly occurs in pediatric patients. MLL is often characterized by *KMT2A* rearrangement at 11q23, which can fuse with over 80 different partner genes, including but not limited to AFF1/AF4, MLLT10/AF10, MLLT3/AF9, and MLLT1/EN (Marschalek, 2016). The KMT2A-MLLT3 fusion protein, resulting from the t(9;11)(p22;q23) translocation, is one of the most common and well-studied fusions in *KMT2A*-rearranged leukemia. These rearrangements can fuse otherwise independent genes into a hybrid

gene, resulting in fusion proteins containing domains initially encoded by separate genes. In MLL, the *KMT2A* gene, which codes for an H3K4 lysine methyltransferase (Castiglioni et al., 2022), fuses with another protein-coding gene, generating an oncoprotein (Britten et al., 2019). In this fusion, *KMT2A* retains its *N*-terminus ($KMT2A^N$), which is placed in frame with the *C*-terminus of one of several fusion partners, creating an oncogenic chimeric protein (Yokoyama, 2021). In this translocation, although KMT2A does not contain the H3K4 methylation SET domain, it does contain a CXXC domain that can bind to nonmethylated CpG-rich promoter regions of target genes of KMT2A like the *HOXA9* gene (**Figure 4)**. Upon binding the fusion protein to the CpG regions, it can recruit DOT1L, the Super Elongation Complex (SEC), and other chromatin-modifying enzymes involved in transcription elongation, thereby increasing *HOXA9* expression (Sharma et al., 2022). In mature blood cells, *HOXA9* expression is generally very low or absent, which is necessary for proper cell differentiation and maturation. Continuous expression of *HOXA9* can prevent the differentiation program from proceeding, resulting in uncontrolled proliferation and contributing to leukemia harbor *KMT2A* rearrangement (Adamaki et al., 2015).

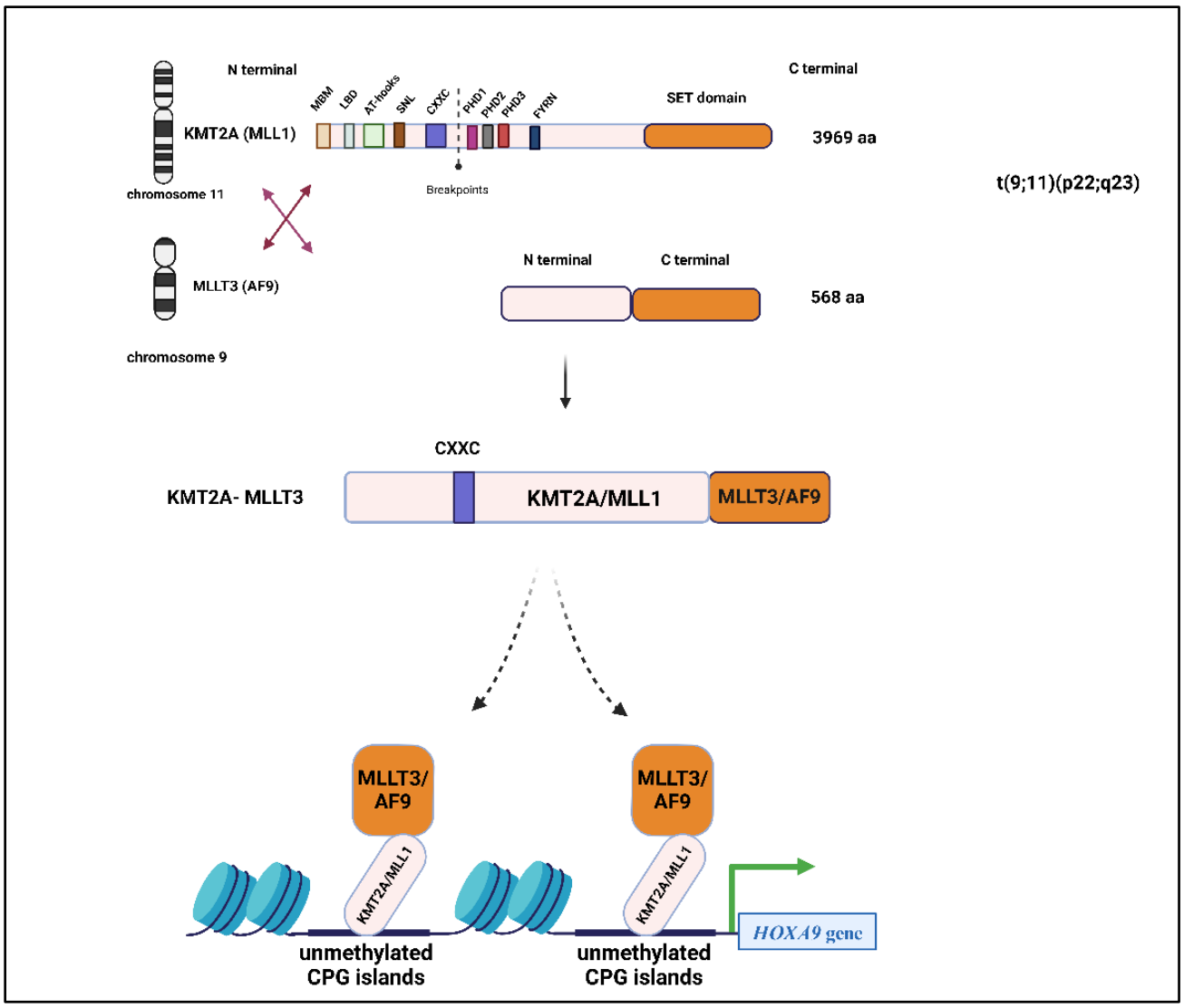

Figure 4: Schematic representation of the *KMT2A (MLL1) and MLLT3 (AF9)* gene translocation in MLL. The KMT2A-MLLT3 fusion protein binds to unmethylated CpG islands within the promoter regions of target genes such as *HOXA9*. Created with BioRender.com

1.5 DOT1L

1.5.1 DOT1L has H3K79 methyltransferase activity

DOT1L (KMT4) is a non-SET domain histone lysine methyltransferase and the sole enzyme responsible for catalyzing mono-, di-, and tri-methylation of histone H3 at lysine 79 (K79me1, me2, or me3) using S-adenosyl methionine (SAM) as a cofactor (Feng et al., 2002; van Leeuwen et al., 2002)**.** The H3K79me2 modification is located within the gene body of active genes and is associated with transcription elongation. The specific localization of H3K79me2 along the gene body reflects its functional role in supporting transcriptional elongation and maintaining an open chromatin state throughout the transcriptional process rather than being associated with transcription initiation at promoters. H3K79me2 plays a chief role in several biological processes, such as cell cycle regulation, DNA damage response, development, and hematopoiesis (Jones et al., 2008; Yang et al., 2023). Studies highlight its pivotal role, with research indicating that loss of DOT1L in mice leads to embryonic death. DOT1L plays a critical role in hematopoiesis development, guiding the differentiation of pluripotent hematopoietic stem cells into multipotent progenitors and ultimately into various mature cell types (Wille & Sridharan, 2022b). Research in human and mouse models has elucidated its importance in hematopoietic development. Interestingly, DOT1L also acts as a barrier during the reprogramming of somatic cells like mouse neural stem cells and human fibroblasts into induced pluripotent stem cells (iPSCs). This suggests that the presence of DOT1L or its activity can impede the successful reprogramming process. Consequently, inhibiting DOT1L emerges as a promising strategy to facilitate the formation of iPSCs (Wille & Sridharan, 2022a, 2022b).

Like other histone post-translational modifications, H3K79me2 is reversible. While the enzyme responsible for removing H3K79me2 is still a topic of debate, research suggests that histone demethylases KDM2B may play a role. These enzymes specifically target and remove methyl groups from histone H3 at lysine 79, contributing to the dynamic regulation of chromatin structure and gene expression (Kang et al., 2018).

Aberrant DOT1L activity is found in various types of leukemia, including mixed lineage leukemia (MLL) with *KMT2A* gene rearrangements with various fusion partners. The exact mechanism of DOT1L function in these contexts remains elusive. However, the evidence shows that the KMT2A

fusion protein, which results from rearrangements between *KMT2A* and fusion partners, mostly A*F10 (MLLT10), ENL (MLLT1), AF9 (MLLT3)*, can direct DOT1L to subsets of genes involved in HSC development in various AML subtypes, including MLL. This includes the homeobox *HOXA* genes, especially the *HOXA9* gene (Arnold et al., 2022). The specific localization of H3K79me2 along the gene body reflects its functional role in supporting transcriptional elongation and maintaining an open chromatin state throughout the transcriptional process rather than being associated with transcription initiation at promoters.

1.5.2 DotCom complex and Super elongation complex (SEC)

DOT1L functions as the central component of the DotCom macromolecular (∼2 MDa), multi-subunit complex, encompassing *KMT2A (MLL1)* translocation partners such as AF10 (MLLT10), ENL (MLLT1), and AF9 (MLLT3) (Mohan et al., 2010)**.** MLLT3 and MLLT1, besides functioning as components of the DotCom complex, also act as subunits within the super elongation complex (SEC), alongside other components such as AFF1, AFF4, and ELL.

The Super Elongation Complex (SEC) is an essential player in gene expression, specifically during the elongation phase of transcription. This complex is made up of several important transcription elongation factors, including ELL1-3, EAF1/2, P-TEFb, AFF1, AFF4, MLLT3 (AF9), and MLLT1 (ENL) and Menin. These factors can be recruited to specific genes that facilitate the transition from transcription initiation to elongation and recruit necessary RNA processing factors (Brzezinka et al., 2020).

1.5.3 DOT1L structure

DOT1L comprises more than 1530 amino acids, containing an N-terminal histone methyltransferase domain (aa 1–332, a non-SET domain catalytic domain) and a long C-terminal region that may mediate interaction with fusion partners such as AF10, AF9 (MLLT3), and eleven-nineteen lysine-rich leukemia (ENL). DOT1L is predicted to contain three separate MLLT3 binding motifs and four tandem coiled-coil (CC) domains (aa 419–670), which are involved in AF10 binding (Zhang et al., 2018).

1.6 Insights into crosstalks modulating DOT1L methyltransferase activity

Histone crosstalk refers to the interaction between different histone modifications that regulate gene expression and chromatin structure. There are two primary types of histone crosstalk: trans histone crosstalk and cis crosstalk. Trans-histone crosstalk involves interactions between histone modifications that occur on different histone tails within a nucleosome. However, cis-histone crosstalk involves interactions between histone modifications that occur on the same histone on the same nucleosome **(Figure 5)**.

K79 on histone H3 is situated in loop 1 of histone H3 fold in the nucleosome, positioned where it is accessible to the solvent and located close to the junction connecting the H3/H4 tetramer with the H2A/H2B dimer (Luger et al., 1997). Multiple studies have indicated that this distinct placement of H3K79 within the nucleosome involves DOT1L in crosstalk with other histone modifications, ultimately contributing to regulating DOT1L enzymatic activity. Several studies have indicated that in trans histone crosstalk, DOT1L interacts with H2BK120ub, the basic region of histone H4 tail, and the nucleosome acidic patch, impacting DOT1L methyltransferase activity and functionality.

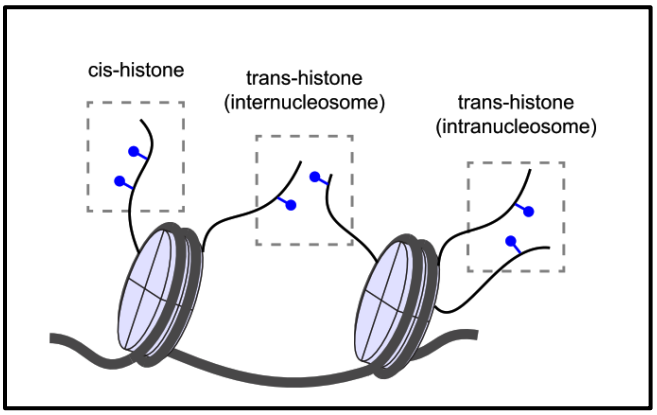

Figure 5: Schematic representation of different types of histone PTMs crosstalk. The figure was adapted with permission from (Lempiäinen & Garcia, 2023).

1.6.1 Players can affect the activity of DOT1L

Research studies have shown that DOT1L methyltransferase activity can be affected by several factors, including the monoubiquitination of H2B at lysine 120 (H2BK120ub), residues R15-R16-

R17-H18-R19 on the histone H4 tail, and the acidic patch on the nucleosome. These factors will be discussed in detail below.

1.6.1.1 Monoubiquitination of H2B (H2Bub)

While polyubiquitination designates proteins for degradation by the 26S proteasome, monoubiquitination of histones serves as a signaling mechanism and can associated with transcriptional activation, transcription elongation (Luger et al., 1997), DNA damage response (Kari et al., 2011), DNA replication (Trujillo & Osley, 2012), positioning of nucleosome (Batta et al., 2011), segregation of chromatin (Latham et al., 2011) and chromatin boundary and transcription repression (Tamburri et al., 2020). Monoubiquitation on histone H2B involves attaching a 76-amino acid protein, roughly 8.5 kDa in size, to histone H2B weighing approximately 13-15 kDa. While monoubiquitation of histone H2B can occur at different residues, such as lysine 34 and 125 (*in vitro*), the monoubiquitation of histone at lysine 120 has garnered significant attention in recent years. Mono-ubiquitination of histones does not always affect transcriptional progression and activation. For example, mono-ubiquitination of histone H2A (H2AK119ub), catalyzed by PRC1 and PRC2, can repress transcription (Tamburri et al., 2020).

1.6.1.2 Monoubiquitination of H2B at lysine 120 (H2BK120ub)

Histone mono-ubiquitination and poly-ubiquitination are both ATP-dependent reactions that link with ubiquitin-activating enzyme E1, ubiquitin-conjugating enzyme E2, and ubiquitin ligase E3. In yeast, H2B is monoubiquitinated on lysine 123 (K123) by the E2 ubiquitin-conjugating enzyme RAD6 and the E3 ubiquitin ligase BRE1. In mammals, this modification occurs on lysine 120 (K120) with RAD6's orthologs UBE2A and UBE2B as the E2 enzymes, and BRE's homologs RNF20/RNF40 as the E3 ligase complex. H2BK120ub in mammals is mediated by the E3 ubiquitin ligase ring finger protein (RNF20–RNF40) complex. RNF20 and RNF40 exist as a heterodimeric complex containing two copies of each polypeptide (Zhang et al., 2018). Both RNF20 and RNF40 contain a carboxyl-terminal RING domain, which is essential for ubiquitin ligase activity and the formation of heterodimeric complexes RNF20/RNF40 (Wood et al., 2003).

H2BK120ub involves the recruitment of the RNF20–RNF40 complex to chromatin via the human PAF1 (RNA polymerase II-associated factor 1) complex. The PAF1 complex associates with RNA polymerase II on the chromatin of actively transcribed genes, playing a critical role in transcription

initiation, elongation, and 3′-end processing. During transcription elongation, RNA polymerase II pauses upon encountering a nucleosome, which acts as a physical barrier. This pause facilitates the recruitment of factors such as the PAF1 complex and the RNF20-RNF40 complex. These factors, including the FACT complex (Facilitates Chromatin Transcription), promote the displacement of one H2A/H2B dimer from the nucleosome, forming a hexasome that Pol II can more easily traverse, thereby enhancing transcriptional efficiency. This mechanism is repeated on successive nucleosomes, thereby increasing overall transcription efficiency during each round of transcription (Belotserkovskaya et al., 2003; Fu et al., 2021; Orphanides et al., 1998).

Like various other modifications to histones, H2BK120ub is reversible and relies on a harmonized interplay between enzymes responsible for adding this modification (writers) and those involved in its removal (eraser). The balance between H2B and deubiquitination is crucial for regular cell growth, maintaining the proper physiological function of the cells, and preventing cryptic transcription. Ubiquitin attached to H2B can be cleaved off by a category of thiol proteases recognized as deubiquitylating enzymes (DUBs). In mammals, USP3, USP7, USP12, USP22, USP44, USP46, and USP49 are all recognized to play a role in the deubiquitylation of H2B (Fuchs & Oren, 2014; Joo et al., 2011; Nicassio et al., 2007; van der Knaap et al., 2005; Zhang et al., 2008). Among these enzymes, USP22 stands out as a specific deubiquitinase, demonstrating precision in removing a mono-ubiquitin molecule from H2BK120ub (Jeusset & McManus, 2017; Zhang et al., 2008). USP22 is a key subunit of the human SAGA complex (hSAGA), a multiprotein transcriptional cofactor complex that is required for the transcription activators in eukaryotes (Lee & Workman, 2007). SAGA (Spt-Ada-Gcn5 acetyltransferase) is a highly conserved transcriptional coactivator that consists of two distinct enzymatic activities, histone acetylation, and deubiquitylation, establish specific epigenetic patterns on chromatin and thereby regulate gene expression. the Gcn5 subunit of SAGA possesses histone acetyltransferase (HAT) activity, catalyzing the acetylation of histones which promotes an open chromatin structure that facilitates transcriptional machinery access to DNA. Moreover, USP22 which is a component of the SAGA complex, plays a crucial role in transcriptional regulation by precisely controlling the levels of H2BK120ub (Cheon et al., 2020).

1.6.1.3 The role of H2BK120ub on DOT1L enzyme activity

Research studies have shown that the methylation of histone H3K79 by DOT1L is a distinctive feature of actively transcribed genes, relying on the H2BK120ub and Lys34 (H2BK34ub). Cryo-EM structures have shown that H2BK120ub secures the DOT1L methyltransferase to nucleosomes, increasing the methylation of histone H3K79 (**Figure 6)**. The ubiquitin on H2B anchors Dot1L at one edge of the nucleosome, enabling the enzyme to assume a poised or active state (Worden et al., 2019). Furthermore, the structural analysis has demonstrated that H2BK34ub prompts an almost identical orientation and binding pattern of DOT1L on the nucleosome, similar to the effect of H2BK120ub. This affects the positioning of DOT1L into a productive conformation through direct ubiquitin-enzyme contacts (Ai et al., 2022).

DOT1L can interact with the Ser-2 and Ser-5 phosphorylated C-terminal domain of actively transcribing RNA polymerase II through a region uniquely conserved in multicellular DOT1 proteins. Genome-wide profiling analyses indicate that DOT1L occupancy largely overlaps with RNAPII at actively transcribed genes in embryonic carcinoma NCCIT cells. These analyses also reveal that actively transcribed genes exhibit both H3K79 methylation and H2BK120ub signal enrichment distributed similarly in these cells. This suggests that DOT1L and H2BK120ub are involved in transcription elongation and can increase the transcription rate (Kim et al., 2012).

Depletion of histone H2BK120ub ubiquitination reduces H3K79me2 levels along the *HOXA9* gene after using proteasome inhibitors like bortezomib. This further demonstrates that DOT1L activity relies on H2BK120ub and that both play a role in transcription elongation, particularly in leukemia and *HOXA9* gene expression (J. L. Kamens et al., 2023).

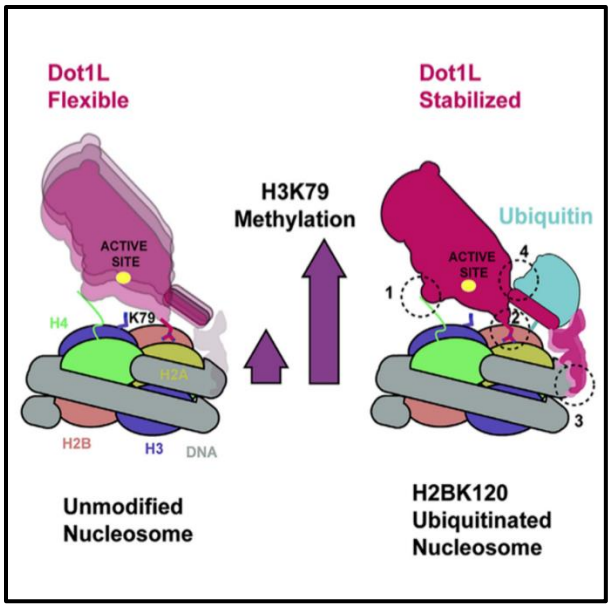

Figure 6: The role of H2BK120 ubiquitination in stabilizing DOT1L and enhancing its methylation activity on H3K79. On the left, DOT1L is shown in a flexible conformation when bound to an unmodified nucleosome, resulting in lower H3K79 methylation activity. On the right, the presence of ubiquitinated H2BK120 (H2BK120ub) stabilizes DOT1L, positioning its active site directly over H3K79. This stabilization promotes higher H3K79 methylation. The figure was adopted with permission from (Worden et al., 2019).

1.6.1.4 The role of the basic region in histone H4 tail in DOT1L enzyme activity

The N-terminal tail of histone H4, specifically amino acids 15 to 19, can further interact with and enhance DOT1L methyltransferase activity. This interaction is especially effective when DOT1L is already stabilized on the nucleosome by the presence of H2BK120ub. This concurrent binding of the H4 tail and ubiquitin to DOT1L positions the enzyme's catalytic site directly over H3K79, ensuring specificity for this residue. The synergistic effect of H4 tail interaction and H2BK120ub highlights the complex regulation of DOT1L activity, crucial for precise histone methylation and proper gene expression (Worden et al., 2019). Moreover, acetylation of lysine 16 on histone H4 directly stimulates the catalytic activity of DOT1L on nucleosomes. While H4K16ac alone promotes the catalytic conformation of DOT1L, the presence of H2BK120ub further enhances this

activity. This allosteric regulation by H2BK120ub and H4K16ac optimizes the catalytic rate of DOT1L, facilitating the di- and trimethylation of H3K79 (Lee et al., 2018).

1.6.1.4 The role of nucleosome acidic patch in DOT1L enzyme activity

The term "acidic patch" on the nucleosome refers to a negatively charged region formed by aspartate (D) and glutamate (E) residues on histones H2A and H2B. Specifically, the acidic residues include Aspartate (D89, D90) and Glutamate (E91) on histone H2A, and Aspartate (D77, D78) and Glutamate (E79, E80) on histone H2B. These acidic residues contribute to the overall negative charge of the patch. The acidic patch serves as an anchoring site for various biological molecules, including transcription factors, chromatin-binding proteins, and enzymes. These interactions are pivotal in regulating the accessibility of DNA within the nucleosome, influencing the structural organization of chromatin, and ultimately governing gene expression. The structure revealed that DOT1L anchors to the acidic patch, which aids DOT1L in stabilizing the nucleosome and assuming a conformation poised for methylation (Worden et al., 2019).

1.7 Histone H3K36 methylation

Histone H3 can be methylated at lysine 36 (H3K36) with mono-, di- and tri-methylations (H3K36me1/me2/me3) by using S-adenosyl methionine (SAM) as a cofactor. Trimethylation of histone H3 at lysine 36 is involved in DNA damage repair and multiple transcriptional-related events, such as the regulation of transcriptional activity, transcription elongation, and pre-mRNA alternative splicing (Bhattacharya et al., 2021; Li et al., 2013; Nilsen & Graveley, 2010; Yoh et al., 2008). Evidence has shown that in mammalian cells, mono- and di-methylating H3K36 can be mediated by several redundant enzymes, including NSD1 (KMT3B) (Rayasam et al., 2003), NSD2 (KMT3G) (Li et al., 2009), NSD3 (KMT3F) (Rahman et al., 2011), ASH1L (KMT2H) (Tanaka et al., 2007), SETD3 (Eom et al., 2011), SETMAR (Lee et al., 2005), and SMYD2 (Brown et al., 2006; Sun et al., 2020). However, SET2 is the only enzyme that can trimethylate histone H3 at lysine 36 (Edmunds et al., 2008). SETD2 is recruited by the Ser2-phosphorylated C-terminal domain (CTD) of RNA polymerase II during the elongation phase of transcription to the genes and is distributed in the gene body at the 3-end. SETD2 is recruited to the RNAPII elongation complex via SPT6S in mammalian cells (Sun et al., 2020; Youdell et al., 2008). The SRI domain located in

the C terminal of the SET2 enzyme is involved in mediating the interaction with the Ser2 phosphorylated C-terminal domain of RNAPII (Kizer et al., 2005; Morris et al., 2005).

H3K36me3 plays a multifaceted role in gene expression, enhancing transcription elongation and gene activity while crucially preventing cryptic transcription within genes. By marking actively transcribed regions, H3K36me3 helps maintain transcriptional fidelity by preventing RNA polymerase from initiating transcription at inappropriate sites within genes. In mammals, H3K36me3 on gene bodies acts as a repressor of aberrant intragenic transcription by facilitating the recruitment of DNMT3B, a DNA methyltransferase that prevents cryptic gene activation (Weinberg et al., 2019). Moreover, H3K36me3 plays an important role in alternative splicing regulation, a process by which different combinations of exons are joined together to produce multiple mRNA variants from a single gene. Studies have shown that alternative splicing regulation is mediated through the recruitment of specific splicing factors to H3K36me3-marked regions of the genome. H3K36me3 acts as a binding platform for splicing factors and other associated proteins. As an example, MRG15/MORF4L1 is a highly conserved protein in eukaryotes that contains a chromodomain (CHD) recognizing methylation of lysine 36 on histone H3 (H3K36me3) in chromatin. MRG15 can interact with splicing factors such as PTB (polypyrimidine tract-binding protein), facilitating their recruitment to chromatin (Devoucoux et al., 2022). H3K36me3 is removed by specific histone demethylases named KDM2A (Verrier et al., 2011).

1.7.1 Crosstalk between H3K36me3 and other active histone modifications

The RNA polymerase II elongation complex not only recruits SET2 but also the RNF20/40 complex through PAF1, which ubiquitinates H2BK120, indicating a potential interplay between these two histone modifications (Silvija Bilokapic & Mario Halic, 2019; Song & Ahn, 2010). There have been reports of extensive crosstalk between the SETD2-dependent H3K36me3 and other histone marks, such as H2BK120 ubiquitination and H3K79me2 (Silvija Bilokapic & Mario Halic, 2019; Anna Skucha et al., 2018) . H3K36me3 and H2BK120ub are both found in the gene bodies of active genes and are associated with transcription elongation. Evidence indicated that SET2 interacts with H2BK120ub, implying that ubiquitin facilitates the placement of SET2 on the nucleosome. The biochemical research, which compares H2BK120 ubiquitinated nucleosomes to

unmodified nucleosomes and demonstrates elevated SET2 tri-methylation activity, supports this observation (S. Bilokapic & M. Halic, 2019; Vlaming et al., 2014).

Moreover, a strong correlation was shown between the localization of the H3K36me3 and H3K79me2 marks in the *HOXA9* gene body in acute myeloid leukemia. They showed that the *HOXA9* gene exhibits an H3K36me3-H3K79me2 signature on its gene bodies (Anna Skucha et al., 2018). This suggests SETD2-dependent H3K36me3 modification is coupled with H3K79me2 in the *HOXA9* gene in acute myeloid leukemia. We should keep in mind that ChIP-Seq data provide valuable insights into the distinct distribution patterns of different histone modifications across the gene body. H3K79me2, a mark associated with active transcription, is enriched in regions starting around the transcription start site (TSS), extending through the gene body, and diminishing towards the 3' end. On the other hand, H3K36me3 shows a distinct pattern, with peaks beginning towards the 3' end of genes. Therefore, these two marks do not completely overlap throughout the gene body. Although these two modifications can coexist in the gene bodies, they do not overlap completely over the gene bodies.

Discovering interaction partners of SET2 offers crucial insights into its function in transcription elongation, especially within MOLM-13 cells, which represent mixed lineage leukemia. Understanding this role not only clarifies the role of SETD2 in transcription processes but also sheds light on its potential influence on *HOXA9* expression in mixed lineage leukemia.

1.8 Proteasome

The 26s proteasome is a large proteolytic complex that is responsible for the degradation and recycling of proteins, a process requiring metabolic energy. It recognizes, unfolds, and cleaves proteins that are destined for removal, usually by prior attachment to polymers of ubiquitin, consisting of 76 amino acids, and has a molecular mass of approximately 8.5 kDa. This tagging process is called ubiquitination and involves a cascade of enzymes: E1 (ubiquitin-activating enzyme), E2 (ubiquitin-conjugating enzyme), and E3 (ubiquitin-ligase enzyme). The 26S proteasome macromolecular machine comprises two subcomplexes, the 19S regulatory particle (RP) and the 20S core particle (CP), which contain at least 33 different subunits. The 20S proteasome characterizes the catalytic part of the 26S proteasome involved in the proteolysis of

proteins marked for degradation by the ubiquitin system (**Figure 7)** (Hershko & Ciechanover, 1998).

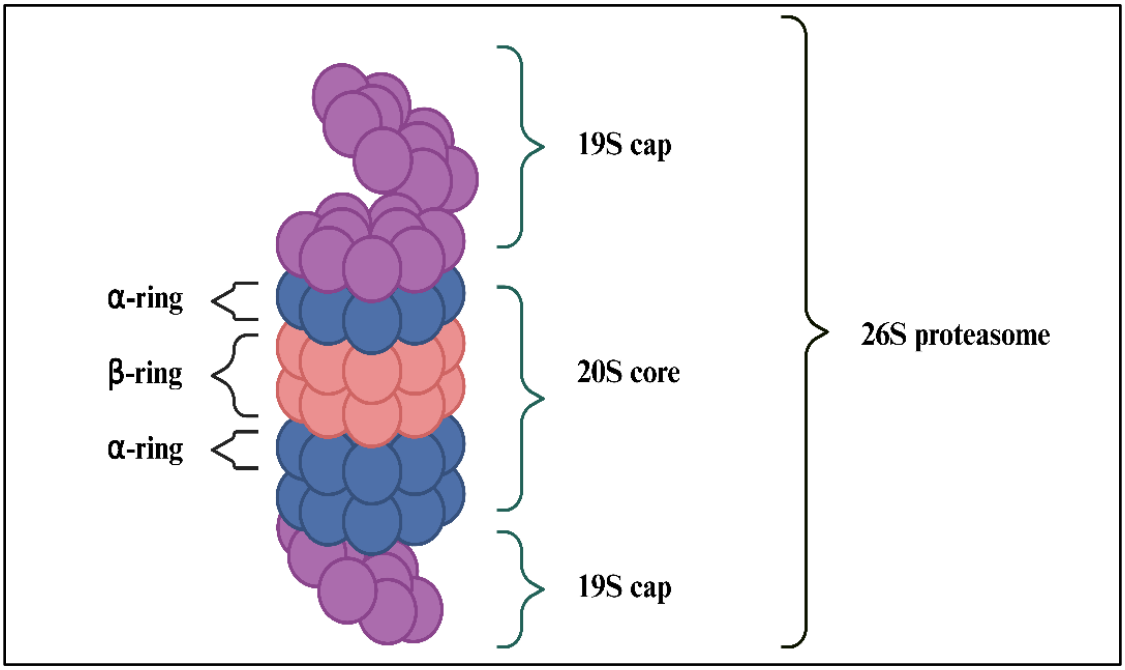

Figure 7: Schematic representation of the 26s proteasome macromolecular machine is composed of two subcomplexes, the 19S regulatory particle (RP) and the 20S core particle (CP), which together contain at least 33 different subunits. Created with BioRender.com

Proteosomes can be classified into two main groups:

1. Constitutive Proteasome
2. Immunoproteasome

The constitutive proteasome exists in almost all cell types and is responsible for the degradation of intracellular proteins under normal physiological conditions. It contains three distinct catalytic β subunits: β1 (Y, *PSMB6*), β2 (Z, *PSMB7*), and β5 (X, *PSMB5*), which are known to cleave peptide bonds after acidic, basic, and hydrophobic residues, respectively.

However, the immunoproteasome is a specialized form of the proteasome found predominantly in immune cells, such as lymphocytes and antigen-presenting cells (Früh et al., 1994). Immunoproteasome has three active sites, including β1i (LMP2, low molecular weight protein 2,

PSMB9), β2i (MECL1, multi catalytic endopeptidase complex-like 1, *PSMB10*), and β5i (LMP7, low molecular weight protein 7, *PSMB8*), respectively (Tanaka, 1998).

1.9 Proteasome inhibitor

Proteasome inhibitors can block the activity of the proteasome complex responsible for degrading intracellular proteins. By inhibiting the proteasome, the breakdown of proteins that regulate cell cycle progression, apoptosis, and other critical cellular processes are blocked, accumulating these proteins and ultimately affecting cell viability. This mechanism is specifically efficient against cancer cells, which rely more on the proteasome for their fast growth and survival. Proteasome inhibitors primarily target the 20S core of the 26S proteasome complex (**Figure 8)**.

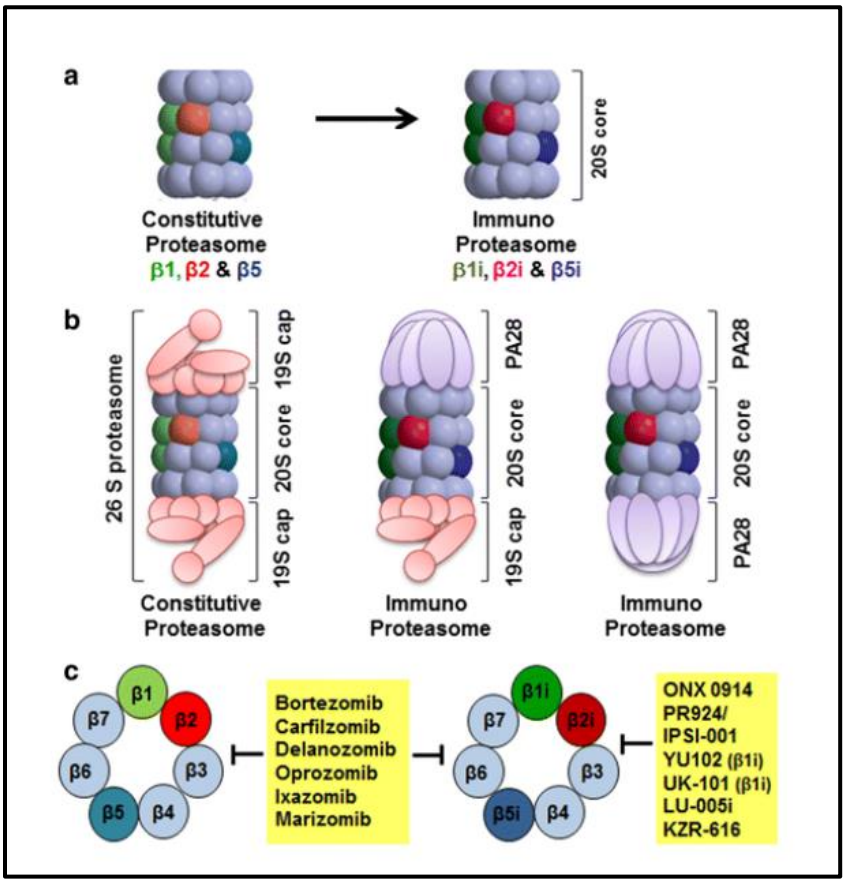

Figure 8: Subunit composition and inhibitors targeting constitutive and immunoproteasomes. **A)** 20S core proteasome. **B)** fully assembled immunoproteasome with various cap proteins. **C)**

Clinically active and experimental inhibitors of constitutive- and/or immunoproteasome. The figure was adapted with permission from (Verbrugge et al., 2015).

1.9.1 Bortezomib

Bortezomib is a proteasome inhibitor that targets both constitutive and immunoproteasomes. It inhibits active sites of the β-subunits (particularly β5) within the 20S core particle, thereby preventing the degradation of ubiquitinated proteins and leading to their accumulation within the cell, ultimately inducing cell death. Bortezomib, a boronic acid peptide, was approved for the treatment of therapy-refractory multiple myeloma about a decade ago.

1.9.2 Bortezomib in clinical trials and clinical practice

Bortezomib has shown significant apoptotic-inducing activity in many tumor cell lines and animal models. The molecular formula of bortezomib is $C_{19}H_{25}BN_4O_4$ and its chemical IUPAC name is [3-methyl-1-(3-phenyl-2-pyrazin-2-ylcarbonylamino-propanoyl) amino-butyl] boronic acid. Bortezomib can be distributed into tissues from the plasma within 10 minutes after intravenous which is a very short time. Its half-life is also about 40 hours (Schwartz & Davidson, 2004). Cytochrome p450 enzymes are primarily responsible for metabolizing the bortezomib in the body. Pharmacodynamic research showed that administering bortezomib to patients in doses ranging from 0.13 to 2.0 mg/m² (milligrams per square meter of body surface area) caused a dose-dependent inhibition of proteasome activity. One hour after administration, proteasome inhibition in whole blood samples peaked at 75% or higher (Papandreou et al., 2004). Because bortezomib is a reversible inhibitor of the 26S proteasome, it usually becomes undetectable 72 hours after administration and the inhibited proteasome activity recovers.

Bortezomib-induced cell growth inhibition and apoptosis induction were observed *in vitro* in many different kinds of malignant cells, including multiple myeloma, prostate cancer, pancreatic cancer, renal cell carcinoma, and squamous cell carcinoma (Adams, 2002; Jagannath et al., 2005; Kondagunta et al., 2004; Richardson et al., 2005; Shah et al., 2001). Bortezomib effectively inhibits cell proliferation in multiple myeloma cell lines, with IC50 values ranging from 3 to 20 nanomolar (nM). It exhibits strong growth-inhibitory effects on both drug-sensitive and drug-resistant human multiple myeloma cells (Hideshima et al., 2001).

1.9.3 Impact of proteasome inhibition on *HOXA9* gene expression and H2BK120ub level

Proteasome inhibitors can reduce ubiquitinated histones, especially uH2B, which is essential for proper transcription elongation. The loss of uH2B significantly disrupts transcription**.** This finding underscores that the ubiquitination of histone H2B is intricately linked to the transcription process (Fierz et al., 2011), supporting the evidence that uH2B is associated with active transcription (Davie & Murphy, 1990).

Bortezomib, as a proteasome inhibitor, can indirectly affect H2BK120ub, in addition to its direct effects on apoptosis and cell growth inhibition in tumors. When the proteasome system is inhibited, such as by bortezomib, the cellular ubiquitin pool becomes depleted due to the accumulation of ubiquitinated proteins in the cytoplasm awaiting degradation. Under normal conditions, ubiquitin is recycled from degraded proteins by the proteasome, maintaining a sufficient supply for various cellular functions. However, proteasome inhibition disrupts this recycling process, leading to a shortage of free ubiquitin in the cytoplasm. To compensate for this shortage, ubiquitin is mobilized from other cellular compartments, including the nucleus. Histones, which are ubiquitinated at specific residues like H2BK120, serve as a significant source of ubiquitin within the nucleus. The depletion of ubiquitin in the cytoplasm results in ubiquitin being removed from these histones, leading to a reduction in histone ubiquitination. This de-ubiquitination process allows ubiquitin to move freely from the nucleus to the cytoplasm, attempting to restore the balance needed for the tagging of cytoplasmic proteins. The loss of ubiquitin from histones disrupts crucial epigenetic marks that are vital for chromatin structure and transcriptional regulation. Histone ubiquitination, particularly at H2BK120, plays a key role in transcription elongation, and its reduction can lead to altered gene expression. In the context of leukemia, this disruption may affect the expression of oncogenes such as *HOXA9*, further linking proteasome inhibition to broader epigenetic changes that contribute to disease progression. Studies utilizing bortezomib have shown a decrease in H2BK120ub levels **(Figure 9)**, resulting in subsequent reductions in H3K79me2 levels in acute lymphoblastic leukemia (ALL) and *HOXA9* gene expression (Jennifer L Kamens et al., 2023).

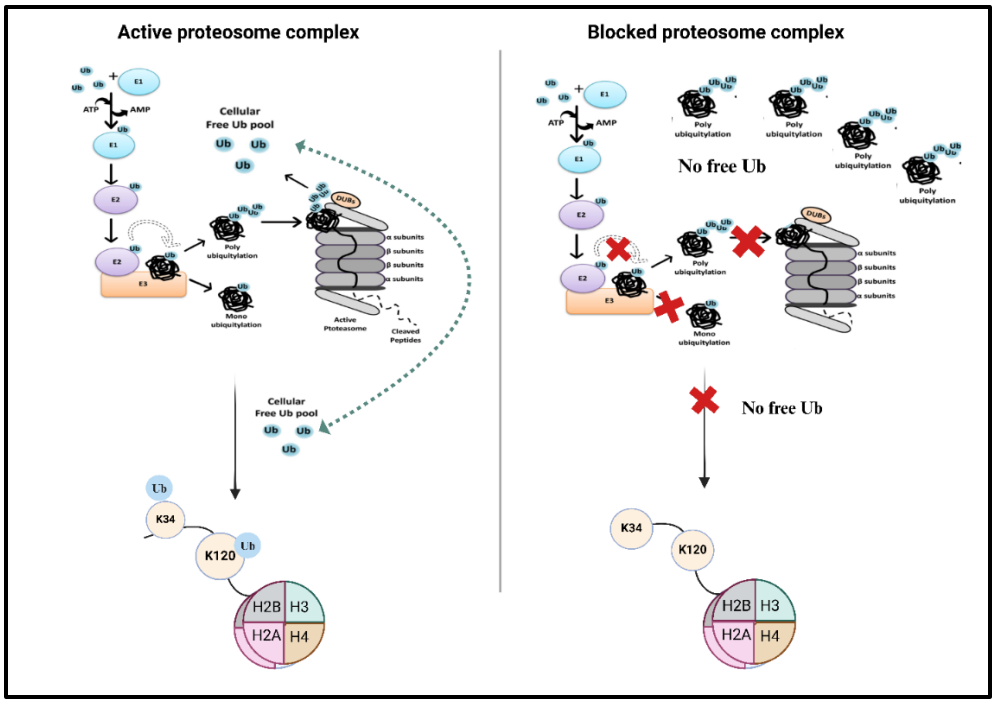

Figure 9: Schematic representation of the effect of active proteasome complex and blocked proteasome complex on histone mono ubiquitination of histone H2B. Created with BioRender.com.

1.10 Histone variants

Histones can be classified mainly into two groups:

- **Replication and cell cycle-dependent (RD) or canonical histones**
- **Replication and cell cycle-independent (RI) or variants**

The following briefly describes the distinctions between the canonical histones (RD) and histone variant (RI):

RD histones, produced during the S-phase, are replication-dependent, while histone variants are replication-independent and expressed continuously throughout the cell cycle. In animals, genes encoding RD histones are typically in multiple copies and recognized as highly conserved proteins. The genes encoding the RD histone tend to be grouped together in the genome across metazoans. In mammals, two primary loci encompass multiple histone genes. The larger cluster, *HIST1*, is situated on human chromosome 6 and encompasses 55 histone genes. Correspondingly, the *Hist1*

cluster on mouse chromosome 13 also contains 51 histone genes. The smaller cluster, *HIST2*, is positioned on chromosome 1 in humans and *Hist2* on chromosome 3 in mice, housing at least six RD histones. In every species, there are typically between 10 to 20 genes encoding each of the core RD histones (Wang et al., 1997)**.** Conversely, histone variant genes are often found as single or double copies and display significant variability among species. Unlike RD histone genes that lack introns, histone variant genes might contain introns and usually possess a polyadenylated mRNA tail at the end, differing in structure from canonical histones.

The process of RI histone integration into chromatin differs from RD. While RD histones incorporate into new nucleosomes during the S phase, RI assembly replaces existing nucleosomes, influencing the structure and function of chromatin. This replacement can result in changes to the local chromatin environment, affecting gene expression and other cellular processes. Therefore, RD histones are initially involved in nucleosome formation, and later, RI histones can be incorporated into these nucleosomes, impacting the dynamics and properties of the chromatin structure (Henikoff & Smith, 2015)**.** Research has revealed diverse histone variants within the core histones (H2A, H2B, H3) and the linker histone (H1).

1.10.1 Histone H3s

In mammals, cells express numerous histone H3s, including H3.1, H3.2, H3.3, CENP-A, H3.Y, H3t, and H3.X, which possess crucial regulatory roles within somatic cells. The H3.1 and H3.2 are predominantly expressed during the S phase of the cell cycle and are categorized as replication-dependent histones (RD). While H3.3, CENP-A, H3.Y, H3t, and H3.X are H3 variants whose expression takes place continuously across the cell cycle without dependence on replication (RI). H3.1 and H3.2 share a 99% sequence identity and a 96% sequence similarity with H3.3 variant. The difference lies in only five residues: four residues (amino acids 87–90) in the globular region and one residue at position 31 in the tail (S31) **(Figure 10)** (Goldberg et al., 2010)**.**

The genes responsible for the replication-dependent (RD) histone H3s are grouped in clusters that contain several gene copies. In humans, there are three copies of genes encoding H3.2 situated within a histone cluster on chromosome 1, while ten copies of genes encoding H3.1 are clustered on chromosome 6p22. These genes lack introns, and their resulting transcripts do not undergo polyadenylation (Marzluff et al., 2002). The arrangement of these genes in a sequence enables

H3.1 and H3.2 to be expressed at the same time, helping in the production of the large quantity of histone necessary for duplicating the genome in the S phase.

In contrast, the genes encoding the histone variant H3.3, represented by *H3F3A* and *H3F3B* in humans, are located outside the histone gene clusters. Similar to most other eukaryotic genes, these genes contain introns, and their messenger RNAs (mRNAs) are characterized by poly(A) tails. The histone variant H3.3 remains one of the most conserved proteins found among various eukaryotic species, displaying an identical protein sequence across all examined vertebrates. Despite the H3.3 protein sequences from *H3F3A* and *H3F3B* being identical in amino acid composition, differences emerge in their codon usage. Notably, the codon usage in *H3F3A* seems more aligned with genes linked to cell proliferation, while *H3F3B* codon usage resembles genes associated with differentiation. These data suggest that through evolutionary changes, H3f3a and H3f3b might have undergone optimization for distinct transcriptional programs (Klein & Knoepfler, 2023; Malik & Henikoff, 2003; Muhire et al., 2019).

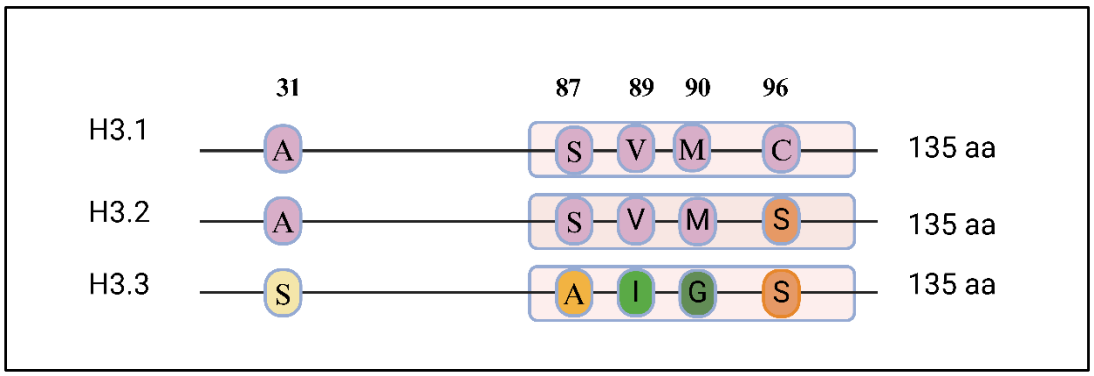

Figure 10: Schematic representation of histone H3 structure differences: H3.1 and H3.2 share 99% sequence identity and 96% sequence similarity with the H3.3 variant. The differences lie in only five residues: four residues (amino acids 87–90) in the globular region and one residue at position 31 in the tail (S31).

1.10.2 The genomic distribution of H3s

H3.1/H3.2 exhibits consistent distribution across both active and inactive genes throughout the genome in the S phase of the cell cycle in a replication-linked pathway manner. In contrast, the H3.3 variant selectively inserts into actively transcribed genes and specific regions of constitutive heterochromatin, such as telomeres and pericentric heterochromatin, throughout the entire cell cycle, based on its specific requirements.

1.10.2.1 H3.3 variant in constitutive heterochromatin regions

H3.3 was initially recognized as a component exclusive to active chromatin (Ahmad & Henikoff, 2002). However, it was subsequently discovered that H3.3 is not only incorporated into active chromatin but also deposits within constitutive heterochromatin, playing a significant role in both euchromatin and heterochromatin contexts.

Previous sections mentioned that the histone H3.3 variant differs from H3.1/2 at five positions, including a serine at position 31. Studies have indicated that this serine residue undergoes phosphorylation (H3.3S31Ph) within constitutive heterochromatin sites, such as telomeres and pericentric repeats (Wong et al., 2009). This modification of serine 31 in H3.3 plays a vital role in regulating heterochromatin accessibility during replication by modulating the activity of the KDM4B histone demethylase. KDM4B, identified as lysine (K)-specific demethylase 4B and recognized for its demethylating activity on H3K9, specifically binds to H3.3K9me3 at telomeres in mouse embryonic stem cells (ESCs). This interaction leads to removing this modification, ultimately enhancing chromatin accessibility and aiding in the facilitation of replication processes. The absence of KDM4B leads to replication stress and DNA damage within telomeric heterochromatin in mouse ESCs (Udugama et al., 2022). It is worth noting that H3.3S31Ph also plays a role in active chromatin, stimulating the activity of the acetyltransferase p300, which can lead to the acetylation of enhancers(Martire et al., 2019).

1.10.2.2 H3.3 in euchromatic regions

Histone H3.3 is mainly incorporated into nucleosomes within active regulatory elements, such as promoters and enhancers, in mammalian genomes (Martire & Banaszynski, 2020)**.** These specific nucleosomes are suggested to possess distinct physical characteristics that could potentially

destabilize the nucleosome core particle, creating a potential "window of opportunity" for the transcriptional machinery to access the DNA. Studies have demonstrated that without H3.3, regulatory elements near promoters become less accessible. This reduced accessibility is associated with lower levels of transcription factor binding and footprinting, a decrease in chromatin modifications linked to transcription factor activity, and reduced engagement of RNA polymerase II at these promoters. Therefore, incorporating H3.3 into active promoters can increase DNA accessibility and promote the binding of transcription factors in mouse embryonic stem cells (Tafessu et al., 2023). Additionally, loss of H3.3 leads to a reduction in chromatin accessibility, a decrease in the activity of the transcriptional coactivator p300, diminished histone H3 acetylation at lysine 27 (H3K27ac), and a reduction in the presence of the BRD4 (acetyl lysine reader) at promoters (Martire & Banaszynski, 2020). Active histone PTM marks, including H3K79me2, H3K4me3, H3K4me2, H3K9ac, and H3K14, were also enriched on H3.3 in the *Drosophila* system. Surprisingly, H3.3 was depleted in H3K9me2 (McKittrick et al., 2004).

1.10.3 Chaperoning of histones: Facilitating nucleosome deposition

Different chaperone complexes deposit histone H3s to form nucleosomes, which will be discussed below.

Accurate incorporation of both RD and RI histones into euchromatin and heterochromatin is facilitated by three important chaperone complexes: HIRA, ATRX/DAXX, and CAF-1.

Histone chaperones play a crucial role in facilitating chromatin assembly and disassembly. The term 'chaperone' refers to proteins that prevent or correct inaccurate interactions arising from the exposure of interactive surfaces to the cellular environment. Because histones possess a notably high positive charge, histone chaperones serve as a protective barrier, preventing nonspecific interactions with negatively charged molecules like DNA, RNA, and other proteins with a negative charge. Many histone chaperones play a role in both assembling and disassembling chromatin. These chaperones can be categorized based on their histone binding preferences. FACT, Nap1, and Chz1 are among the chaperones responsible for facilitating the assembly of histone H2A-H2B complexes. Histone H3/H4 chaperones include the HIRA complex, CAF-1 (chromatin assembly factor 1), Asf1 (anti-silencing factor 1), Rtt106 (regulation of Ty1 transposition), Spt6, Vps75, and Nap1.

Histone chaperones play a crucial role in chromatin structure through either replication-dependent or replication-independent machines. For instance, histone chaperones CAF-1 operate through a replication-dependent pathway, whereas the HIRA complex functions in a replication-independent manner. Certain histone chaperones, like Asf1 and Rtt106, are observed to participate in both pathways (Amin et al., 2013)**.**

This section discussed the importance of three histone chaperone systems: HIRA, CAF-1, and FACT.

1.10.3.1 HIRA chaperone mediates replication-independent nucleosome assembly in active and inactive regions

HIRA is a histone chaperone that is evolutionarily conserved and plays a crucial role in assembling nucleosomes independently of replication. HIRA plays a crucial role in nucleosome organization. Depletion of HIRA in cells results in a global reduction in nucleosome occupancy at gene sequences. HIRA is essential for maintaining nucleosome architecture in both euchromatic and heterochromatic loci. The Electrophoretic Mobility Shift Assay (EMSA) demonstrated the binding preference of the HIRA complex, specifically associating with histones H3-H4 and not with H2A/H2B. This specificity highlights the distinct function of the HIRA complex as a chaperone specifically involved in the facilitation of nucleosome assembly for histones H3-H4. In mammals, the HIRA complex comprises three fundamental subunits: HIRA, UBN1 (Ubinuclein 1), and CABIN1 (calcineurin-binding protein 1)(Gal et al., 2015).

The mechanism of H3.3 deposition in the active region involves HIRA. The HIRA complex collaborates in placing the newly synthesized H3.3 into the euchromatic areas. It interacts with two more subunits, UBN1 and CABIN1. The UBN1 subunit within the HIRA complex has a critical function in the specific and direct binding of H3.3, thereby facilitating the precise distribution of H3.3 across the chromatin landscape. Moreover, the HIRA complex plays a role in reusing H3.3 during gene transcription. This mechanism relies on interacting with the chaperone anti-silencing function protein 1 (ASF-1)**.** As discussed earlier, H3.3 is not only incorporated into euchromatin but also in constitutive heterochromatin regions with a different chaperoning system known as the ATRX/DAXX complex (Torné et al., 2020)**.**

1.10.3.2 CAF-1 chaperone mediates replication-dependent nucleosome assembly

Chromatin Assembly Complex 1 (CAF-1) is an evolutionarily conserved histone chaperone responsible for depositing $(H3\text{-}H4)_2$ tetramers during the replication-dependent chromatin assembly process. CAF-1 is a protein complex made up of three subunits (p150, p60, and p48) in human cells and plays a vital role in multicellular organisms. Depletion of CAF-1 results in developmental arrest during the early embryonic stage in mice. In the context of human cells, the absence of CAF-1 disrupts S-phase progression, causing cells to undergo arrest in the early or mid-S phase.

Histone H3.1 and H3.2 employ the chaperone CAF-1 to facilitate the assembly of nucleosomes that are dependent on replication during the S-phase. CAF-1 guarantees the placement of H3.1/H3.2 during the active replication phase at specific replication locations, and even when the cell is not in the replication phase, it helps position these histones at sites involved in DNA repair (Adam et al., 2016; Tagami et al., 2004).

1.10.3.3 FACT (Facilitates Chromatin Transcription) chaperone mediates replication-dependent and replication-independent nucleosome assembly

FACT is a histone chaperone widely conserved and named for its capacity to enhance RNA Pol II elongation through nucleosomes *in vitro***.** The structure and function of FACT are extensively conserved across all eukaryotes, consisting of two subunits, SPT16 (Suppressor of Ty 16) and SSRP1 (Structure Specific Recognition Protein 1). Both components of FACT, Spt16 and Pob3, possess regions at their C-termini, characterized by high acidity. The presence of an acidic feature in the C-terminal regions of both Spt16 and Pob3, a trait commonly observed in histone chaperones, contributes to their ability to bind to histones H2A and H2B. This facilitates the incorporation of these histones into the nucleosome structure. FACT is actively involved in nucleosome assembly/disassembly processes, specifically in incorporating histones H2A and H2B into the nucleosome structure. It plays a crucial role in transcription, virus infection, DNA replication, DNA repair, chromatin maintenance, and cell differentiation (Kemble et al., 2015). s

1.11 Hypothesis

Genes crucial for driving leukemia exhibit higher activity of DOT1L and RNF20/40. These factors collectively contribute to increased transcriptional elongation and accelerated transcription of leukemic genes like *HOXA9*.

1.12 Aims

1.12.1 Determine whether genes important to mixed lineage leukemia are marked with H3K79me2

To determine the association of H3K79me2 and DOT1L with genes crucial in leukemia, particularly focusing on *HOXA9*, which plays a significant role in leukemogenesis, especially in leukemia harbor *KMT2A*-rearrangement, we conducted bioinformatic analyses of the broad H3K79me2 domains across various leukemic cell lines. Histone modification H3K79me2 is known to be enriched at actively transcribed genes, and its specific distribution on key leukemia-associated genes can provide insights into their regulatory mechanisms and potential therapeutic targets.

1.12.2 Determine DOT1L transcript, protein, and modification levels in MOLM-13 and K562 cell lines

Investigation into DOT1L aims to deepen our understanding of its role in the MOLM-13 which is mixed linage leukemia cell lines. K562 cell line was used as a reference cell line. For this aim, I utilized cell lysis and acid-extracted histone techniques, along with immunoblotting and RT-qPCR analyses, to precisely quantify DOT1L protein level, product level, and transcript level across different cell line models.

1.12.3 Determine the level of H2BK120 monoubiquitination in MOLM-13 and K562 cell lines

This study seeks to uncover how this specific histone modification is regulated differently in distinct types of leukemia by comparing the levels of H2B K120 monoubiquitination between MOLM-13 and K562 cell lines. I utilized acid-extracted histone and immunoblotting techniques to determine the level of H2B K120 monoubiquitination.

1.12.4 Determine the impact of bortezomib on H2BK120ub, H3K79me2, and H3K36me3 modifications and *HOXA9* gene expression after treatment with bortezomib in MOLM-13 cell line

I chose to investigate the impact of bortezomib on H2BK120ub, H3K79me2, H3K36me3 modifications, and *HOXA9* gene expression in the MOLM-13 cell line. Previous studies have demonstrated that proteasome inhibitors can reduce ubiquitinated histones, particularly uH2B, essential for proper transcription elongation. The loss of uH2B significantly disrupts transcription (Fierz et al., 2011). This underscores the intricate link between H2B ubiquitination and the transcription process, highlighting uH2B's association with active transcription (Davie & Murphy, 1990). Motivated by this understanding, I began exploring the impact of proteasome inhibitors on uH2B and other histone modifications linked to transcription. In 2022, Dr. Davie and I decided to integrate bortezomib, an established FDA-approved treatment for multiple myeloma, into our research. In 2023, a study examined bortezomib's effects on histone modifications, specifically its impact on uH2B and *HOXA9* expression. Although the study revealed that bortezomib affects these modifications, such as H2BK120ub and H3K79me2, it focused on ALL rather than MLL.

Thus, my investigation aims to fill this knowledge gap by providing crucial data specific to MOLM-13, shedding light on how bortezomib influences these epigenetic markers and gene expression patterns in the context of mixed lineage leukemia. Understanding these effects is essential for uncovering unique vulnerabilities and potential therapeutic strategies tailored to KMT2A-MLLT3 leukemias.

In this aim, I utilized acid-extracted histone, immunoblotting, and RT-qPCR techniques to determine the impact of bortezomib on H2BK120ub, H3K79me2, and H3K36me3 modifications and the *HOXA9* transcript level.

1.12.5 Determine the concurrent presence of H3K79me2 and H3K36me3 on the same histone (Cis-histone pattern) in leukemic cells

Analyzing ChIP-seq data using Partek Flow, it became apparent that these two PTMs, H3K79me2 and H3K36me3, might co-occur throughout part of the *HOXA9* gene body. My approach aims to explore whether they are present on the same histone H3. By understanding how these PTMs interact in MOLM-13, this study aims to uncover novel epigenetic mechanisms underlying leukemia pathogenesis.

In this aim, I utilized the histone Coimmunoprecipitation (Co-IP) / immunoblotting techniques to determine the concurrent presence of H3K79me2 and H3K36me3 on the same histone**.**

1.12.6 Determine the levels of histone H3s (H3.1, H3.2 and H3.3) and the H3K79me2 modification level in H3s in leukemia cell lines

Investigating the levels of histone H3s (H3.1, H3.2, and H3.3) and their associated H3K79me2 modification in leukemia cell lines is critical for understanding their roles in chromatin dynamics and gene regulation. Histone H3s, such as H3.1, H3.2, and H3.3, possess distinct incorporation patterns and influence chromatin structure, thereby impacting gene expression in leukemia. The H3K79me2 modification, regulated by DOT1L, is pivotal in transcriptional regulation and has been implicated in leukemogenesis. In this study, I used the acetic acid-urea-Triton X-100 polyacrylamide gel electrophoresis (AUT-PAGE)/ immunoblotting techniques to determine the level of H3s and K79me2 levels in these histones.

Integrating the hypothesis: I hypothesize that increased activity of DOT1L and RNF20/40 leads to enhanced transcriptional elongation of leukemic genes like *HOXA9*. Each aim of my project is designed to test different aspects of this hypothesis, from identifying key histone modifications (H3K79me2 and H2BK120ub) associated with the *HOXA9* gene to understand how manipulating these histone marks (with bortezomib) impacts *HOXA9* gene expression. Collectively, these aims will provide comprehensive insights into how the interplay of DOT1L, RNF20/40, and their associated histone modifications drives leukemia.

Chapter 2

2. Material and methods

2.1 Cell Culture

2.1.1 Cell lines

The human leukemic cell lines MOLM-13 and K562 cell lines were used in this study. MOLM-13 cells were obtained from DSMZ (Leibniz Institute - DSMZ German Collection of Microorganisms and Cell Cultures GmbH). K562 cells were obtained from ATCC (ATCC.ORG). MOLM-13 and K562 cells were used from passage numbers 3 to 5. Detailed information about the cell lines is summarized in **Table 1.**

Table 1: Cell lines used in this study are summarized in this table.

Cell line	Leukemia type	Patient age	Patient gender
K562	Chronic myelogenous leukemia	53-year-old	female
MOLM-13	Acute myeloid leukemia	20-year-old	male

2.1.2 Cell culture conditions

All cells were cultured in suspension within 175 cm^2 tissue culture flasks, using 14 mL of RPMI 1640 medium and 10 mL of cell suspension per flask. The flasks were maintained within a 37°C incubator with 5% (v/v) carbon dioxide (CO_2) and a standard oxygen (O_2) level of 20% (v/v). RPMI 1640 medium, supplemented with L-glutamine (2 mM final concentration) and 25 mM HEPES, was used for subculturing and culturing MOLM-13 and K562 cell lines. The medium was fortified with 10% (v/v) fetal bovine serum (FBS) from Corning®, and 1% Antibiotic-Antimycotic solution, which included 10,000 units/ mL penicillin G, 10,000 µg/ mL streptomycin, and 250 ng/ mL amphotericin B, from Gibco®.

2.1.3 Cell passaging

The confluent cells were sub-cultured after reaching approximately 90% confluency, indicating nearly complete coverage of the culture surface with cells. Typically, the cells were cultivated in a T175 flask with a volume of 25 mL. Once the cell density reached 1 x 10^6 cells/mL, indicative of optimal growth, they were sub-cultured by transferring 10 mL of cells into a new flask. Subsequently, 14 mL of fresh medium was added to promote continued growth and maintain optimal conditions. The T175 flask was then placed back into a 37°C incubator for 3 to 4 days to facilitate further cell proliferation before further analysis or experimentation. Notably, MOLM-13 cells typically require 3 to 4 days to reach a density of 1 x 10^6 cells/mL, while K562 cells typically achieve this density within 2 to 3 days.

2.1.4 Cell counting

The Olympus Model R1 Cell Counter (Cambridge Scientific ID: 26640) was used for cell counting **(Figure 11)**. Trypan blue is a dye used in cell biology to distinguish between viable (live) and non-viable (dead) cells in a population. Viable cells have intact cell membranes that exclude the dye, appearing clear or slightly refractive under a microscope. In contrast, non-viable cells have compromised membranes that allow the dye to penetrate, resulting in a blue stain. To perform the assay, a 10-microliter cell suspension was mixed with an equal volume of Gibco™ Trypan Blue Solution, 0.4% (Catalog No.15250061), and thoroughly combined for 1-2 minutes. Subsequently, this mixture was applied to the Olympus cell counting slide. Cell counting procedures followed the manufacturer's instructions to determine the precise cell concentration. The number of viable or live cells (unstained) and non-viable or dead cells (blue-stained) were recorded. Cell viability was measured as a percentage of viable cells out of the total cell count. Cells were also examined using a Zeiss microscope luminaire with 10x magnification.

.

Figure 11 : The Olympus Model R1 Cell Counter (Cambridge Scientific ID: 26640) and Olympus cell counting slide were shown.

2.1.5 Cell storage and recovery

Cells were grown in culture for the cryopreservation of cells until they reached 90% confluency. Before initiating the cryopreservation procedure, cryovials were labeled with details, including the cell type, passage number, number of cells per vial, initials, and the labeling date. The process of cell counting using the Olympus automated cell counter and Gibco™ Trypan Blue Solution, 0.4% (Catalog No.15250061) (1:1) was thoroughly explained in the preceding section. A 10-microliter cell suspension was mixed with an equal volume of Gibco™ Trypan Blue Solution, 0.4% (Catalog No.15250061), and completely combined for 1-2 minutes. Subsequently, this mixture was applied to the Olympus cell counting slide. Cell counting procedures followed the manufacturer's instructions to determine the precise cell concentration. The number of viable or live cells (unstained) and non-viable or dead cells (blue-stained) were recorded. Cell viability was measured as a percentage of viable cells out of the total cell count. Following labeling the vials, the cells were centrifuged at 200 g using a microcentrifuge for 10 minutes at room temperature. The supernatant was carefully removed without disturbing the cell pellet. Subsequently, the cell pellet was resuspended by flicking the tube in a freezing medium comprising 95% (v/v) appropriate medium and 5% (v/v) dimethyl sulfoxide (DMSO) (Sigma). One milliliter of the cell suspension

(1 x 10^6 cells/mL) was then aliquoted into cryovials (Thermo Fisher Scientific) and promptly transferred into a Styrofoam cooler for transportation and storage in a -80°C freezer. After 24 hours of storage at -80°C, the cells were transferred to a liquid nitrogen tank for long-term preservation.

For cell revival, the appropriate medium was first prewarmed in a 37°C water bath. Then, 9 mL of prewarmed medium was transferred into a 15 mL tube. The vial of cells was then removed from the -80°C freezer or liquid nitrogen and transferred into a cooler full of ice to the cell culture room. The cryovials of frozen cells were fast-thawed in a 37°C water bath and closely observed until the cells were mostly defrosted. The surface of the vial was immediately decontaminated by spraying 70% ethanol. The content of the vial was quickly transferred into the prepared 15 mL centrifuge tube containing 9 mL of the appropriate medium and centrifuged at 150 g for 10 minutes at room temperature. The supernatant (media and DMSO) was aspirated without disturbing the pellet, and the pellet was resuspended in 5 mL of growth medium. The entire amount of the suspension was then transferred to a 25 mL cell culture flask. The cells were allowed to revive in the 25 mL flask through overnight incubation at 37°C. The cells were checked daily until they reached the required confluency for passaging.

2.1.6 Treatment conditions

Bortezomib, a class of drugs known as proteasome inhibitors, was used to treat the cells. Cells at 80-90% confluence were employed in the treatment study. Cell counts were obtained before and after treatment using the Olympus Model R1 automated cell counter. The cells were treated with 5 nM of bortezomib inhibitor for 2 and 4 hours. Subsequently, histone extraction for western blot analysis and RNA extraction for gene expression measurement were performed. Bortezomib was provided in powder form and dissolved in 100% DMSO to create a 10.84 M stock solution. To achieve a final concentration of 5 nM, intermediate stock solutions of 10 mM and 10 µM were made. The calculated volume was taken from the 10 µM stock and added to the cells to reach a 5 nM concentration. DMSO (0.1%) was added to the control cells for the control vehicle. To prepare the 0.1% DMSO solution, a 1% DMSO stock was first prepared, from which the 0.1% DMSO working solution was made and used for the control cells. DMSO was passed through a filter to ensure the removal of any potential particulate contaminants before use.

2.2 Protein-Based Techniques

This study utilized various protein-based methods, including histone extraction, cell lysate preparation, Bradford assay, BSA assay, SDS-PAGE and western blotting, AUT-PAGE and western blotting, and two-dimensional gel electrophoresis.

2.2.1 Histone extraction

A minimum of 50 million MOLM-13 or K562 cells were collected and harvested by centrifugation at 300 g and 4°C using a Thermo Scientific ST16R Refrigerated Centrifuge for 10 minutes to form a pellet. PMSF (phenylmethylsulfonyl fluoride), a serine protease inhibitor, was added directly to the MOLM-13 cells before centrifugation to reduce protease activity, which is particularly high in MOLM-13 cells and can cause clipping of histone H3. The final concentration of PMSF in total cells was 2mM. After centrifugation, the supernatant was discarded, and the pellet was retained. Next, the cell pellet was washed once with 10 mL of ice-cold 1X PBS buffer containing protease and phosphatase inhibitors (137 mM NaCl, 2.7 mM KCl, 10 mM Na_2HPO_4, 1.8 mM KH_2PO_4, 5 mM sodium butyrate, pH adjusted to 7.4) and spun for 10 minutes at 300 g at 4°C in the Thermo Scientific ST16R Refrigerated Centrifuge. After this wash, the supernatant was discarded.

As the first lysis step, the cell pellet was resuspended in 1 mL of 1X PBSB with 0.5% (v/v) Triton X-100 buffer containing protease and phosphatase inhibitors (Catalog number A32961, ThermoFisher). The resuspended cells were homogenized 10 times using a homogenizer with a Teflon or glass pestle. The homogenized sample was then transferred into a 15 mL centrifugation tube. The cell suspension was passed through a syringe with a 22-gauge needle 5 times. Cells were then centrifuged at 10,000 g for 10 minutes at 4°C using an Eppendorf™ 5424 Microcentrifuge, and the supernatant was discarded. As the second lysis step, the pellet containing the nuclei was resuspended in 1 mL of RSB buffer (3 mM MgCl2, 10 mM Tris-base, and 10 mM NaCl) in a 1.5 mL microcentrifuge tube and passed through a syringe with a 22-gauge needle 5 times. Then, 111 µL of 4 N H_2SO_4 was added to the solution (containing the nuclei pellet and RSB buffer) and mixed well to reach a final concentration of 0.4 N H_2SO_4 in 1 mL. Histones and other basic proteins are soluble in H_2SO_4, while DNA and most cellular proteins are not. The sample was then left on ice for 20 minutes. The sample was centrifuged at 16,000 g for 10 minutes using an Eppendorf™ 5424 Microcentrifuge at 4˚C. The supernatant was retained, and 25% (w/v) TCA (trichloroacetic acid) was added to the supernatant. To achieve 25% (w/v) TCA, 370 µL of 100% TCA was added

to the RSB solution containing 0.4 N H_2SO_4. The samples were left on ice for a minimum of 20 minutes or incubated overnight in the refrigerator. The samples were then centrifuged at 16,000 g for 10 minutes using an Eppendorf™ 5424 Microcentrifuge at 4˚C. The pellet containing histones was washed as follows: after each wash, the samples were centrifuged at 16,000 g for 5 minutes using an Eppendorf™ 5424 Microcentrifuge at 4˚C, and the supernatant (acetone) was carefully removed without disturbing the histone-precipitated pellet. The pellet was washed twice in 1 mL acetone and air-dried for 20 minutes at room temperature. The air-dried pellet (histones) was then resuspended in 40 to 50 µL of ddH2O. Histones were quantified using the Bradford assay. Histones are very basic proteins and have a high concentration of lysine and arginine amino acids. The Bradford assay relies on the ability of the Coomassie Brilliant Blue dye to effectively bind to these residues, offering a reliable assessment of their concentration.

2.2.2 Total cellular lysate

About 30 million cells were cultured and collected. PMSF was added directly to the MOLM-13 cells before pelleting down (2 mM final concentration of PMSF). Then, the cells were pelleted down at 300 g using Thermo Scientific ST16R Refrigerated Centrifuge for 10 minutes. The supernatant was carefully discarded, and the pellet was retained. Subsequently, the cell pellet was washed once with 10 mL of ice-cold 1X PBSB buffer containing protease and phosphatase inhibitors (137 mM NaCl, 2.7 mM KCl, 10 mM Na2HPO4, 1.8 mM KH2PO4, 5 mM sodium butyrate, pH adjusted to 7.4). The supernatant was discarded after spinning for 10 minutes at 300g with Thermo Scientific ST16R Refrigerated Centrifuge. The pellet was then resuspended in RIPA buffer (50 mM Tris-HCl, 150 mM NaCl, 2 mM EDTA, 10% Triton X-100, 0.5% sodium deoxycholate, 0.1% SDS) and incubated in a cold room on a rotator for 20 minutes. Subsequently, the sample was centrifuged at 13,000 g for 10 minutes at 4°C using Eppendorf™ 5424 Microcentrifuge, and the supernatant was collected.

2.2.3 Bradford assay

The standards were prepared according to **Table 2** (adapted from the "Coomassie Plus (Bradford) Assay Reagent, Catalog Numbers 23238), based on the desired working range. Instead of albumin, histone calf thymus 2 µg/µL was used for making standards. Standards (calf thymus) and unknown samples were diluted in 1.5 mL microcentrifuge tubes as per**.**

Table 2: Preparation of diluted calf thymus histones standards for test tubes (Normal assay). Working range 100 – 2,000 µg/ mL

Tube (Standards)	Vol of ddH2O (ul)	Vol of calf thymus histone 2 ug/ul (ul)	Conc calf thymus histone (ug/ul) in stock	Final conc calf thymus histone (ug/ul)	Final Vol (ul)
A	0	30	2	2	30
B	7.5	22.5	2	1.5	30
C	15	15	2	1	30
D	22.5	7.5	2	0.5	30
E	18	12	0.5 (Made from 2ug/ul stock)	0.2	30
F	24	6	0.5 (Made from 2ug/ul stock)	0.1	30
G	30	0	0	0	30

Ten µL of each prepared standard was pipetted into different wells of a 96-well plate. Each well was then added with 300 µL of the Coomassie Plus Reagent and thoroughly mixed. For unknown samples, a total volume of 30 µL was achieved by adding 29 µL of water and 1 µL of histones. Subsequently, 10 µL of each unknown sample was pipetted into the wells of the 96-well plate. Three hundred µL of the Coomassie Plus Reagent was added to each well and mixed well. The samples were incubated for 10 minutes at room temperature (RT). A microplate reader, SpectraMAX M3, was used for absorbance measurement. The selected protein quantification method was the 96-well plate, Bradford. The standards, blank, and unknown samples were defined on the plate, and absorbance was measured at 595 nm. The absorbance measurements were recorded, and a standard curve was prepared by plotting the average blank-corrected 595 nm measurement for each protein standard against its concentration in µg/µL. The protein concentration of each unknown sample was determined using the standard curve.

2.2.4 BCA assay

The BCA assay was used to determine the protein concentration in lysate. The standards were prepared based on **Table 3**, which was adapted from the Pierce™ BCA Protein Assay Kit (Catalog Numbers XB338070), according to the desired working range. The Pierce™ BCA Protein Assay Kit comprises three components: BCA Reagent A, BCA Reagent B, and Albumin Standard Ampules (2 µg/µl).

Table 3: BSA standard dilution scheme for the microplate procedure and the test tube procedure using the standard protocol (working range = 25–2,000 µg/mL)

Tube (Standards)	Vol of ddH2O (ul)	Vol of Albumin (ul)	The concentration of Albumin (ug/ul) stock	Final Concentration of Albumin (ug/ul)	Final Vol (ul)
a	0	50	2	2	50
b	12.5	37.5	2	1.5	50
c	25	25	2	1	50
d	37.5	12.5	2	0.5	50
e	45	5	2	0.2	50
f	40	10	0.5 (Made from 2 ug/ul BSA stock)	0.1	50
g	45	5		0.05	50
			0.5 (Made from 2 ug/ul BSA stock)		50
h	47.5	2.5	0.5 (Made from 2 ug/ul BSA stock)	0.025	50

Procedure

Mix BCA reagent A with BCA reagent B at a 50:1 ratio (50:1, Reagent A: B) to create a working reagent. Two hundred µL of each prepared working reagent was pipetted into different wells of a 96-well plate. To each well, 25 µL of sample or standards was added and mixed well. For unknown samples, a total volume of 50 µL was achieved by adding 49 µL of water and 1 µL of the unknown sample. The 96-well plate was then incubated for 30 minutes at 37°C. Absorbance was measured at 562 nm using a microplate reader, SpectraMAX M3. The selected protein quantification method was the 96-well plate BCA method. Standards, blanks, and unknown samples were defined on the plate, and absorbance was measured at 562 nm. Absorbance measurements were recorded, and a standard curve was prepared by plotting the average blank-corrected 562 nm measurement for each protein standard against its concentration in µg/µL. The protein concentration of each unknown sample was determined using the standard curve.

2.3 Electrophoresis techniques

2.3.1 Sodium dodecyl-sulfate polyacrylamide gel electrophoresis (SDS-PAGE)

Sodium dodecyl sulfate-polyacrylamide gel electrophoresis (SDS-PAGE) is a widely employed technique for the separation of protein mixtures based on their molecular weights. This method starts by denaturing the proteins, which means it unfolds and disrupts their native structures. This denaturation step ensures that the proteins are uniformly charged and coated with SDS molecules, allowing them to migrate primarily based on their size when subjected to an electric field during electrophoresis (Laemmli, 1970).

2.3.2 SDS-PAGE and Western Blotting

Acid-extracted histones and total cellular lysate were denatured with 2X SDS loading buffer, consisting of 0.0625 M Tris-HCl (pH 6.8), 5% glycerol, 2% SDS, 0.1% bromophenol blue, and 2.5% β-mercaptoethanol (Laemmli, 1970). After adding the SDS loading buffer, samples were heated to 95°C for 5 minutes and then loaded onto polyacrylamide gels with varying percentages (10%, 12%, or 15%) based on the molecular weight of target proteins. The gel was run at 200V for 1 hour using a running buffer containing 25 mM Tris, 192 mM glycine, and 0.1% SDS. Following electrophoresis, proteins were transferred from the gel to either a 0.45 µm nitrocellulose (NC) or PVDF membrane using the Trans-Blot Turbo Transfer System (Bio-Rad). NC and PVDF

membranes can be used for different reasons. NC is mostly used for histones due to its high protein binding capacity, low background noise, and strong retention of small (<25 kDa) and basic proteins. PVDF is used for higher molecular weight proteins (>25 kDa) and has a higher binding capacity for hydrophobic and dipole proteins. It is also resistant to harsh chemicals. PVDF membranes need activation in methanol before use, which involves soaking the membrane in methanol for about 1 minute, making the hydrophobic PVDF membrane more hydrophilic, improving protein binding, and ensuring efficient transfer. After transferring the gel onto the NC or PVDF membrane, the membrane was stained with 0.5% Ponceau S and 5% acetic acid for 5 minutes. The membrane was then destined in 1X TBST buffer and blocked with 5% skim milk powder in 1X TBST for 1 hour at room temperature on a rocking platform. After blocking, the membrane was incubated overnight at 4°C with a primary antibody, appropriately diluted in 3% skim milk in 1X TBST, as per the manufacturer's instructions. The membrane was washed three times with 1X TBST for 10 minutes each at room temperature. Subsequently, the membrane was incubated for 1 hour at room temperature with the corresponding horseradish peroxidase-conjugated anti-IgG secondary antibody diluted in 3% skim milk. Following secondary antibody incubation, the membrane was washed three times for 15 minutes with 1X TBST at room temperature. Finally, the target protein bands on the membrane were visualized using Thermo Scientific™ Pierce™ ECL Western Blotting Substrate (Catalog No. PI32106). In the AZURE400 machine, the "chemiblot" option was selected, followed by the chemiluminescence with ECL option. The membrane was placed on the black tray and on the upper shelf. In the AZURE400 machine, the "chemiblot" option was selected, followed by the chemiluminescence with ECL option. Images were taken with different exposure times, and the TIF files were saved.

2.3.3 Acetic acid-urea-Triton-X100 polyacrylamide gel (AUT) electrophoresis

AUT gels can separate basic histones and their subtypes based on charge, mass, and hydrophobicity (Waterborg, 2002). Fifteen % polyacrylamide AUT (acetic acid/ 6 M urea/ /0.375 % Triton X-100) minilab gel was prepared using the following recipe, which is summarized in **Table 4 and Table 5.**

Table 4: Recipe for 1mm plate (separating gel)

Materials	Gel (1 mm)	stock
Urea	3.2 g	64 g
Acrylamide/bis(30:0:8)	4 ml	80 ml
4% Temed/43.1 Acetic acid	1 ml	20 ml
0.004 % Riboflavin	0.8 ml	16 ml
0.2 M Triton X-100	160 µl	3 ml
Thiodiglycol	80 µl	1.6 ml
	8 mL (per gel)	160 mL (total stock)

Table 5: Recipe for 1mm plate (stacking gel)

Materials	Gel (1 mm)	stock
Urea	0.8 gr	32 gr
Acrylamide/bis(30:0:8)	0.5 ml	20 ml
0.004 % Riboflavin	0.25 ml	10 ml
0.2 M Triton X-100	0.2 ml	8 ml
Thiodiglycol	40 µl	1.6 ml
3M KAc (pH 4)	20 µl	0.8 ml
	2 mL **(per gel)**	**80** mL **(total stock)**

Procedure

First, the gel was poured with separating buffer and placed in front of a light box for approximately 2 to 3 hours. Next, isopropanol was added to the gel to prevent drying. Riboflavin is the catalyst for polymerization. After polymerization of the separating gel, isopropanol was removed, and the stacking gel was poured on top of the separating gel. The stacking gel was allowed to polymerize for about 1 to 2 hours in front of the lightbox. Then, the acid-extracted histones were mixed with 2X AUT-sample buffer (0.75 M KAc pH 4.0, 30% (w/v) sucrose, 0.1% (w/v) pyronin Y) and loaded onto an AUT gel. A running buffer of 0.9 N acetic acid was used, and the gel was electrophoresed at 200V for 2 hours at room temperature (can be done in a cold room at 4°C). It is crucial to correctly attach the electrical leads between the power supply and the electrophoresis system during the electrophoresis process to ensure proper separation of proteins. Specifically, you should connect the positive (+) lead to the upper reservoir and the negative (-) lead to the lower reservoir. This configuration is opposite to the standard setup used in SDS-PAGE electrophoresis, where the positive lead is usually attached to the lower reservoir and the negative lead to the upper reservoir.

Then, the gel was stained with a solution containing 0.25% Coomassie Blue G-250, prepared with a mixture of 45% methanol and 9% acetic acid. The gel was initially in a strong destaining buffer comprising 10% acetic acid, 30% methanol, and 60% distilled water (ddH2O) for at least 4 hours on a shaker. This was followed by a weak destaining solution consisting of 10% methanol, 5% acetic acid, and 85% distilled water (ddH2O). (Delcuve & Davie, 1992). Finally, the destained gel was imaged with AZURE400. In the AZURE400 machine, the 'Protein Gels with Dyes' option was selected, and the gel was placed on top of the Orange Tray or Trans White Table. The 'Auto Image' option was then used, and the TIF file was saved.

2.3.4 Acetic acid-urea-Triton-X100 polyacrylamide gel (AUT) electrophoresis western blotting

The acid-extracted histones were mixed with 2X AUT-sample buffer (0.75 M KAc pH 4.0, 30% (w/v) sucrose, 0.1% (w/v) pyronin Y) and loaded onto an AUT gel. A running buffer of 0.9 N acetic acid was used, and the gel was electrophoresed at 200V for 2 hours at room temperature (it can be done in a cold room at 4°C). It can also be run in a cold room at 4°C as an alternative (Delcuve & Davie, 1992).

AUT western blotting is quite similar to SDS-PAGE immunoblotting. However, to achieve a satisfactory transfer of basic proteins from AUT gels to nitrocellulose, polyacrylamide gels need to be equilibrated in two steps. First, the gel was submerged in glacial acetic acid (50 mM) and 0.5% SDS (equilibration buffer 1; 2 x 30 minutes) to displace Triton X-100 and to allow histone to bind SDS, followed by a 2 x 30-minute incubation in a Tris-SDS buffer (equilibration buffer 2; 1 M Tris-HCl at 62.5 mM pH 6.8, 2.3% SDS, 5% β-mercaptoethanol). After equilibration, the gel was transferred to a nitrocellulose (NC) membrane using the Trans-Blot Turbo Transfer System (Bio-Rad). The membrane was stained with 0.5% Ponceau S and 5% acetic acid for 5 minutes. The membrane was then destined in 1X TBST buffer and blocked with 5% skim milk powder in 1X TBST for 1 hour at room temperature on a rocking platform. After blocking, the membrane was incubated overnight at 4°C with a primary antibody, appropriately diluted in 3% skim milk in 1X TBST. The following day, the membrane was washed three times with 1X TBST for 10 minutes at room temperature. Subsequently, the membrane was incubated for 1 hour at room temperature with the corresponding horseradish peroxidase-conjugated secondary antibody, diluted in 3% skim milk in 1X TBST milk. Following secondary antibody incubation, the membrane was washed three times for 15 minutes with 1X TBST at room temperature. Finally, the target protein bands on the membrane were visualized using Thermo Scientific™ Pierce™ ECL Western Blotting Substrate (Catalog No. PI32106). In the AZURE400 machine, the "chemiblot" option was selected, followed by the chemiluminescence with ECL option. The membrane was placed on the black tray and on the upper shelf. Images were taken with different exposure times, and the TIF files were saved.

2.3.5 Two-dimensional gel electrophoresis

The two-dimensional gel system consists of acetic acid-urea-triton polyacrylamide gel (AUT-PAGE) analysis in the first dimension and standard sodium dodecyl sulfate polyacrylamide gel (SDS-PAGE) in the second dimension. This method allows for high-resolution separation of modified histone species and histone variants in relatively short periods.

First, a (1mm width) 15% AUT-PAGE gel was prepared (please refer to the AUT-PAGE section for detailed preparation notes). The acid-extracted histones were mixed with 2X AUT-sample buffer (00.75 M KAc pH 4.0, 30% (w/v) sucrose, 0.1% (w/v) pyronin Y) and then loaded onto the 15% acetic acid-urea minilab gel, and electrophoresis was conducted at 200 V for 2 hours in room temperature (can be done in a cold room at 4°C). The gel was then stained with 0.25% (w/v)

Coomassie Blue G-250 in 45% (v/v) methanol and 9% (v/v) acetic acid and destained by diffusion in the strong destained buffer (please refer to the AUT-PAGE section for details).

Next, the track of interest was cut from the gel and equilibrated for 20 to 30 minutes in buffer 0 (10% glycerol, 5% β-mercaptoethanol, 2.3% sodium dodecyl sulfate, and 62.5 mM Tris-HCl, pH 6.8). A 1.5 mm width 15% polyacrylamide-SDS gel was then cast without a comb (standard SDS gel with separating and stacking parts; please refer to the SDS-PAGE section for details). The track of interest from the AUT-PAGE gel was applied horizontally to the top of the second-dimension polyacrylamide-SDS stacking gel and gently pushed down. It was then sealed with melted 1% agarose in buffer 0 and allowed to solidify. Electrophoresis was performed for 2 hours at 200 V room temperature (could also be run in cold room 4c). The gel was stained and destained as previously described (with Coomassie Blue and destaining using strong and then weak buffers). Finally, the destained gel was imaged with AZURE400. In the AZURE400 machine, the 'Protein Gels with Dyes' option was selected, and the gel was placed on top of the Orange Tray or Trans White Table. The 'Auto Image' option was then used, and the TIF file was saved. Please keep in mind that the width of the SDS gel should be greater than that of the AUT gel so that it can be inserted into the plate easily. Cast the AUT gel at 1 mm and the SDS-PAGE gel at 1.5 mm. The instructions for making the 2D gel are summarized in **Figure 12.**

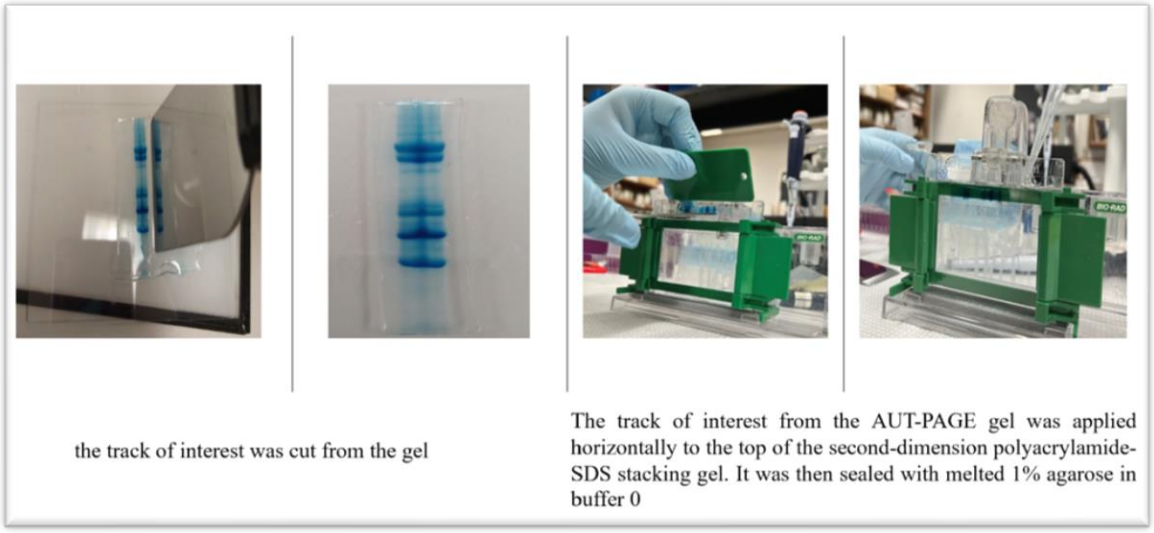

Figure 12: The instructions for making the 2D gel are shown in Figure.

2.3.6 Agarose gel electrophoresis

One percent (1%) agarose gel was used to separate the DNA according to bp size PCR product analyses. For 1% agarose gel, 0.5 g of agarose (Invitrogen) was dissolved in 50 mL of 1X TAE buffer (40 mM Tris base, 20 mM Acetic Acid, and 1 mM EDTA pH 8.0). Once mixed, it was heated in the microwave for 2 minutes until agarose completely dissolved in 1X TAE. Then let it cool down for seconds and then 5 μL of SYBR Safe DNA gel stain (Invitrogen) was added to the mixture and let it solidify. One volume of loading Dye was mixed with 5 volumes of DNA sample and loaded into the 1% agarose gel. The gel was run for 1 hour at voltage 120, and a 1X TAE buffer was used as a running buffer for the electrophoresis of the agarose gel. The gel was visualized using the AZURE400 imaging machine. In the AZURE400 machine, the Nucleic acid gels with Dyes option was selected, and the gel was placed directly on the bottom of the machine (no tray is needed). The 'Auto Image' option was then used, and the TIF file was saved.

2.4 Immunoblotting antibody list

Acid-extracted histones from MOLM-13 and K562 cell lines were resolved using 15% SDS-PAGE and 15% AUT gels to PTMs and histone H3.3 variants. An 8% SDS-PAGE gel was also used to determine DOT1L protein levels in MOLM-13 and K562 cell lines. Immunoblotting analyses were performed with specific antibodies to detect histone PTMs, histone variants, and proteins summarized in Table 6.

Table 6: list of antibodies that were used in this study

Antibody	Company	Catalog No
H3K79me2	Active motif	91399
H3.3	Millipore	09-838
H3K36me3	Thermofisher	MA5-42755
Ubiquitinated Histone H2B (Lys123)	Millipore	MABE1785
β-Actin antibody	Millipore	A5316
Dot1L	Abcam	ab239358
Histone H3	Sigma-Aldrich	07-690

2.4.1 Dot blot

First, the nitrocellulose membrane was labeled accordingly. Various concentrations (from 1 µg/mL to 10 µg/mL) of protein were applied to the membrane and allowed to air-dry at room temperature for several minutes. The membrane was then baked between Whatman filter papers for 30 minutes at 65°C in an oven. Next, the membrane was blocked with 1X TBST buffer containing 5% skim milk for 30 minutes. Three washes with 1X TBST followed this, each lasting 5 minutes. The membrane was then incubated overnight in a cold room with the primary antibody in a 1X TBST solution containing 3% skim milk. The primary antibodies targeted both H3.1K79me2 and H3.3K79me2 to distinguish between the two and determine if the K79me2 modification occurs at the same levels in both histone variants. The following day, the membrane was washed again in 1X TBST and then incubated for one hour with the secondary antibody in a 1X TBST solution containing 3% skim milk. The incubation with the secondary antibody was performed in a plastic bag to ensure even distribution, and the membrane was wrapped accordingly to avoid drying out. After the incubation, the membrane was washed with 1X TBST. Finally, the membrane was visualized using Thermo Scientific™ Pierce™ ECL Western Blotting Substrate (Catalog No. PI32106) for 10 minutes with AZURE 400. For imaging, from the available protocols on the machine, the chemiblot option was selected, followed by the chemiluminescence with ECL option. Peptides were aliquoted to a stock concentration of 1 µL/mL. From 1 µL/mL stock, 5 µL, 2 µL, and 1 µL aliquots were taken and added to the blot to determine their respective concentrations.

2.5 RNA-Based Techniques

2.5.1 Total RNA extraction and cDNA synthesis

Before initiating RNA extraction, the entire workspace was thoroughly cleaned using RNaseZap to ensure an RNase-free environment and prevent RNA degradation due to RNase contamination. Approximately 10 million cells from each cell line were grown at 90% confluence and then harvested by centrifugation at 300 g at 4°C for 10 minutes using a Thermo Scientific ST16R Refrigerated Centrifuge. The media were discarded, and the cells were washed with 10 mL of ice-cold 1X PBS, followed by centrifugation at 300 g at 4°C for another 10 minutes using a Thermo Scientific ST16R Refrigerated Centrifuge. Total RNA extraction was performed using the RNeasy Plus Mini Kit (Cat#74134, Qiagen, Germany) following the manufacturer's instructions. After

washing the cells with 1X PBS, the pellet was lysed with RLT buffer containing β-mercaptoethanol (10 µL per 1 mL of RLT buffer) to denature proteins and prevent RNA degradation. Then, the lysate was then processed through a QIAshredder column by centrifugation at maximum speed (13,500 rpm) for 2 minutes using an Eppendorf™ 5424 Microcentrifuge. Next, the supernatant was collected and mixed with 70% ethanol and passed through an RNeasy mini-column, repeating the process if necessary to ensure complete sample passage. RNeasy mini-column is used to elute the purified RNA from the silica membrane. Then, the column was washed twice with the provided washing buffer, and RNA was eluted with RNase-free water and stored at -80°C. RNA concentration and purity were assessed using the A260/A280 and A260/A230 ratios with a Nanodrop 2000 (Thermo Fisher Scientific). Following RNA isolation and purification, DNase I treatment was performed using the RQ1 kit (Thermo Fisher Scientific) to remove any genomic DNA, by incubating the RNA sample with DNase and reaction buffer at 37°C for 30 minutes, followed by the addition of DNase stop solution and incubation at 65°C for 10 minutes. Subsequently, cDNA synthesis was conducted using the iScript Reverse Transcription Supermix for RT-qPCR (Bio-Rad, USA) according to the manufacturer's instructions, with the PCR protocol set at 25°C for 5 minutes, 46°C for 20 minutes, and 95°C for 1 minute, followed by a cool-down step at 4°C.

2.5.2 Primer design and primer sequencing

The gene transcripts were obtained from Ensembl (https://www.ensembl.org/), and the transcript variant that best suited the experimental needs was selected. Once identified, the transcript sequence was retrieved. The primer design, involving the use of the transcript sequence to design primers for RT-qPCR, is detailed in **Table 7**. The key factors in primer design include GC content, melting temperature (Tm), primer length, and avoiding secondary structures such as hairpins or dimers. Specific forward and reverse primers targeting the gene of interest were designed using IDT PrimerQuest. Subsequently, primer specificity was ensured using tools like Primer-BLAST (https://www.ncbi.nlm.nih.gov/tools/primer-blast/). Following primer design, a gradient real-time PCR was performed to confirm the absence of primer dimers for each primer, with annealing temperatures selected based on melt curve peak and Cq values. Finally, PCR products were run on a 1% agarose gel to verify the absence of primer dimers. To validate the amplicon sequence after RT-qPCR, the PCR product was first purified using a PCR purification kit to remove contaminants.

The purified DNA was then quantified and submitted for sequencing. After sequencing, the obtained sequence data confirmed the accuracy of the amplification and the fidelity of the RT-qPCR process.

2.5.3 Quantitative PCR (qPCR)

For each PCR sample, a mixture was prepared by combining 10 microliters of SYBR Green master mix (Fisher Scientific), 1 microliter each of forward and reverse primers, 7 microliters of nuclease-free water, and 1 microliter of previously synthesized cDNA, resulting in a total reaction volume of 20 microliters. The mixture was then thoroughly mixed. Following preparation, 96-well plates were utilized, and the QuantStudio™ thermocycler from Thermo Fisher Scientific was employed for amplification. The PCR conditions were set as follows. Initially, the reaction mixture was subjected to an initial denaturation step at 95°C for 2 minutes, followed by denaturation at 95°C for 30 seconds, annealing at 60°C for 30 seconds for 40 cycles, and extension at 72°C for 1 minute. Subsequently, a melt curve analysis was performed by heating the samples to 95°C for 15 seconds, followed by annealing at 50°C for 1 minute and final denaturation at 95°C for 15 seconds. These temperature cycles allowed for the amplification of specific DNA fragments and subsequent analysis of the PCR products. The time and temperature profiles are shown in **Figure 13.** Quantitative or real-time polymerase chain reaction (qRT-PCR) was conducted in triplicate. The cycle threshold (Ct) values obtained were normalized to the corresponding GAPDH or B-actin expression using the ΔCt method, wherein higher ΔCt values indicated lower amounts of the transcript. In certain experiments, the levels of targets were determined using the ΔΔCt method, where ΔCt values for each cell line were normalized to an appropriate control. Fold changes were calculated using the 2^ΔΔCt formula.

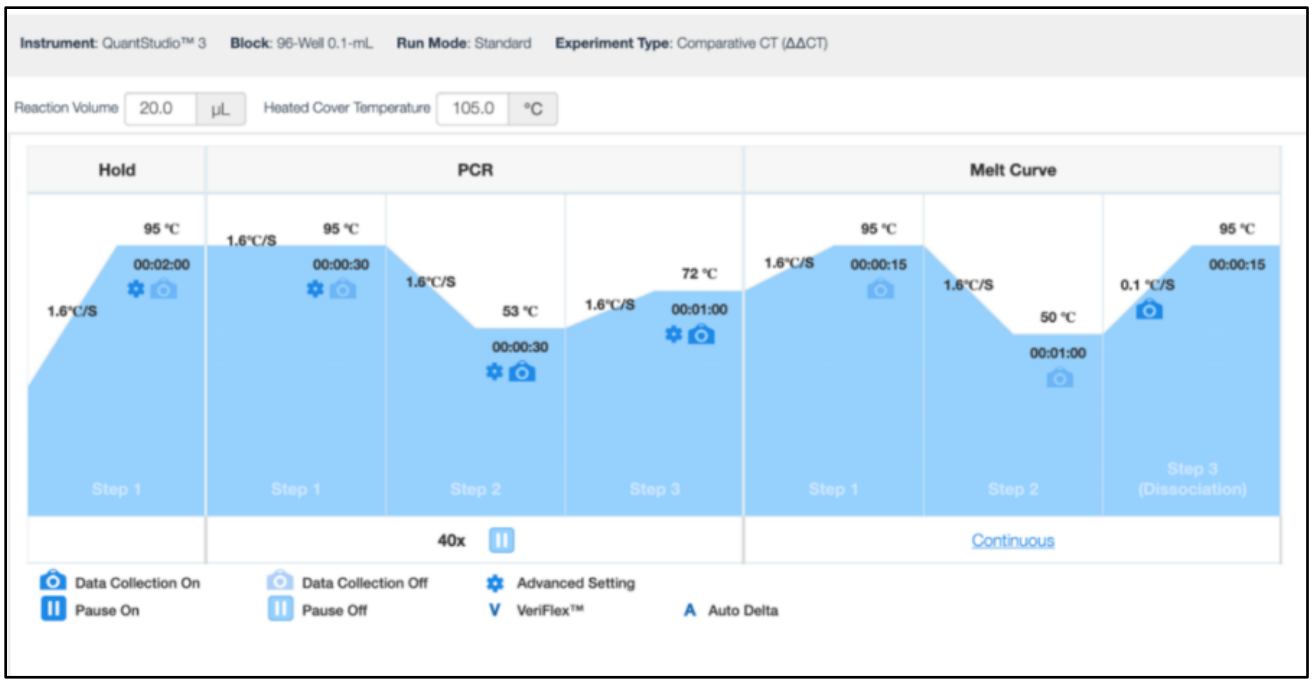

Figure 13: The time and temperature profile needed for quantitative or real-time polymerase chain reaction (qRT-PCR)

Table 7: List of primers used for RT-qPCR analysis (5’ to 3’)

primer	Sequences
DOT1L	F:GGAGAAGCTGTTGAAGGAGAAG R:GCTCTTCTCTAGCTCCACAATG
HOXA9	F:CCCATCGATCCCAATAACCCA R:AGTTCCAGGGTCTGGTGTTT
GAPDH	F:CAACAGCGACACCCACTCCT R:CACCCTGTTGCTGTAGCCAAA
B-actin	F: TGGAACGGTGAAGGTGACAG R:AACAACGCATCTCATATTTGGAA

2.6 Histone Co-Immunoprecipitation (Co-IP)

Cells were cultured, and approximately 50 million cells were used for the experiment. PMSF was added directly to the MOLM-13 cells before pelleting down (2 mM final concentration of PMSF). The cells were then pelleted and washed in PBS 1X before being centrifuged at 300 g at 4°C for 10 minutes using a Thermo Scientific ST16R Refrigerated Centrifuge. Following this, the cells were resuspended in cell lysis buffer containing (5mM HEPES pH 8.0, 85 mM KCl, 0.5% (w/v) NP-40 supplemented with protease and phosphatase inhibitor cocktails (PhosSTOP and cOmplete, Mini, EDTA-free; Roche Diagnostics). The suspension was incubated with shaking at 4°C for 10 minutes and then centrifuged at 2000 g for 10 minutes using an Eppendorf™ 5424 Microcentrifuge. The resulting nuclear pellet was resuspended in 1–2 mL of micrococcal nuclease (MNase) digestion buffer (10 mM Tris-HCl, pH 7.5, 0.25 M sucrose, 75 mM NaCl), also supplemented with the phosphatase/protease inhibitor cocktails, and the absorbance at 260 nm (A260) was measured. To fragment the chromatin, 2.5 units of MNase per A260 of nuclear suspension was added in the presence of 3 mM CaCl2 and incubated at 37°C for 25 minutes. The MNase buffer was prepared using a stock solution with a concentration of 22.5 units per microliter. The amount of MNase buffer added to the lysed cells was determined based on the A260 absorbance measurement of the lysed cell sample. Then, the reaction was stopped by the addition of EDTA at pH 8.0, to a final concentration of 5 mM. Subsequently, the nuclei were lysed by the addition of SDS to a final concentration of 0.5% and rotation at room temperature for 60 minutes, leading to the dissociation of histones from DNA. Insoluble material was removed by centrifugation at 2000 g for 10 minutes using Thermo Scientific ST16R Refrigerated Centrifuge, and the soluble material was diluted to 0.1% SDS with RIPA buffer (10 mM Tris-HCl, pH 8.0, 1% Triton-X-100, 0.1% SDS, 0.1% sodium deoxycholate), supplemented with phosphatase/protease inhibitors. This will serve as the INPUT.

Then, 2 mL of the input was precleared with a 50% slurry of protein A/G Plus agarose (HiTrap® NHS-activated)**.** After centrifugation at 2000 × g for 10 minutes, the beads were removed, and the A260 was measured. Subsequently, 1 µg of antibody per A260 of precleared extract was added and incubated overnight at 4°C. Anti-H3K36me3 (Recombinant Rabbit Monoclonal Antibody (RM155), ChIP-Verified) and isotype-specific nonrelated IgG as negative control (EMD Millipore) were used. After overnight incubation, 60 µl of hydrated Dyna beads Protein A/G per mL of Input sample (diluted in RIPA buffer) was added to the extract. (Firstly,

the beads were washed with RIPA buffer and resuspended again in RIPA to be added to the incubated input sample with the target Ab). Then, the input sample with the target Ab and hydrated Dyna beads Protein A/G was incubated at 4˚C for 3 hours with rotation in the cold room. After incubation, the target protein bound to Dyna beads was separated using a magnetic stand, which allowed the beads with bound proteins to adhere to the magnet, leaving the unbound proteins in the supernatant. The supernatant, containing proteins that were not bound to the Dyna beads, was carefully transferred to a new tube. This process is crucial for immunodepletion (ID), where specific proteins of interest are selectively removed from the sample. The immunodepleted sample (ID) refers to the supernatant that remains after this process, enriched with proteins that were not bound to the Dyna beads and devoid of the targeted proteins originally bound to the beads. This will be the IMMUNODEPLETED or (ID). The remaining beads were washed with RIPA buffer. This will serve as the IMMUNOPRECIPITATED (IP). The INPUT, ID, and IP were resuspended in the 2X sample buffer and were loaded on SDS-PAGE and Immunoblotting experiments (refer to SDS-PAGE and Western Blot methodology) for IP efficiency and western blotting (Khan et al., 2017).

2.7 Staining methods

2.7.1 Ponceau staining

The proteins transferred to the nitrocellulose or PVDF membrane were stained with Ponceau S stain, which contained 0.5% (w/v) Ponceau S dissolved in 1% (v/v) acetic acid for 1 minute on a rocker. Then the membrane was washed with 1X TBST for 5 minutes.

2.7.2 Coomassie blue staining

The SDS or AUT gel can be stained with 0.1% (w/v) Coomassie Blue G250 in 40% methanol and 10% acetic acid to determine the quality of extracted proteins or histones, or for quantification.

2. 8 Bioinformatic analysis

2.8.1 ChIP Sequence analyses

To map genes associated with the broadest active histone mark of H3K79me2, as well as DOT1L and DNase I, available ChIP-seq data were analyzed by Dr. Davie.

Data Collection: Analyses were conducted using publicly available ChIP-Seq data from the Gene Expression Omnibus (GEO) database. The GEO files for the H3K79me2 ChIP-Seq files for the following cell lines were as follows: MOLM-13 (GSE149183, GSE43063, GSE113191), MOLM-14 (GSE76745), K562 (GSE29611), Loucy (GSE96166), DND-41 (GSE29611), MV4-11 (GSE79899), and THP-1 (GSE79899). The GEO files for the DNase I-Seq files for MOLM-13 were from GSE149183. DOT1L ChIP-Seq files for MOLM-13 were from GSE149183. RNA-Seq files for the leukemic cell lines were from the following sources: K562, GSE90239, GSE78556, GSE140322; Loucy, GSE155337; DND-41, GSE173867, GSE116873; MOLM-13, GSE113191, GSE181003.

ChIP Sequence analyses (MACS2): FASTQ files were obtained from the European Nucleotide Archive and downloaded to the Partek Flow analytical program (Partek Incorporated, 100 Chesterfield Business Parkway, Chesterfield, Missouri 63005). The Bowtie 2 aligner was used, with sequences being aligned against the human hg38 assembly. Identification of broad H3K79me2 peaks was carried out using the MACS2 broad-peak function. The peaks were annotated using Ensembl transcript release 91.

Broad H3K79me2 Domain: The top 5% of the broadest domains were extracted from the H3K79me2 peaks identified by the MACS2 peak caller. We used the online tool VENNY 2.1 to classify genes per cell type and to identify the genes that were unique to each cell line. The VENNY 2.1 tool was then applied to identify the unique genes with the broadest H3K79me2 domains. We extracted these exclusive genes and performed gene ontology (GO) (biological process) with Enrichr.

2.8.2 RNA Sequence Analyses

RNA-Seq files for the leukemic cell lines were from the following sources: K562, GSE90239, GSE78556, GSE140322; MOLM-13, GSE113191, GSE181003. FASTQ files for the cell lines were obtained from the European Nucleotide Archive and downloaded to the Partek Flow analytical program (Partek Incorporated, 100 Chesterfield Business Parkway, Chesterfield, Missouri 63005). The HISAT 2.1.0 aligner was used, with sequences being aligned against the human hg38 assembly. Quantification was completed using the Partek Flow “quantify to annotation model (Partek E/M)” and the Ensembl transcript release 104. Normalization was carried out using the TPM method.

Chapter 3

3. Results

3.1 Cell lines selection

In this project, two leukemic cell lines were used: MOLM-13, which represents the mixed lineage leukemia (MLL) and contains the KMT2A-MLLT3 fusion protein, and K562, a chronic myeloid leukemia cell line. The MOLM-13 cell line was chosen because it exemplifies mixed lineage leukemia (MLL) with the presence of the KMT2A-MLLT3 fusion protein, which leads to the expression of the *HOXA9* gene. *HOXA9* expression is a key factor in leukemogenesis and is associated with poor prognosis in patients with KMT2A-MLLT3 fusion protein. Using MOLM-13 cells, we can specifically investigate how KMT2A-MLLT3 fusion protein contributes to leukemia development and progression. On the other hand, the K562 cell line was selected as it represents chronic myeloid leukemia (CML) and does not contain the KMT2A-MLLT3 fusion protein nor express *HOXA9*. This cell line was used as a reference, allowing us to explore the differences in cellular and molecular pathways between leukemias with and without the KMT2A-MLLT3 fusion protein.

3.2 Selection and validation of antibodies for H3K79me2 detection

In this study, the main antibody that I used to detect H3K79me2 was the AbFlex® Histone H3K79me2 antibody from Active Motif, which passed my quality control tests (QC) successfully. I have tried at least two other H3K79me2 antibodies that failed QC. I have listed the antibodies that underwent QC in **Table 8** and mentioned the results of the test.

Table 8: List of the antibodies that underwent QC in this study

Name of antibody/company	Catalog No	Fail/Pass
H3K79me2 Invitrogen	PA5-117746	Fail / Detected histone H4 and H3
H3K79me2 Active Motif	39143	Fail/ Detected histone H4
H3K79me2- AbFlex®-Active Motif	91399	Pass/ Detected histone H3

3.2.1 AbFlex® Histone H3K79me2 antibody QC

3.2.1.1 Western blot analysis

Histone H3K79me2 antibody from Active Motif with catalog number 91399 did pass the QC. The first step in testing the antibody was immunoblotting with acid-extracted histones resolved by SDS-PAGE to ensure that the antibody specifically detected histone H3. The H3K79me2 antibody from Active Motif with catalog number 91399 successfully detected the H3 band at 15 kDa.

3.2.1.2 Dot blot analysis with specific peptide

Specific peptides corresponding to the histone variants H3.3 and canonical H3.1 were designed to evaluate the unbiased detection of K79me2 in H3.1 and H3.3.

Rationale: Histone H3.3 and H3.1, despite their high sequence similarity, exhibit several structural differences that may impact antibody recognition and binding specificity. Notably, H3.3 differs from H3.1 at multiple amino acid positions, including positions 31, 87, 89, 90, and 96 (see **Figure 10** in the Introduction). The sequence differences in H3.1 and H3.3 can potentially change the accessibility of epitopes recognized by antibodies specific to modifications such as H3K79me2. Testing the antibody against peptides derived from both H3.1 and H3.3 helps evaluate whether the antibody recognizes the K79me2 equally well on both H3.1 and H3.3 or if there are differences in binding affinity. This approach provides valuable insights into the antibody's specificity and suitability for experimental applications involving different histone variants.

Despite contacting the manufacturer, we did not have access to the epitope information for the H3K79me2 antibody. Therefore, we designed peptides encompassing amino acids 78 to 92 for both H3.1 and H3.3, which include residue 79, the target of the antibody, and cover the most significant structural differences between H3.1 and H3.3. We designed peptides for unmodified H3, H3K79me1 (mono-methylated H3K79), H3K79me2 (di-methylated H3K79), and H3K79me3 (tri-methylated H3K79) for both H3.1 and H3.3 for this purpose. The results indicated a preference for antibody binding to the H3.1K79me2 over H3.3K79me2. Moreover, the antibody specifically recognized the dimethylation of K79 in both H3.1 and H3.3 and did not recognize the unmodified, monomethyl, and trimethyl forms, demonstrating its high specificity (**Figure 14)**.

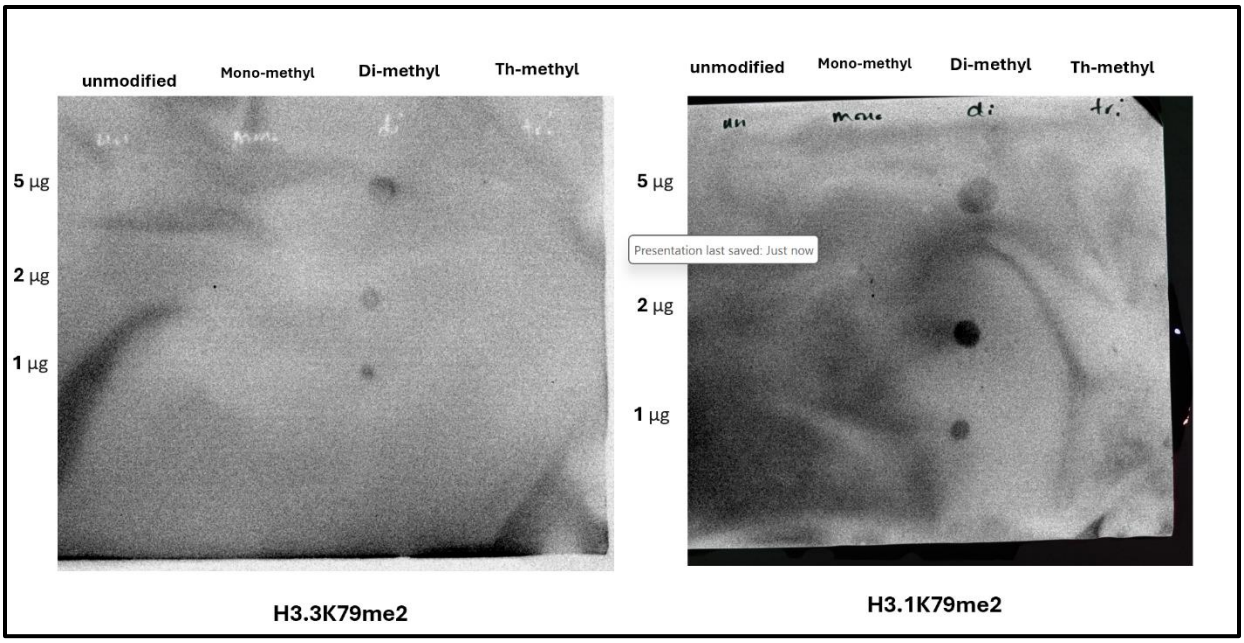

Figure 14: The dot blot results using unmodified, H3K79me1, H3K79me2, and H3K79me3 peptides for H3.1 and H3.3, along with immunoblotting using the H3K79me2 antibody. This was done to assess the antibody's specificity and determine its equal recognition of H3K79me2 modifications on both H3.1 and H3.3.

3.3 Confirmation of histone transfer and quantity consistency using Ponceau S staining

Ponceau S staining was employed to confirm histone transfer onto blots and ensured uniform histone quantities across samples. This method reliably validated the transferring of histones onto the blot and ensured consistent loading of histones in each sample.

3.4 Determine whether the *HOXA9* gene, which is important in leukemogenesis, is marked with H3K79me2 in leukemic cell lines

This aim explores the critical association of H3K79me2 and DOT1L within the *HOXA9* gene, crucial in leukemogenesis, particularly in leukemias containing the KMT2A-MLLT3 fusion protein. We performed bioinformatic analyses of the H3K79me2 domains in MOLM-13 cell lines harboring the KMT2A-MLLT3 fusion protein to elucidate this relationship.

3.4.1 *In silico* analyses of RNA sequencing (RNA-Seq) data

Rationale: The rationale for this experiment is to explain the transcriptional landscape of *HOXA9* in leukemic cell lines with distinct genetic backgrounds. By comparing the expression of *HOXA9* in MOLM-13 (with the KMT2A-MLLT3 protein) and K562 (without the KMT2A-MLLT3 protein), we aim to determine the impact of the KMT2A-MLLT3 fusion on *HOXA* cluster expression, especially *HOXA9*. Given that *HOXA9* plays a critical role in leukemogenesis, understanding its expression profile in different leukemic contexts will provide insights into its regulatory mechanisms and its contribution to the pathogenesis of leukemias harbor KMT2A-MLLT3 fusion protein. This analysis helps to pinpoint *HOXA9* as a potential therapeutic target and biomarker for specific leukemia subtypes, like mixed lineage leukemia.

Dr. Davie conducted data analyses on publicly available RNA sequencing (RNA-Seq) data from MOLM-13 and K562 cells using Partek Flow. Further analyses of the Excel spreadsheets on transcript levels in the cells were conducted by me. The results showed that *HOXA9* is expressed in MOLM-13, which has the KMT2A-MLLT3 fusion protein, but not in K562. The results also revealed that *HOXA9, HOXA10,* and *HOXA11* had the highest transcript level in the *HOXA* cluster in MOLM-13 cells (**Figure 15)**. RNA-Seq data for the leukemic cell lines were obtained from the Gene Expression Omnibus (GEO) database. The GEO accession numbers for each cell line are as follows: K562 (GSE90239, GSE78556, GSE140322), and MOLM-13 (GSE113191, GSE181003).

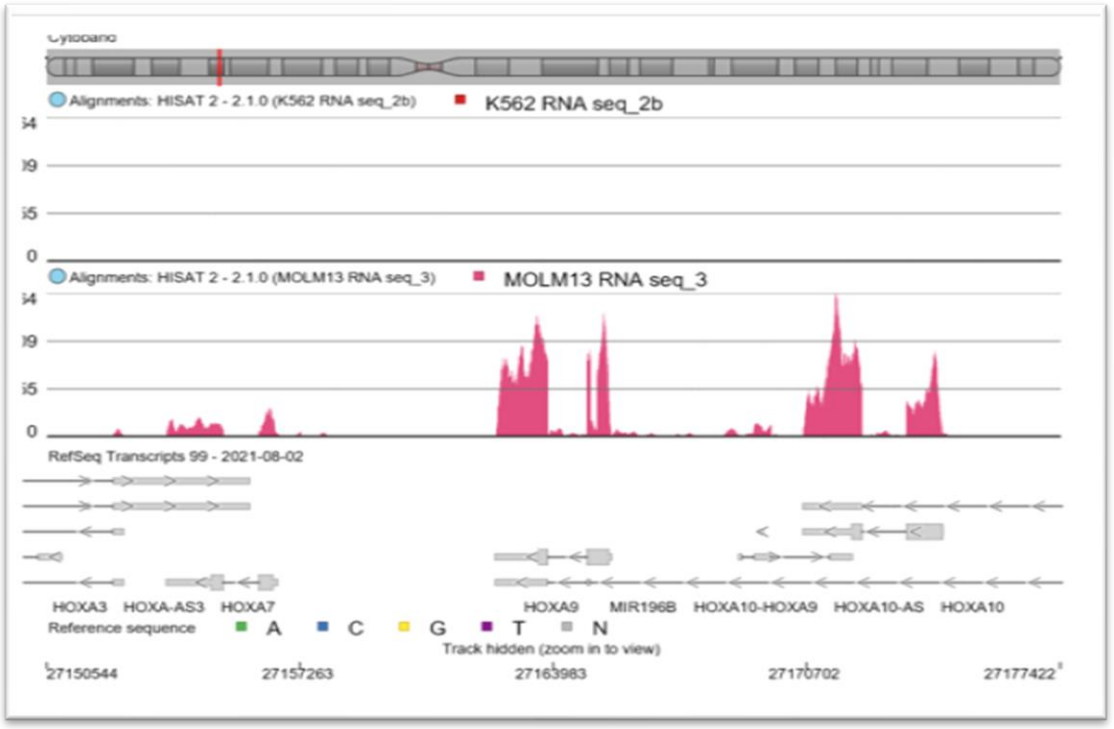

Figure 15 : The RNA-Seq alignment data for two leukemia cell lines, K562 and MOLM-13, focusing on the *HOXA* cluster**.** The first track shows RNA-Seq alignment data for the K562 cell line. The second track shows RNA-Seq alignment data for the MOLM-13 cell line. The y-axis of each track represents the number of reads aligning to the genome, indicative of the expression levels of the genes in this region.

3.4.2 *In silico* analyses of chromatin immunoprecipitation (ChIP-Seq) data

The rationale for this experiment is to investigate the epigenetic landscape of the *HOXA* cluster, exclusively the *HOXA9* in MOLM-13 cells, focusing on the specific histone modifications and chromatin interactions that regulate its expression. By analyzing the association of DOT1L and H3K79me2 within *HOXA9* in MOLM-13 cells, we can understand the role of these epigenetic marks in maintaining an active transcriptional state of *HOXA9* in the presence of the KMT2A-MLLT3 fusion protein. Furthermore, examining DNase I hypersensitivity provides insight into the chromatin accessibility and regulatory potential of the *HOXA9* locus. This comprehensive analysis will shed light on the epigenetic mechanisms that drive *HOXA9* expression in leukemias with KMT2A-MLLT3 fusion, offering potential avenues for targeted epigenetic therapies.

Dr. Davie analyzed the association of DOT1L with the entire *HOXA* cluster in the MOLM-13 cell line using the available ChIP-Seq data. The result showed that the entire *HOXA* including the *HOXA9* gene was associated with DOT1L and H3K79me2 in the MOLM-13 cell line. Furthermore, DNase I hypersensitivity covers the entire *HOXA* cluster including the *HOXA9* broad H3K79me2 domain and regions on either side of the domain. This observation suggests that *HOXA9* has an unstable chromatin structure (**Figure 16)** (Sharma et al., 2022). Analyses were conducted using publicly available ChIP-Seq data obtained from the Gene Expression Omnibus (GEO) database. The GEO accession numbers for the H3K79me2 ChIP-Seq files for the MOLM-13 cell line are as follows: GSE149183, GSE43063, and GSE113191. The GEO files for the DNase I-Seq files for MOLM-13 were also sourced from GSE149183, and the DOT1L ChIP-Seq files for MOLM-13 were obtained from GSE149183 as well.

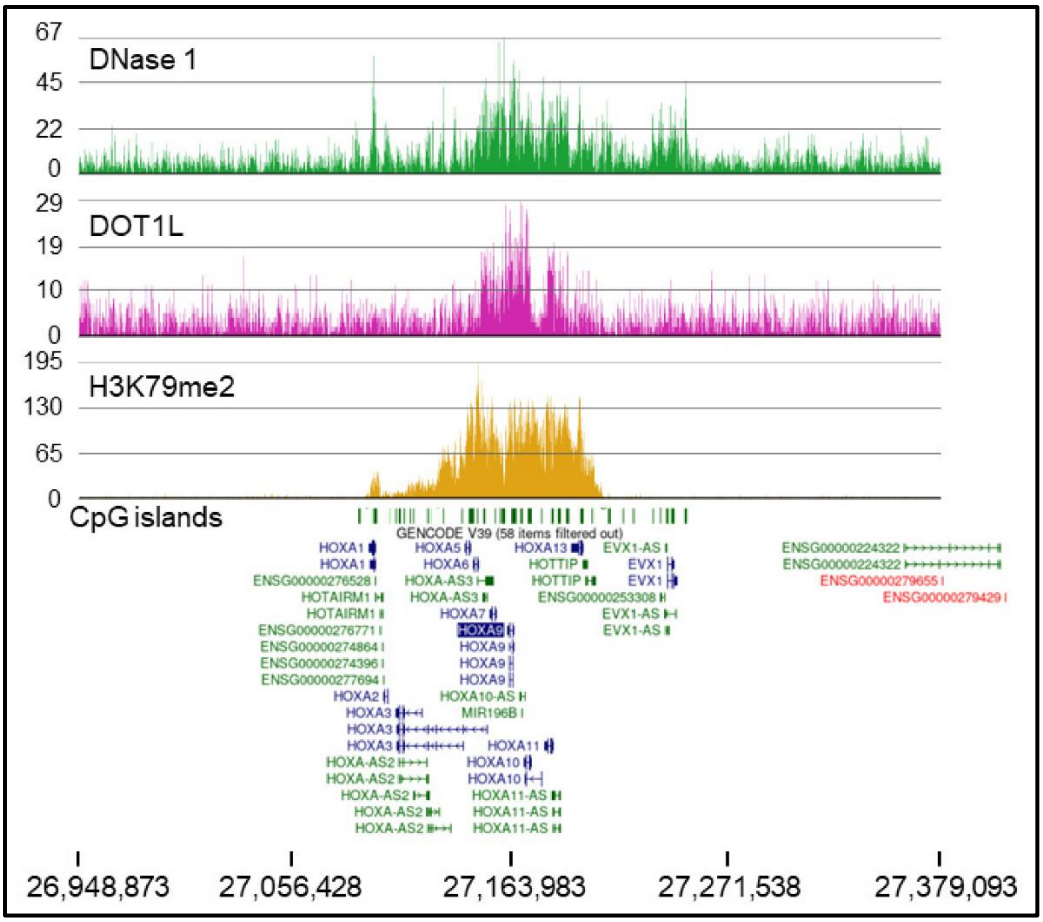

Figure 16: The ChIP-Seq tracks of H3K79me2, DOT1L, and DNase I hypersensitivity within the *HOXA* cluster in MOLM-13. Tracks from top to bottom**: DNase I hypersensitivity (green):** This track shows regions of open chromatin, identified by DNase I hypersensitivity, and the y-axis represents the signal intensity of DNase I hypersensitivity. **DOT1L binding (pink):** This track represents the binding sites of the histone methyltransferase DOT1L. The y-axis indicates the signal intensity of DOT1L binding. **H3K79me2 modification (orange):** This track illustrates the distribution of the H3K79me2 histone modification, an indicator of active transcriptional elongation. The y-axis shows the signal intensity of H3K79me2 modification, with peaks indicating regions enriched with this histone mark. The x-axis denotes the genomic coordinates, ranging from approximately 26,948,873 to 27,379,093, covering the *HOXA* cluster region in the human genome. The gene annotations show various *HOXA* genes, including *HOXA1, HOXA2, HOXA3, HOXA5, HOXA6, HOXA7, HOXA9, HOXA10, HOXA11*, and *HOXA13*. Non-coding RNAs such as *HOTTIP* are also annotated. *HOXA9* is marked in blue.

3.5 Determine DOT1L transcript, protein, and H3K79me2 levels in MOLM-13 and K562 cell lines

3.5.1 *DOT1L* transcript level

Rationale: To further elucidate the role of DOT1L in leukemias involving KMT2A-MLLT3 fusion proteins, it is essential to determine the levels of DOT1L transcript, protein, and its histone modification product (H3K79me2) in MOLM-13 and K562 cell lines. Our previous bioinformatic analyses revealed the distribution of DOT1L along the *HOXA9* gene in MOLM-13 cells. However, understanding the differences in DOT1L expression and activity at the transcript, protein, and modification levels between MOLM-13 (with KMT2A-MLLT3 fusion) and K562 (no KMT2A-MLLT3 fusion) cells can provide deeper insights into the molecular mechanisms driving leukemogenesis in these distinct leukemia types.

DOT1L transcript levels were assessed in both cell lines using reverse transcription-quantitative polymerase chain reaction (RT-qPCR). *GAPDH* served as the reference gene to normalize the expression levels, ensuring accurate comparison between samples. The RT-qPCR protocol included the extraction of total RNA from the cells, followed by the synthesis of cDNA using reverse transcriptase. Specific primers for *DOT1L* and *GAPDH* were designed and validated to ensure amplification efficiency and specificity. The PCR reactions were performed in three biological replicates, with each biological replicate having three technical replicates, to account for technical variability. Biological repeats involve using multiple, independent samples to account for variability within a population, ensuring that results are representative and not specific to a single sample. Technical repeats involve performing the same experiment multiple times on the same sample to assess and correct for procedural variability and measurement errors, thereby ensuring the accuracy and consistency of the results. Quantification of DOT1L transcript levels was conducted using the comparative Cq (threshold cycle). Delta Cq values, which denote the difference in cycle threshold (Cq) values between a target gene and a reference gene, were compared to evaluate gene expression levels in quantitative PCR. The average Cq values for the technical repeats of each replicate are presented in (**Table 9**) for K562 and (**Table 10)** for MOLM-13. The data indicated that the *DOT1L* transcript levels were comparable between the two cell lines, suggesting no significant differential expression of this gene under the conditions tested (**Figure 17)**.

Table 9 : The average Cq values for the technical repeats of each replicate of K562 are shown in this table

K562	Average Cq Replicate 1	Average Cq Replicate 2	Average Cq Replicate 3
GAPDH	20.48	20.57	20.01
DOT1L	26.58	27.40	27.05

Table 10*:* The average Cq values for the technical repeats of each replicate of MOLM-13 are shown in this table

MOLM-13	Average Cq Replicate 1	Average Cq Replicate 2	Average Cq Replicate 3
GAPDH	20.83	20.98	20.52
DOT1L	27.52	28.10	27.78

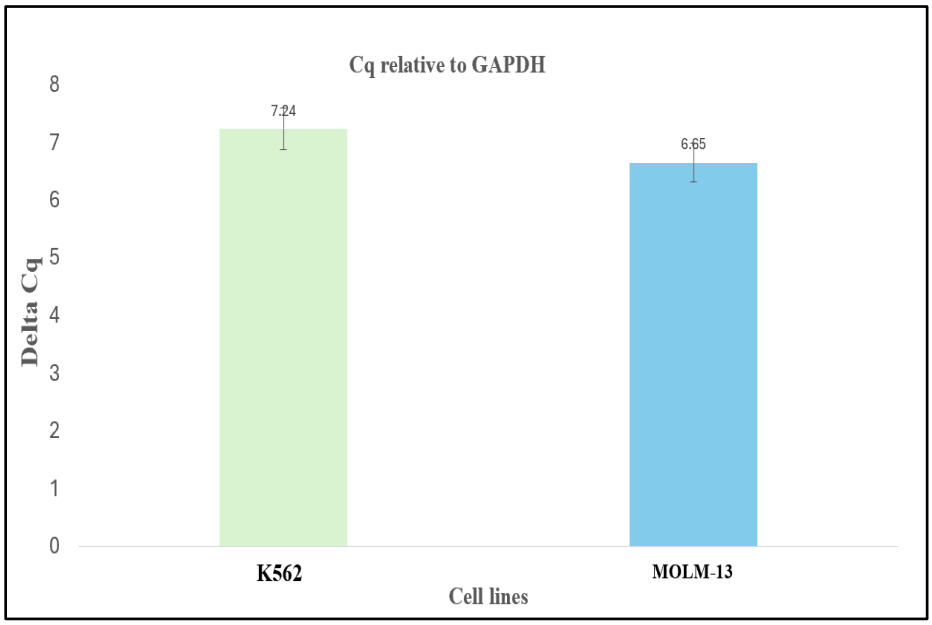

Figure 17: The relative expression levels of *DOT1L* in K562 and MOLM-13 cell lines, normalized to the housekeeping gene *GAPDH*. The y-axis represents the delta Cq values, which indicate the difference in quantification cycles (Cq) between *DOT1L* and *GAPDH*. The error bars represent the standard error of the mean (SEM).

3.5.2 DOT1L protein level

Rationale: Measuring the protein level of DOT1L is essential because transcript levels do not always directly correlate with protein expression due to various regulatory mechanisms in the cell. While transcript levels provide valuable information about gene expression, assessing protein levels is crucial to fully understand the functional implications of DOT1L. Integrating transcript and protein level data offers a more comprehensive view of gene expression regulation.

Proteins (100 ug) from MOLM-13 and K562 were resolved by 15% SDS-PAGE (electrophoresis at 200 V) followed by immunoblotting using a DOT1L antibody. The results show that the protein levels of DOT1L were similar in both cell lines (**Figure 18).**

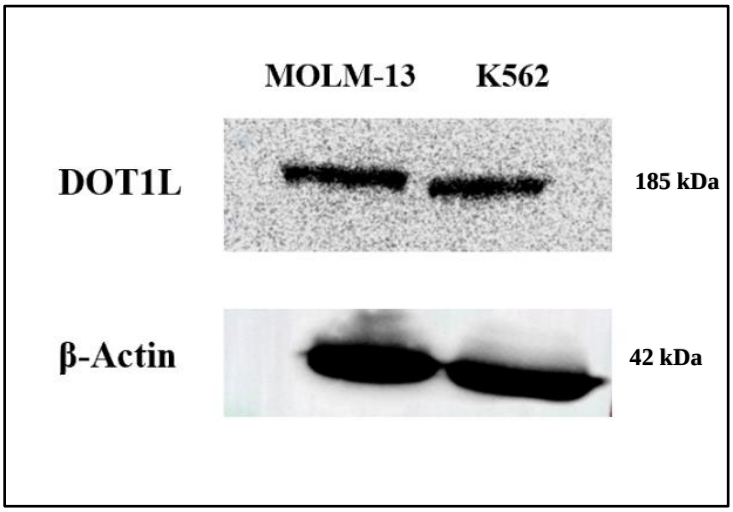

Figure 18: Protein levels of DOT1L, detected at 185 kDa, were measured in MOLM-13 and K562 cells. β-Actin, used as a loading control, was detected at 42 kDa.

3.5.3 DOT1L product (H3K79me2) level

To determine the level of H3K79me2, the product of DOT1L enzyme, in MOLM-13 and K562 cell lines, immunoblotting was performed with the H3K79me2 antibody.

Acid-extracted histones (6 µg) from MOLM-13 and K562 cell lines were resolved by 15% SDS-PAGE (electrophoresis at 200 V) following electrophoresis, immunoblotting was performed using H3K79me2 and H3 antibodies. The results indicated that the H3K79me2 modification level, a product of DOT1L activity, was higher in MOLM-13 compared to K562 (**Figure 19)**.

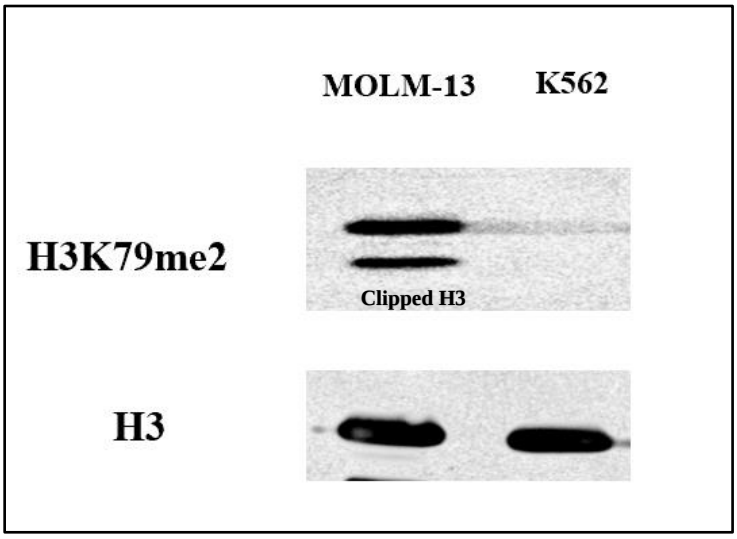

Figure 19 : The level of H3K79me2 in MOLM-13 and K562. Total H3 was used as a loading control. The clipped H3 band was detected.

3.7 Determine the level of H2BK120ub in MOLM-13 and K562 cell lines

Rationale: The critical role of histone H2B lysine 120 mono-ubiquitination (H2BK120ub) in regulating the methyltransferase activities of DOT1L and SET2 has been shown. This modification, facilitated by the RNF20/40 complex, is crucial for directing DOT1L and SET2 to nucleosomal sites, where they catalyze the formation of H3K79me2 and H3K36me3 marks, respectively. Investigating the levels of this modification in MOLM-13 and K562 cells will provide insights into how its abundance influences epigenetic regulation and potentially impacts DOT1L activity in these leukemia cell lines.

Acid-extracted histones (6 µg) from MOLM-13 and K562 cell lines were resolved by 15% SDS-PAGE (electrophoresis at 200 V) following electrophoresis, immunoblotting was performed using immunoblotting using an antibody specific for ubiquitinated histone H2B at lysine 120 (H2BK120ub). The results indicated that MOLM-13 cells, which exhibit higher DOT1L activity than K562 cells, showed elevated levels of H2BK120ub (**Figure 20**).

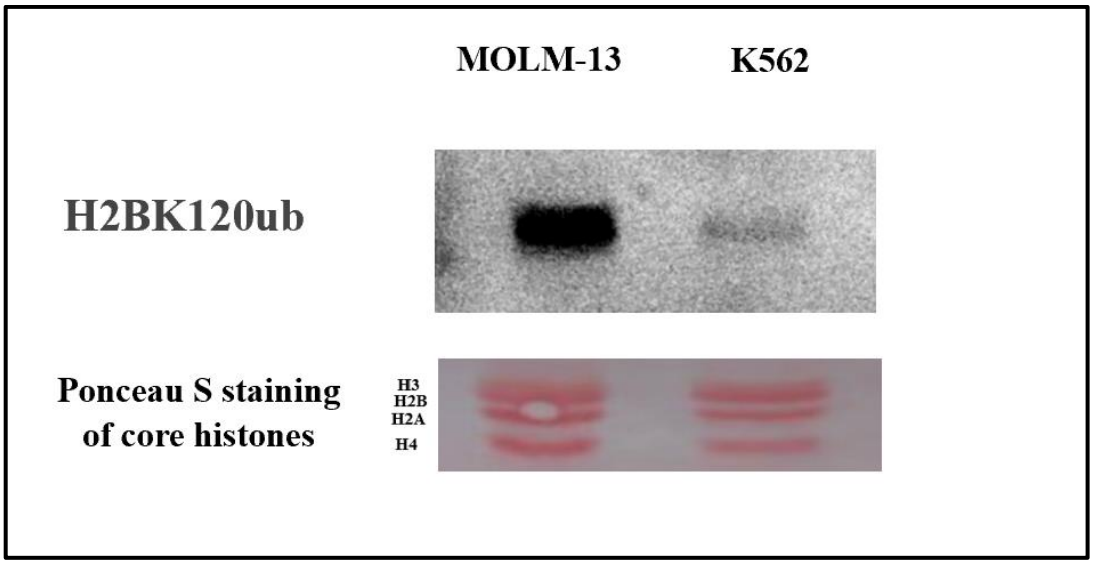

Figure 20: The level of H2B (K120) mono-ubiquitination in MOLM-13 cells compared to K562 cells. Ponceau S staining of core histones is also included.

3.8 Determine the impact of proteasome inhibitor (bortezomib) on modifications that play a role in transcription elongation in MOLM-13 cells

Rationale: Bortezomib, a well-known proteasome inhibitor, not only directly affects the proteasome but also indirectly influences histone modifications such as H2BK120ub. Reduced proteasome activity leads to decreased levels of H2BK120ub, which is essential for proper transcription elongation and chromatin structure, thereby affecting gene expression. Studies have demonstrated that proteasome inhibitors like bortezomib reduce H2BK120ub levels, resulting in subsequent decreases in H3K79me2 levels along the *HOXA9* in acute lymphoblastic leukemia (ALL). These findings underscore the critical role of H2BK120ub in regulating DOT1L activity for *HOXA9* gene transcription (Jennifer L Kamens et al., 2023). I aimed to see how bortezomib, as a proteasome inhibitor, affects key modifications like H2BK120ub, H3K79me2, and H3K36me3, all of which play a role in transcription elongation. I conducted each part of the experiment with three replicates to ensure the results were reproducible.

For this aim, I turned my attention to MOLM-13 cells, which stand out for their high H2BK120ub and H3K79me2 levels. These cells were treated with a low dose of 5 nM bortezomib for 2 and 4 hours. Cell viability was measured before and after treatment for control, 2h, and 4h treatments. The acid-extracted histones were used to determine the level of H2BK120ub, H3K79me2, and H3K36me3 before and after treatment.

3.8.1 Determine the impact of proteasome inhibitor (bortezomib) on H2BK120ub in MOLM-13 cells

About fifty million MOLM-13 cells were treated with 5 nM bortezomib for 2 and 4 hours, after which histones were extracted. Acid-extracted histones (control, 2h, and 4h conditions) from MOLM-13 were resolved by 15% SDS-PAGE (electrophoresis at 200 V) following electrophoresis, immunoblotting was performed using an antibody specific to ubiquitinated histone H2B at lysine 120 (H2BK120ub). Ponceau S-stained with histones labeled is shown. Cell viability, measured before and after treatment, did not change significantly. The results showed that treatment with 5 nM bortezomib for 2 and 4 hours significantly reduced H2BK120ub levels (approximately 2-fold) in MOLM-13 cells (**Figure 21)**.

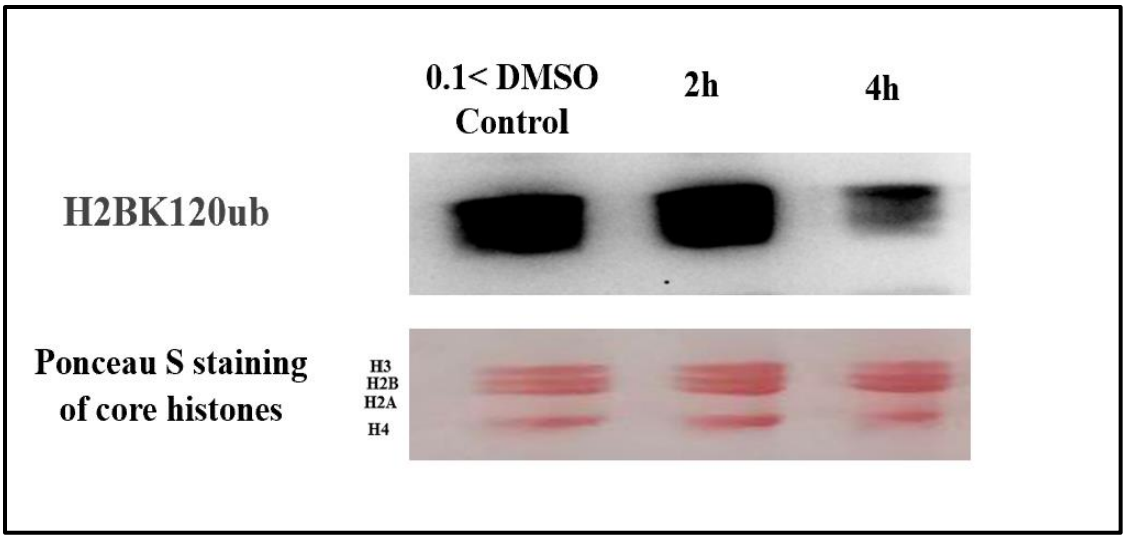

Figure 21: The levels of H2BK120ub were measured in control, 2-hour, and 4-hour treatments with 5 nM bortezomib. Ponceau S staining is also included. The concentration of DMSO was 0.000046% in control, 2-hour, and 4-hour treatment groups.

3.8.2 Determine the impact of proteasome inhibitor (bortezomib) on H3K79me2 levels in MOLM-13 cells

Acid-extracted histones (control, 2h, and 4h conditions) from MOLM-13 were resolved by 15% SDS-PAGE (electrophoresis at 200 V) following electrophoresis, immunoblotting was performed using an H3K79me2 antibody. The results showed that H3K79me2, a product of the DOT1L enzyme, exhibited a decrease after 4 hours of treatment with 5 nM bortezomib (about 2-fold) (**Figure 22**).

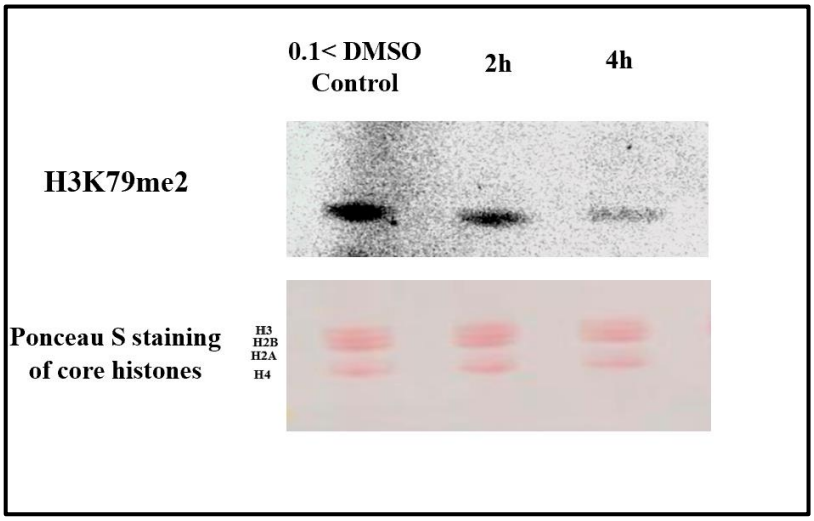

Figure 22 : The levels of H3K79me2 were measured in control, 2-hour, and 4-hour treatments with 5 nM bortezomib. Ponceau S staining is also included. The concentration of DMSO was 0.000046% in control, 2-hour, and 4-hour treatment groups.

*3.8.*3 Determine the impact of proteasome inhibitor (bortezomib) on H3K36me3 levels in MOLM-13 cells

Acid-extracted histones (control, 2h, and 4h conditions) from MOLM-13 were resolved by 15% SDS-PAGE (electrophoresis at 200 V) following electrophoresis, immunoblotting was performed using an H3K36me3 antibody**.** The results showed that treatment with 5 nM of bortezomib for 2 and 4 hours did not change the level of H3K36me3, a product of the SETD2 enzyme **(Figure 23).**

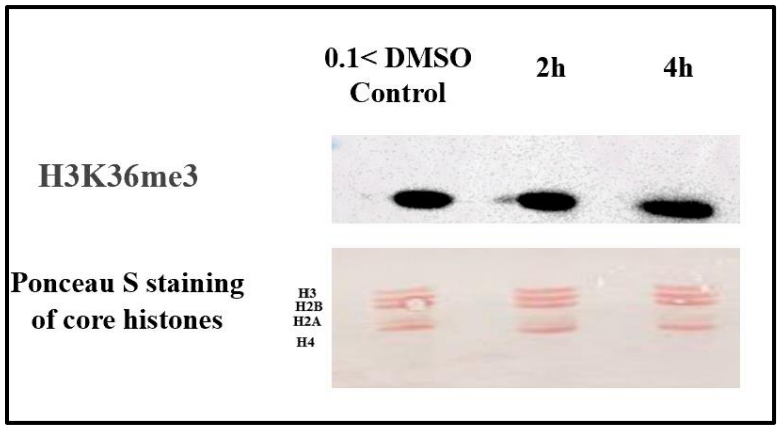

Figure 23 : The levels of H3K36me3 were measured in control, 2-hour, and 4-hour treatments with 5 nM bortezomib. Ponceau S staining is also included. The concentration of DMSO was 0.000046% in control, 2-hour, and 4-hour treatment groups.

3.8.4 Determine the impact of proteasome inhibitor (bortezomib) on *HOXA9* transcript levels in MOLM-13 cells

HOXA9 transcript levels were measured by RT-qPCR before and after treatment with 5 nM of bortezomib for 14 hours, using *β-actin* as the reference gene for normalization. Cell viability was also assessed. The results showed that bortezomib reduced *HOXA9* gene expression (fold change of 0.46). The fold change of 0.46 in the expression of *HOXA9* indicated downregulation of this gene in response to bortezomib treatment. Fold change is a measure used in quantitative PCR (qPCR) to compare the expression levels of a gene between different experimental conditions. It is calculated using the ΔΔCt method, where the threshold cycle (Ct) values of the target gene (in this case, *HOXA9*) are normalized to a reference gene (such as *β-actin*) and then compared between treated and untreated samples. It is worth mentioning that initially, I used *GAPDH* as the reference gene for both the treatment and control conditions. However, the Cq values were inconsistent, and there were significant variations between the control and treatment groups, which is not ideal for RT-qPCR. The reference gene should be consistent before and after treatment. For this reason, I used *β-actin* instead, with β-*actin* showing more consistent levels in control and treated samples.

In this experiment, the ΔCt for *HOXA9* in the control sample was 6.33, while in the treated sample, it was 7.44. The difference in ΔCt values (ΔΔCt) was 1.11. The fold change was then calculated as 2^(-ΔΔCt), which equals 2^(-1.11), resulting in approximately 0.46. A fold change of less than 1 indicates a reduction in gene expression, as the negative exponent signifies a fractional decrease (**Figure 24)**. This downregulation suggests that bortezomib suppresses the transcription of *HOXA9*, which could be relevant to understanding the molecular mechanisms of its therapeutic effects.

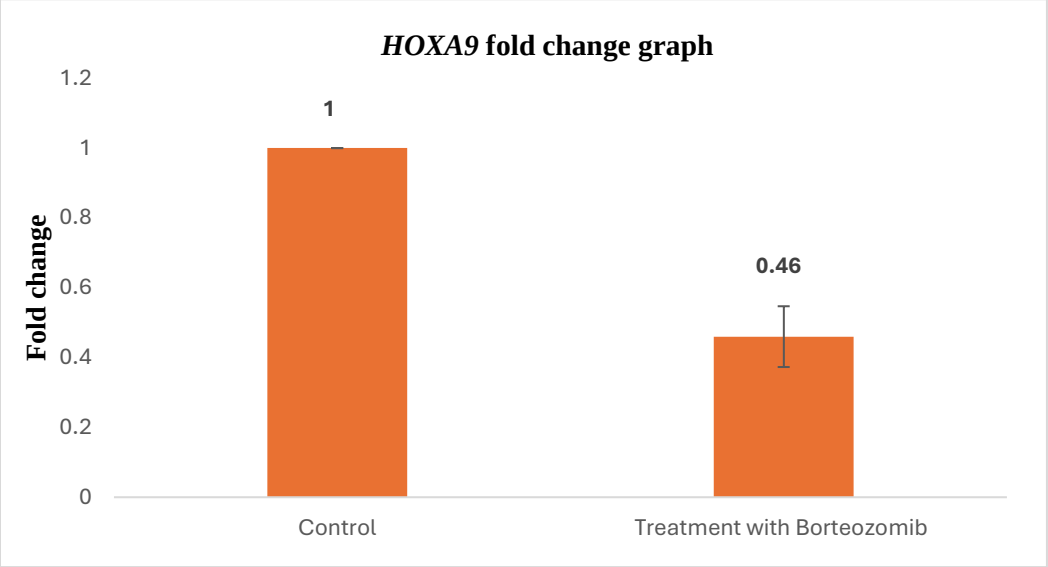

Figure 24: *HOXA9* fold change in control and 5 nM bortezomib-treated conditions after 14 hours of treatment. Fold changes were measured using β-actin as the reference gene. Error bars represent SEM.

3.9 Determining the concurrent presence of H3K79me2 and H3K36me3 on the same histone in MOLM-13 and K562 cells

3.9.1 *In silico* analyses of ChIP-Seq data

Rationale: Previous studies have demonstrated a strong correlation between H3K36me3 and DOT1L-dependent H3K79me2 marks on gene bodies of *HOXA9* in acute myeloid leukemia (AML) (A. Skucha et al., 2018). This relationship suggests that the SETD2-dependent H3K36me3

modification is intricately linked with H3K79me2 in the *HOXA9* gene in acute myeloid leukemia. To investigate the crosstalk between H3K79me2 and H3K36me3 along the *HOXA9* in MOLM-13 cells, which are a model of mixed lineage leukemia is poorly investigated. It is crucial to first analyze available ChIP-seq tracks to observe the patterns of distribution of H3K36me2 and H3K79me2 along the *HOXA9* gene in MOLM-13. Subsequently, histone Co-IP experiments can be performed to determine if these two modifications coexist on the same histone.

Dr. Davie analyzed the association of H3K79me2, H3K36me3, H3K27ac, H3K4me3, DOT1L, and DNase I hypersensitivity within the entire *HOXA* cluster in MOLM-13 cells. Analysis of the available ChIP-seq data reveals that the *HOXA9* gene in MOLM-13 cells, which carry the KMT2A-MLLT3 fusion protein, exhibits enrichment not only of H3K79me2 but also of H3K36me3 and other active marks **(Figure 25)**. The GEO files for H3K36me3, DOT1L, H3K4me3, and H3K27ac were from the following sources: H3K36me3 (GSE189894), DOT1L (GSE149183), H3K4me3 (GSE113191) , H3K27ac (GSE173600) , H3K79me2 (GSE149185) and DNase I **(**GSE149183).

Typically, H3K79me2 initiates immediately after the transcription start site (TSS), extends through the gene body, and diminishes towards the 3' end, whereas H3K36me3 predominantly marks the 3' end of the active gene bodies. While both modifications decorate gene bodies, their distributions only partially overlap. The coexistence of H3K79me2 and H3K36me3 within the *HOXA9* gene body in MOLM-13 cells suggests a potential crosstalk mechanism that could enhance the transcription rate of the *HOXA9* gene in MOLM-13 cells. Upon closer examination of **Figure 25**, the entire *HOXA* cluster, encompassing HOXA1-11 genes, as well as long non-coding and intergenic regions, also shows enrichment of H3K79me2. This pattern suggests an unusual spread of H3K79me2 across the entire region; typically, H3K79me2 begins at gene promoters and extends towards the 3' end. Conversely, H3K36me3 specifically decorates *HOXA9* and *HOXA10* gene bodies emphasizing its role in regulating *HOXA9* transcription.

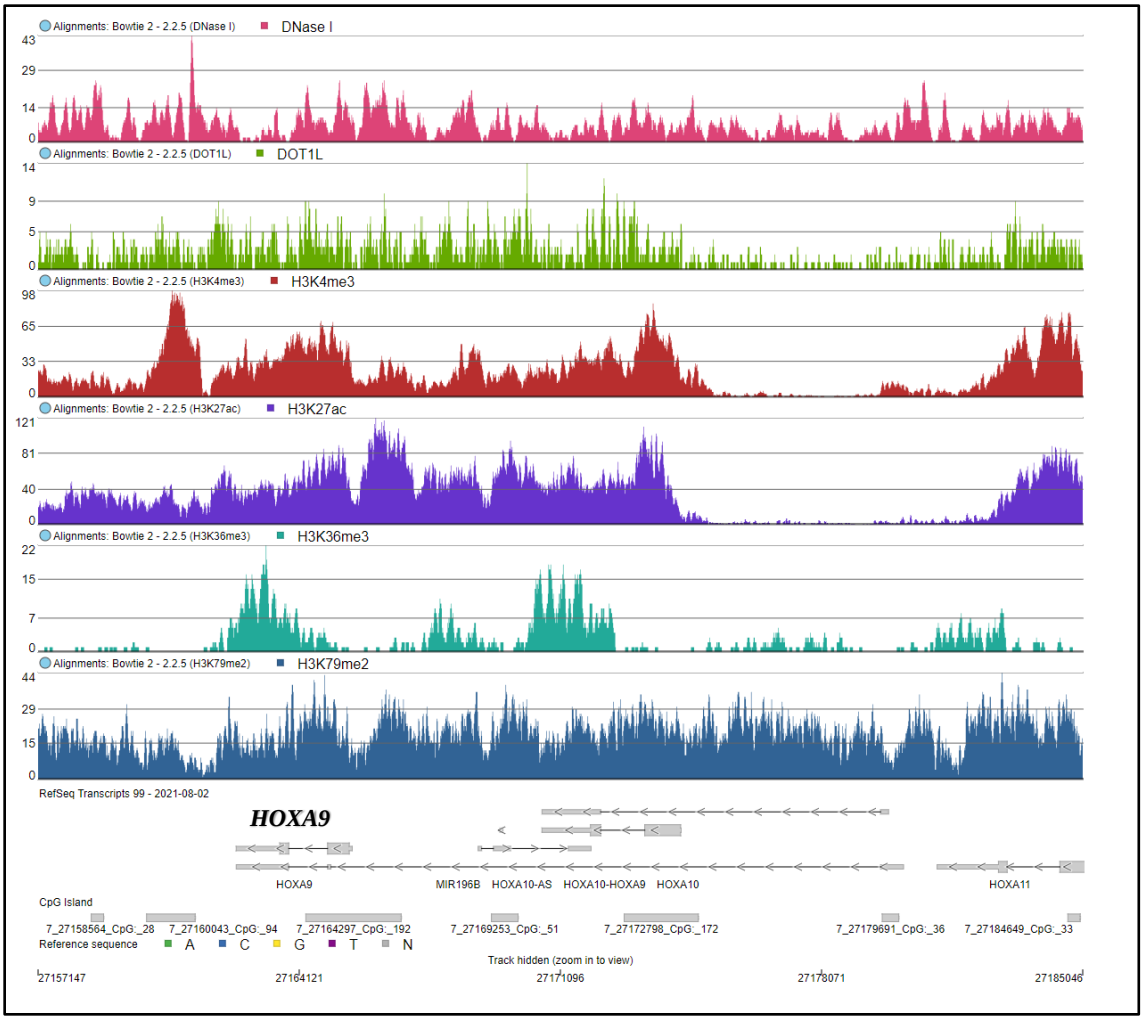

Figure 25 : The ChIP-Seq tracks for H3K79me2, H3K36me3, H3K27ac, H3K4me3, DOT1L, and DNase I hypersensitivity are shown. Tracks in order from top to bottom as shown in the image: **DNase I Hypersensitivity** (peaks in pink), showing regions of open chromatin. **DOT1L** (peaks in green), showing the binding sites of the DOT1L protein within the *HOXA* cluster. **H3K4me3** (peaks in red), showing trimethylation of histone H3 at lysine 4, within the *HOXA* cluster. **H3K27ac** (peaks in purple), showing acetylation of histone H3 at lysine 27, within the *HOXA* cluster. **H3K36m (**peaks in green), showing trimethylation of histone H3 at lysine 36, within the *HOXA* cluster. **H3K79me2** (peaks in blue), showing dimethylation of histone H3 at lysine 79, within the *HOXA* cluster.

3.9.2 Determining the concurrent presence of H3K79me2 and H3K36me3 on the same histone (Cis-histone pattern) in MOLM-13

Analysis of the available ChIP-seq data reveals that the *HOXA9* gene in MOLM-13 cells, which carry the KMT2A-MLLT3 fusion protein, exhibits enrichment not only of H3K79me2 but also of H3K36me3 thus, the histone Co-IP was used to investigate whether these two modifications can coexist on the same histone H3 in leukemic cells.

Approximately 50 million cells were used for the histone Co-IP experiment. A portion of the samples (80 µg each), including Input, ID (immuno-depleted), and IP (immunoprecipitated with H3K36me3 antibody) samples, were resuspended in 2X sample buffer and loaded onto a 15% SDS-PAGE gel. This gel was used to assess IP efficiency using the H3K36me3 antibody which is shown in **Figure 26A**. I was specifically looking for a clear enrichment of H3K36me3 in the IP sample compared to the Input and ID samples, as this would indicate successful immunoprecipitation of H3K36me3 marked histones. Additionally, a control IgG antibody was used as a negative control. The IgG antibody was added to an input sample, immunoprecipitated, and run on the gel, followed by immunoblotting with the H3K36me3 antibody. The results showed no IP band in the IgG control, indicating that the H3K36me3 antibody was specific and not binding non-specifically. After confirming that the antibody successfully pulled down H3K36me3, the remaining samples from INPUT, ID (immuno-depleted), and IP (immunoprecipitated with H3K36me3 antibody) were used for immunoblotting with an H3K79me2 antibody **(Figure 26B).**

The results showed that H3K79me2 and H3K36me3 are concurrent in the same histone H3 in MOLM-13 cells. The presence of IP bands in the immunoblotting with the H3K79me2 antibody after initial immunoprecipitation with the H3K36me3 antibody indicates that MOLM-13 cells carry both H3K36me3 and H3K79me2 modifications **(Figure 26B)**. This suggests that these two histone modifications co-occur on the same histone H3. However, the IP efficiency with H3K36me3 showed some presence in the ID (immuno-depleted) sample, indicating that the antibody was not 100% efficient in pulling down all H3K36me3. In the immunoblotting with the H3K79me2 antibody, the ID band is stronger than the IP band, suggesting that a significant portion of histones marked with H3K79me2 are not associated with H3K36me3. This implies that while some histones have both H3K36me3 and H3K79me2 modifications, a considerable amount of H3K79me2-modified histones are not associated with H3K36me3.

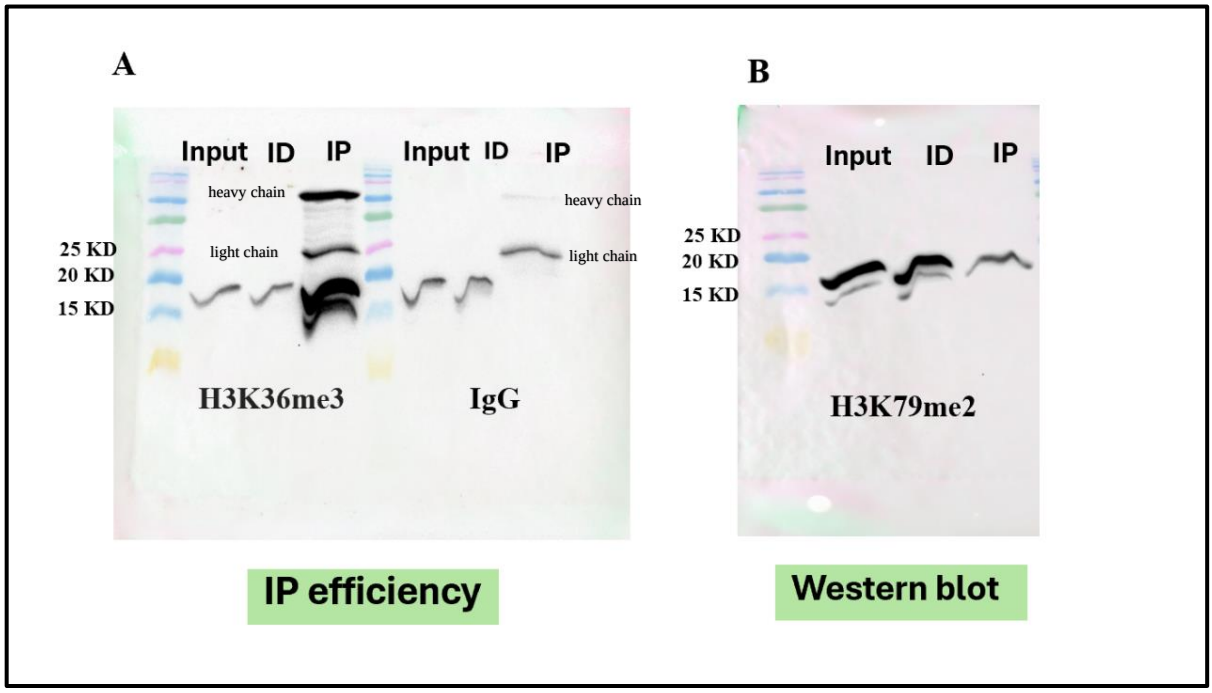

Figure 26. (A) The IP efficiency for H3K36me3 in MOLM-13 cells. A control IgG antibody was used as a negative control. **(B).** Immunoblotting the Input, ID (immuno-depleted), and IP (immunoprecipitated with H3K36me3 antibody) with an H3K79me2 antibody in MOLM-13 cells.

3.9.3 Determining the concurrent presence of H3K79me2 and H3K36me3 on the same histone (Cis-histone pattern) in K562 cells

Approximately 50 million cells were used for the histone Co-IP experiment. A portion of the samples (80 µg each), including Input, ID (immuno-depleted), and IP (immunoprecipitated with H3K36me3 antibody) samples, were resuspended in 2X sample buffer and loaded onto a 15% SDS-PAGE gel. This gel was used to assess IP efficiency using the H3K36me3 antibody which is shown in **Figure 27A**. I was specifically looking for a clear enrichment of H3K36me3 in the IP sample compared to the Input and ID samples, as this would indicate successful immunoprecipitation of H3K36me3. The remaining samples from INPUT, ID (immuno-depleted), and IP (immunoprecipitated with H3K36me3 antibody) were used for immunoblotting with an H3K79me2 antibody **(Figure 27B).**

The results showed that H3K79me2 and H3K36me3 are concurrent in the same histone H3 in K562 cells **(Figure 28B).** The presence of IP bands in the immunoblotting with the H3K79me2 antibody after initial immunoprecipitation with the H3K36me3 antibody indicates that K562 cells carry both H3K36me3 and H3K79me2 modifications. This suggests that these two histone modifications co-occur on the same histone H3. However, the IP efficiency with H3K36me3 showed some presence in the ID (immuno-depleted) sample, indicating that the antibody was not 100% efficient in pulling down all H3K36me3. In the immunoblotting with the H3K79me2 antibody, the ID band is stronger than the IP band, suggesting that a significant portion of histones marked with H3K79me2 are not associated with H3K36me3. This implies that while some histones have both H3K36me3 and H3K79me2 modifications, a considerable amount of H3K79me2-modified histones are not associated with H3K36me3 in K562 cells. These findings suggest that the co-occurrence of H3K79me2 with H3K36me3 is minimal, likely due to the intrinsically low levels of H3K79me2 in K562 cells.

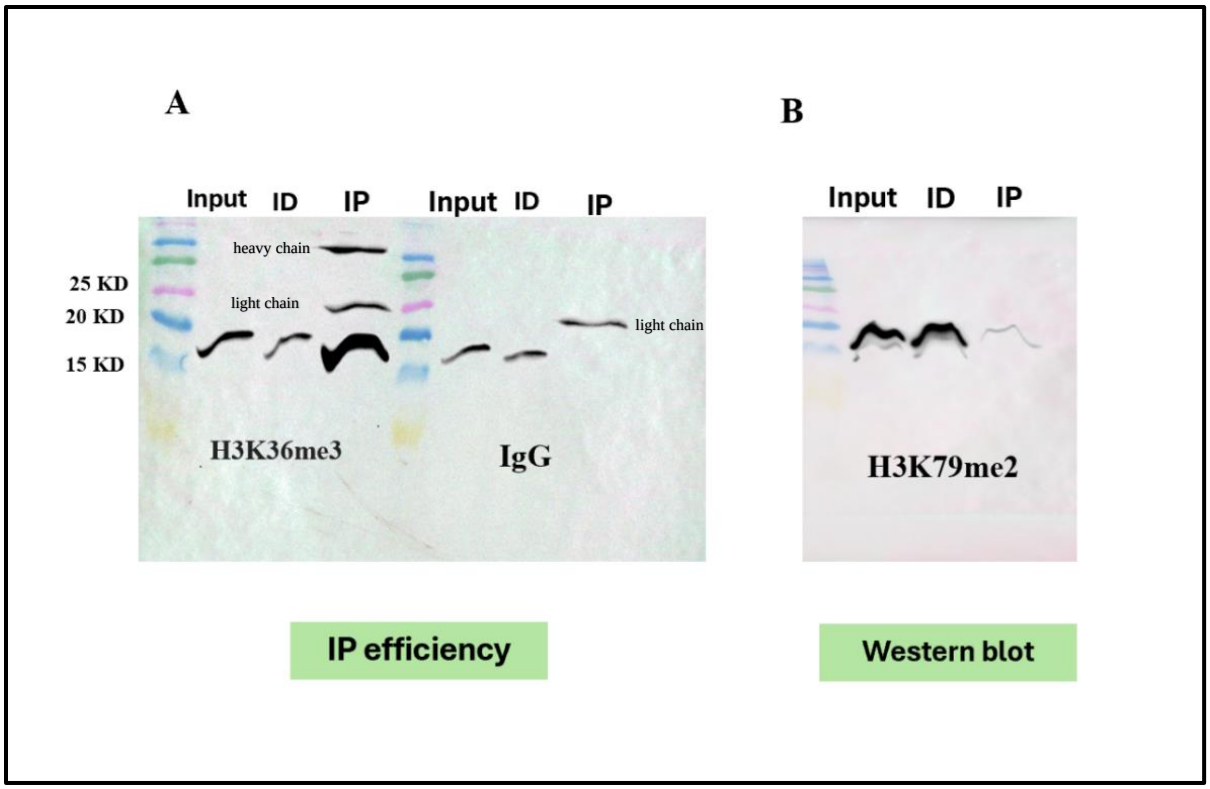

Figure 29: (A) The IP efficiency for H3K36me3 in K562 cells. A control IgG antibody was used as a negative control. **(B)** Immunoblotting the Input, ID (immuno-depleted), and IP (immunoprecipitated with H3K36me3 antibody) with an H3K79me2 antibody in K562 cells.

3.10 Determine the levels of histone H3 variants and H3K79me2 in H3 variants in MOLM-13 and K562 cells

3.10.1 Determine the protein levels of canonical histone H3 (H3.1 and H3.2) and H3.3 variant

The levels of histone H3.1, H3.2, and H3.3 in MOLM-13 and K562 cells were determined using AUT gel electrophoresis. Acid-extracted histones (9 μg) from each cell line were prepared by mixing with 2X AUT-sample buffer. Human histone standards, which included purified H3.1, H3.2, and H3.3 proteins, were used to validate the migration positions of the histone H3s. The samples and histone standards were loaded onto an AUT gel and subjected to electrophoresis at 200 V for 3 hours. Following electrophoresis, the gel was stained with Coomassie Blue and destained to visualize the bands corresponding to histone H3s. The results indicated that H3.1

exhibited the highest levels in both MOLM-13 and K562 cell lines, while H3.3 showed the lowest levels in both cell types **(Figure 28).** The levels of the histone H3s followed the order of H3.1 > H3.2 > H3.3 in both MOLM-13 and K562 cell lines.

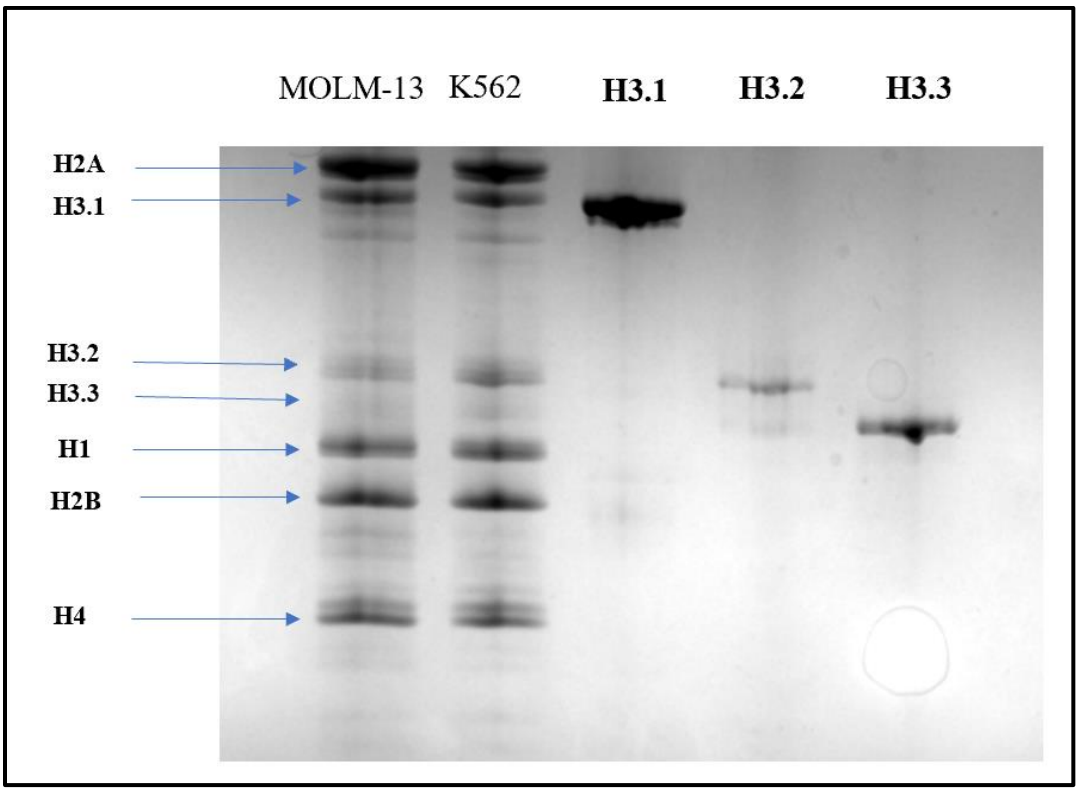

Figure 30 : Histones (canonicals and variants) from MOLM-13 and K562 cells alongside human histone standards, specifically purified H3.1, H3.2, and H3.3 proteins, which were used to verify the migration positions of the H3.1, H3.2, and H3.3.

3.10.2 Two-dimensional gel electrophoresis used for high-resolution separation of histone H3s

The two-dimensional gel system consists of acetic acid-urea-triton polyacrylamide gel (AUT-PAGE) analysis in the first dimension and standard sodium dodecyl sulfate polyacrylamide gel (SDS-PAGE) in the second dimension. This method allows for high-resolution separation of modified histone species and histone variants in relatively short periods. MOLM-13 acid-extracted histones were used in this 2D gel PAGE study (**Figure 29)**.

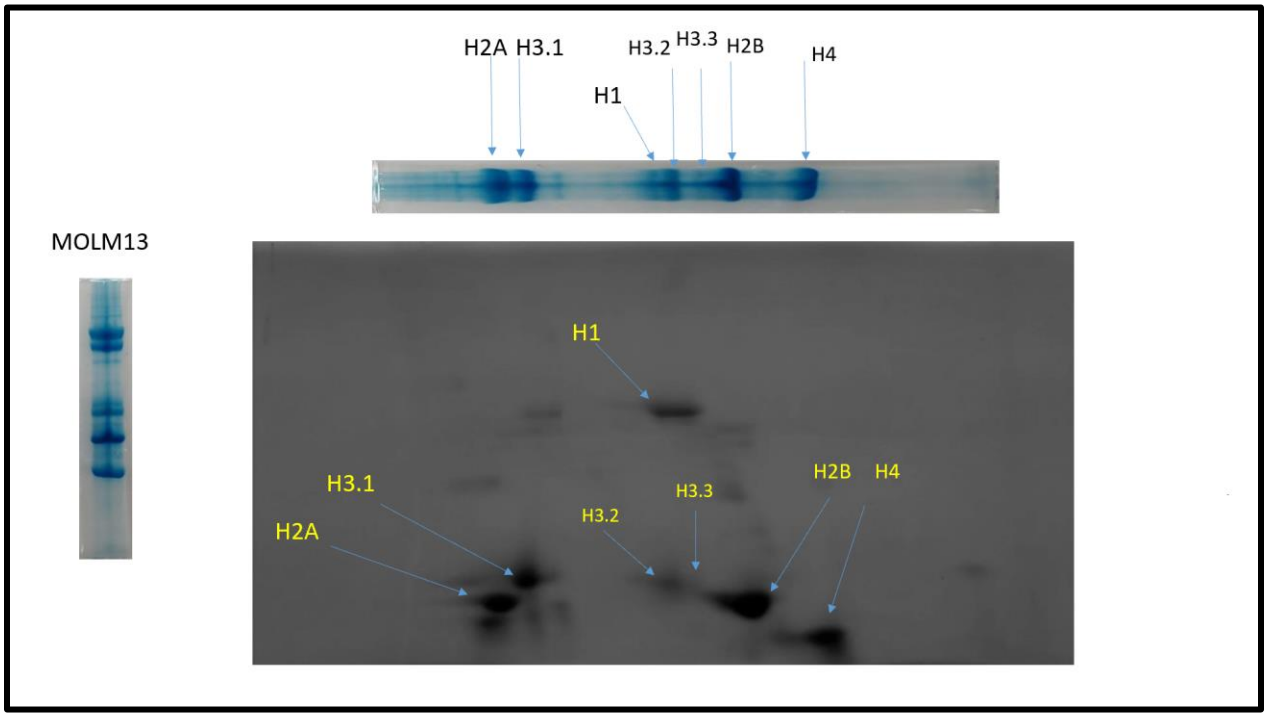

Figure 31: Two-Dimensional (2D) PAGE system consisting of acetic acid-urea-triton polyacrylamide gel (AUT-PAGE) analysis in the first dimension and standard sodium dodecyl sulfate polyacrylamide gel (SDS-PAGE) in the second dimension. The MOLM-13 histones were labeled.

3.10.3. Protein level of H3.3 in MOLM-13 and K562 cells

To determine the level of histone H3.3 variant more specifically, AUT immunoblotting was used to confirm the level of H3.3 variant in MOLM-13 and K562 cell lines. Acid-extracted histones (6 µg) from MOLM-13 and K562 cell lines cell lines were prepared by mixing with 2X AUT sample buffer. The samples were then loaded onto an AUT gel and subjected to electrophoresis at 200 V for 3 hours. After electrophoresis, the gel was transferred to nitrocellulose and then immunoblotted using an H3.3 antibody. The results showed that the level of H3.3 is similar in MOLM-13 and K562 cell lines (**Figure 30).**

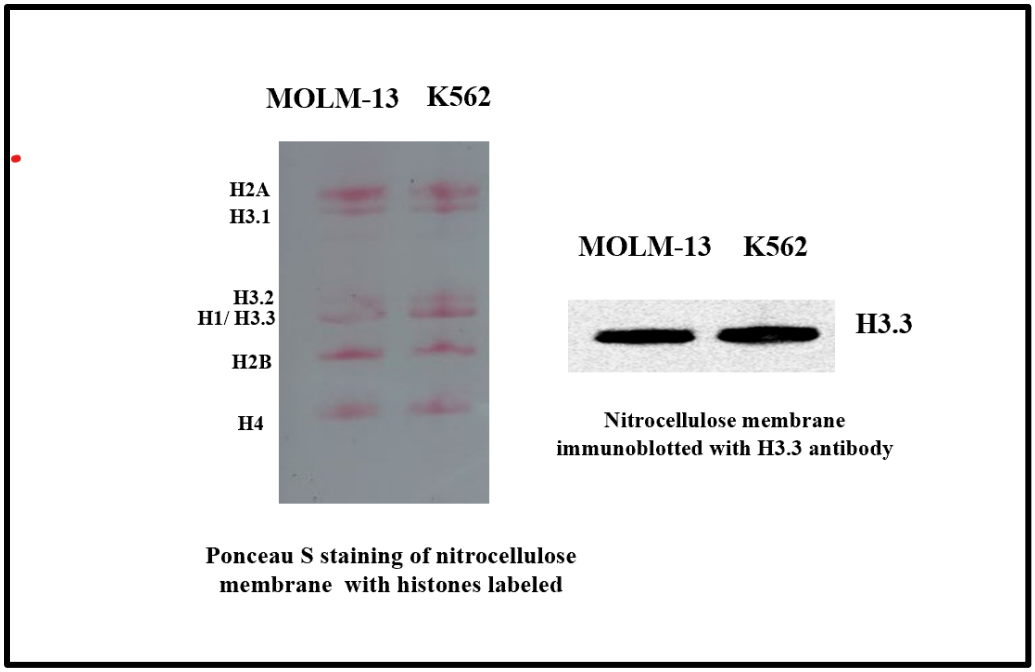

Figure 32: The level of histone H3.3 variants in MOLM-13 and K562 cell lines. Ponceau S staining of histone variants is included.

3.10.4. Determine whether H3.3 is preferentially dimethylated at K79 in MOLM-13 and K562 cells

AUT immunoblotting was used to determine the levels of H3.1 K79me2, H3.2 K79me2, and H3.3 K79me2. As mentioned earlier, the protein level of histone H3.3 is the lowest compared to H3.2 and H3.1 in both cell lines. However, the AUT immunoblot using the H3K79me2 antibody showed that the H3.3K79me2 level is similar to that of H3.2K79me2. Considering the lower protein level of H3.3 but modified at the same level as H3.2K79me2, this indicates that H3.3 is preferentially dimethylated at K79 in MOLM-13 and K562 cell lines (**Figure 31)**.

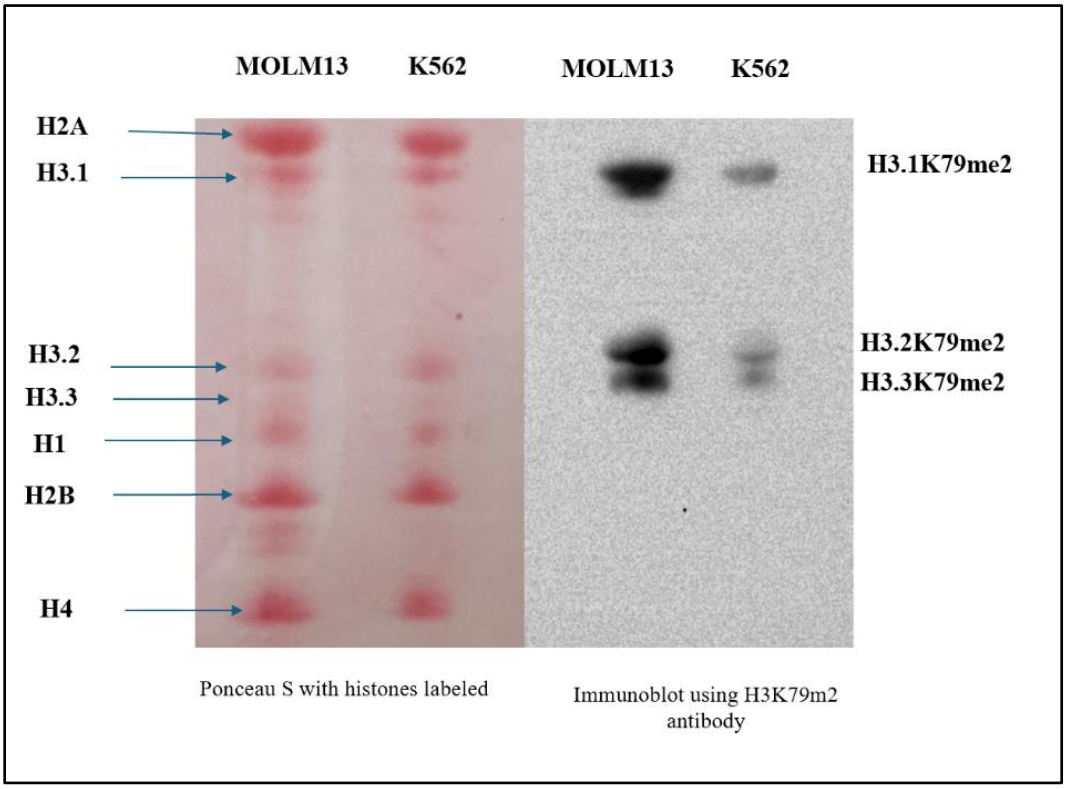

Figure 33: The level of H3.1K79me2, H3.2K79me2, and H3.3K79me2 in MOLM-13 and K562 cell lines.

Chapter 4

4. Discussion

4.1 Quality control (QC) and importance of QC in studies dependent upon antibodies

Selecting an antibody that is specific for detecting post-translational modifications is a significant challenge, as I encountered many issues in finding one that specifically detects H3K79me2. Most of my results rely on the H3K79me2 antibody, which is why finding a good one was a priority. After testing several antibodies that failed to meet the required specificity and reliability, I found success with the AbFlex® Histone H3K79me2 antibody from Active Motif, which had passed quality control (QC) tests, including immunoblotting and peptide specificity. This antibody successfully detected dimethylation of H3 at K79, without recognizing unmodified, monomethyl, or trimethyl states. The AbFlex® Histone H3K79me2 antibody showed a preference for binding to H3.1K79me2 over H3.3K79me2. This preference suggests that the H3K79me2 antibody has a higher affinity for H3.1K79me2. Consequently, the levels of H3.3K79me2 might be underestimated in the immunoblot results due to the antibody's lower affinity for this variant.

For the H3K36me3 antibody, QC was performed using AUT gel and SDS gel immunoblotting. However, peptides corresponding to H3K36me3 were not available to check the antibody's specificity. Despite this, the H3K36me3 antibody successfully detected the H3 band in both SDS gel and AUT gel immunoblots.

The H2BK120ub antibody was also tested via SDS gel-immunoblotting and the detected H2BK120ub band with the correct molecular mass.

4.2 Analysis of RNA-Seq, ChIP-Seq, and histone Co-IP in leukemia cell lines, MOLM-13 and K562

We realized and confirmed that *HOXA9* is expressed in MOLM-13 cells but not in the K562 cell line. *HOXA9* expression was also measured in MOLM-13 and K562 cells using RT-qPCR by me and our lab member, Sadhana R.N. Sudhakar. The results showed that *HOXA9* was expressed in MOLM-13 and not detected in the K562 cell line (Cq > 35), confirming the RNA-Seq analyses further.

The presence of the *KMT2A-MLLT3* translocation in MOLM-13 cells was confirmed using chromosome painting by Dr. Sabine Mai’s lab. Additionally, our lab verified the presence of the *KMT2A-MLLT3* fusion transcript in MOLM-13 cells through RT-qPCR, led by Dhanvi Prajapati. These studies support the presence of fusion protein resulting from the *KMT2A-MLLT3*

translocation. Numerous studies have demonstrated the significant role of the KMT2A-MLLT3 fusion protein in mixed lineage leukemia (Milne, 2017). This fusion protein is known to hijack transcriptional machinery (for example, the super elongation complex, SEC), leading to dysregulated expression of critical genes such as *HOXA9*, pivotal in mixed lineage leukemia development **(Figure 32).**

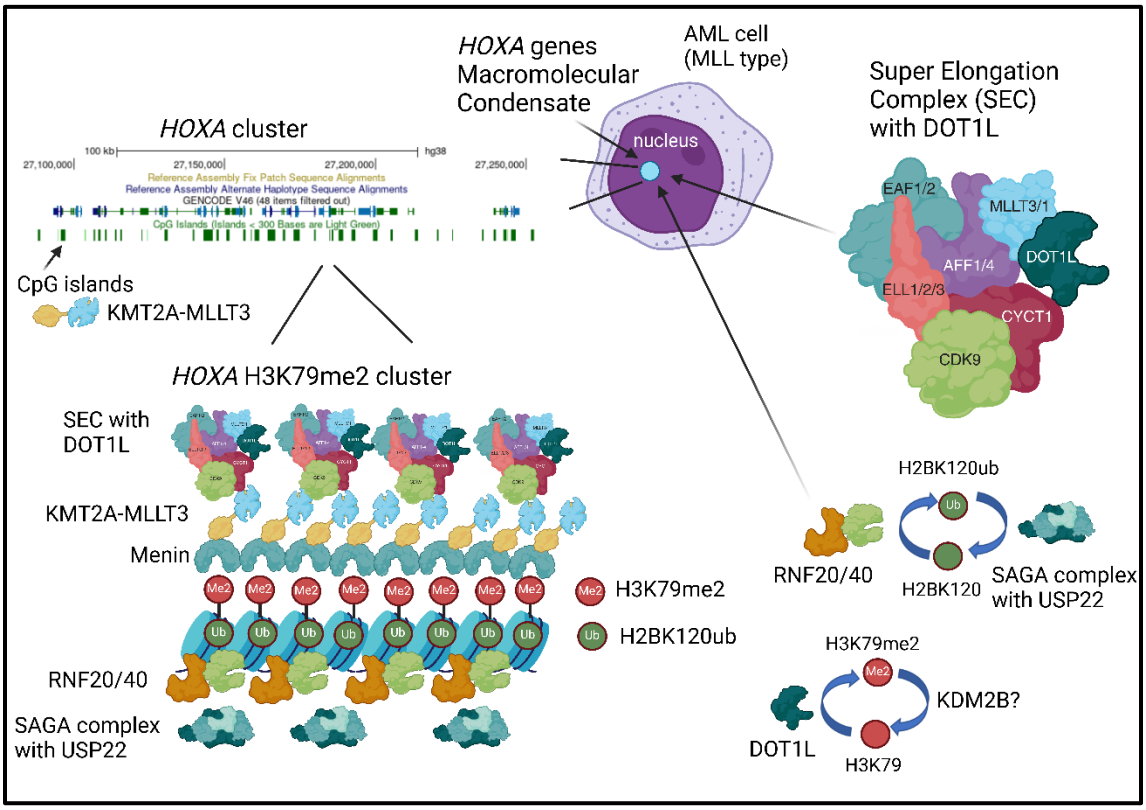

Figure 34: Sequential events through which the KMT2A-MLLT3 fusion protein hijacks the transcriptional machinery and chromatin-modifying enzymes, including the SEC complex, DOT1L, RNF20/40, Menin, and others, to the HOXA cluster, forming a macromolecular condensate region in the nucleus of MLL cell. The *HOXA* gene cluster located on chromosome 7 has been shown in the figure. The CpG islands (green bars) indicate regulatory regions that KMT2A-MLLT3 is recruited to and binds. In the top right corner, DOT1L with Super Elongation Complex (SEC), is shown being recruited to the *HOXA* cluster by KMT2A-MLLT3, facilitating transcriptional elongation and dysregulating target genes such as *HOXA9*. Menin, a reader of H3K79me2 marks, is also depicted as attached to the N-terminus of KMT2A and recruited to the

HOXA9 cluster, where it can read H3K79me2 marks and exert its effects. The RNF20/40 complex enzyme is also recruited to the *HOXA9* cluster, ubiquitinating H2B at lysine 120 (H2BK120ub), which can increase DOT1L methyltransferase activity. Both H3K79me2 and H2BK120ub facilitate transcriptional elongation of *HOXA* cluster genes, especially *HOXA9*. The steady state of the two PTMs, H3K79me2, and H2BK120ub, is shown in the bottom right-hand corner, determined by the enzymes adding the mark and the enzymes removing the mark. USP22, part of the SAGA complex, is recruited to this region to deubiquitinate H2BK120ub and remove this mark. The potential involvement of KDM2B in demethylating H3K79me2 is also suggested.

We observed that the *HOXA* cluster in MOLM-13 cells is decorated with several active marks, including H3K79me2, H3K4me3, H3K27ac, and H3K36me3, while in K562 cells, there are no active marks associated with the *HOXA* cluster. In MOLM-13 cells carrying the KMT2A-MLLT3 fusion protein, a hallmark of mixed lineage leukemia, we found a striking enrichment pattern of H3K79me2 across the entire *HOXA* cluster, spanning from *HOXA1* to *HOXA11* genes, non-coding RNAs, and intergenic regions. Typically, H3K79me2 marks genomic regions beginning downstream of the transcription start site (TSS), extending through the gene body, and diminishing towards the 3' end. However, in the *HOXA* cluster in MOLM-13 cells, the widespread decoration of H3K79me2 suggests a regulatory complexity beyond conventional models **(Figure 32)**. Although H3K4me3 and H3K27ac, both active marks, are present in this domain, they are not as extensive as the H3K79me2 domain. This H3K79me2 cluster also shows the presence of DOT1L and DNAase I hypersensitivity throughout the domain, indicating an unstable nucleosome structure. This instability could be attributed to multiple factors, including nucleosomes with various histone PTMs such as H3K4me3, H3K27ac, H3K36me3, and others, as well as chromatin remodelers (ATP-dependent complexes), writers (DOT1L), and readers (Menin).

I postulate that the *HOXA* H3K79me2 domain in MOLM-13 cells is in a macromolecular condensate in which DOT1L and complexes involved in transcription elongation (e.g. Super Elongation Complex, SEC) are present in high concentrations **(Figure 32)**. The fusion protein would play a role in forming this condensate. This exciting possibility will need to be explored further through imaging methods that visualize unusual structures in the nucleus.

Regarding the H2BK120ub modification, although we did not find ChIP-Seq data for H2BK120ub in MOLM-13 cells, tracks in THP-1 cells, another MLL line with the same KMT2A-MLLT3 fusion protein, showed that H2BK120ub and H3K79me2 have similar distributions along active genes, especially within the *HOXA* gene cluster (Eric Wang et al., 2013). Together, these modifications create an environment conducive to gene activation, potentially transforming the *HOXA* cluster into a central hub for transcriptional machinery **(Figure 32)**.

My results uncovered that MOLM-13 cells exhibit higher levels of H2BK120ub compared to K562 cells. This groundbreaking finding highlights, for the first time, the varying levels of H2BK120ub across different leukemia cell lines. It also demonstrates that cell lines harboring KMT2A-MLLT3 and elevated DOT1L activity correspondingly show increased H2BK120ub levels. Research has demonstrated that RNF20 is essential for KMT2A fusion-mediated leukemogenesis. Suppressing RNF20 expression leads to the inhibition of cell proliferation. Furthermore, RNF20 knockdown results in reduced expression of KMT2A-fusion target genes, including *HOXA9* (E. Wang et al., 2013). These findings suggest that higher levels of H2BK120ub in MOLM-13 cells may be associated with enhanced recruitment and activity of the RNF20/40 complex to active regions like *HOXA9*, contributing to the maintenance and expression of KMT2A fusion target genes, thereby supporting leukemic cell proliferation. However, further research is needed to clarify the specific role and impact of H2BK120ub and RNF20 in KMT2A fusion-driven leukemogenesis.

H3K36me3 and H3K79me2 are both elongation-related marks found along the gene bodies of active genes. The tracks revealed that H3K36me3 and H3K79me2 both decorate the *HOXA9* gene in MOLM-13 cells. However, these two marks are out of synchronization because the H3K79me2 mark usually starts before the H3K36me3 mark along the gene body. For the *HOXA* cluster on MOLM-13 cells, the H3K36me3 has the most intensity over the expressed gene bodies. The tracks, however, do not prove that H3K79me2 and H3K79me2 are on the same histone H3. My histone Co-IP and immunoblot study results showed that some nucleosomes have H3 with K36me3 and K79me2 in MOLM-13 and K562 cells. These two PTMs are located in different nucleosome regions and are unlikely to recruit a reader recognizing both marks. The more likely scenario is that each PTM recruits its reader; Menin for H3K79me2 (Lin et al., 2023) and MRG15 and many others for H3K36me3 (Sharda & Humphrey, 2022).

4.3 Histone PTM dynamics

The steady-state level of histone PTMs reflects the balance between adding and removing these modifications by writer and eraser enzymes in a cell which is crucial for maintaining normal gene expression **(Figure 32)**. Disruptions in this balance can lead to abnormal gene expression, contributing to disease development. Therefore, studying the steady-state levels of PTMs provides valuable insights into cellular mechanisms and can help identify potential therapeutic targets for treating diseases associated with PTM dysregulation, such as mixed lineage leukemia.

H3K79me2 modification, found in active regions and linked to transcriptional elongation, is deposited by DOT1L, removed by KDM2B (Kang et al., 2018), and recognized (reader) by Menin (Lin et al., 2023) **(Figure 32)**. Considering all these factors is crucial for understanding the dynamics of this epigenetic mark.

My result showed that DOT1L protein and transcript levels were similar in MOLM-13 and K562 cells. However, higher levels of H3K79me2 were observed in MOLM-13 cells compared to K562 cells, indicating increased DOT1L activity in MOLM-13. The higher activity of DOT1L might be due to several reasons including, specific recruitment to the genome by fusion protein, the altered SEC complex that has the KMT2A-MLLT3 fusion protein, the presence of H2BK120ub, the lower activity of the H3K79me2 eraser, and the higher presence of its reader. I will explain each of these in detail below.

The higher levels of H3K79me2 in MOLM-13 cells compared to K562 cells are likely due to differences in how DOT1L is recruited to specific genomic sites, influenced by the fusion protein, and its increased enzymatic activity. It seems that in MOLM-13 cells, DOT1L is more effectively recruited to genomic regions associated with genes like *HOXA9* because of the KMT2A-MLLT3 fusion protein that exists in MOLM-13 cells. My findings also revealed that MOLM-13 cells exhibit elevated levels of H2BK120ub compared to K562 cells. Thus, increased H2BK120ub facilitates DOT1L's proper positioning on the nucleosome and its activity, leading to elevated H3K79me2 levels in MOLM-13 cells. This underscores the pivotal role of the H2BK120ub in regulating DOT1L methyltransferase activity to produce H3K79me2. Both DOT1L and H2BK120ub are crucial for transcription elongation, making them essential for activating *HOXA9* gene expression in mixed lineage leukemia. DOT1L has a role in destabilizing the nucleosome without its enzymatic activity as well (Jang et al., 2019). Together, H2BK120ub, which

destabilizes the nucleosome structure (Cao et al., 2020; Jang et al., 2019), and DOT1L may render a nucleosome unstable and result in rapid nucleosome dissolution and reassembly. These events may result in transient nucleosome-free stretches along the *HOXA* H3K79me2 domain that is detected by DNase I.

Considering the dynamics of PTMs, it is crucial to explore enzymes responsible for removing H3K79me2. Although the literature suggests KDM2B may demethylate H3K79me2, uncertainties remain **(Figure 32)**. Lower demethylase activity in MOLM-13 compared to K562 cells might contribute to increased H3K79me2 persistence. Thus, evaluating KDM2B activity in both cell lines would provide clarity on this aspect.

H3K79me2 is recognized by the reader protein called Menin, which is believed to be a component of the Super Elongation Complex crucial for transcriptional regulation (Yokoyama et al., 2005) **(Figure 32)**. Menin also binds to the N-terminal part of KMT2A (Brzezinka et al., 2020). Assessing Menin levels could reveal differential patterns between MOLM-13 and K562 cells. In the case of KMT2A-MLLT3, which is recruited to the *HOXA9* gene, Menin can be robustly recruited there through Menin's binding to the N-terminal part of KMT2A. Since DOT1L and H3K79me2 are also present at this *HOXA9*, Menin can recognize more H3K79me2, potentially amplifying the H3K79me2 effect and enhancing transcriptional regulation. Exploring Menin further could provide valuable insights into the dynamics of H3K79me2 in MOLM-13 and K562 cells.

The H2BK120ub modification, found predominantly in active genomic regions associated with transcriptional elongation, is catalyzed by the E3 ubiquitin ligase complex RNF20/RNF40 and is erased by the deubiquitinates including USP22, USP44, and USP3 **(Figure 32)**. My findings indicate a higher level of H2BK120ub in MOLM-13 cells compared to K562, suggesting enhanced recruitment and activity of the RNF20/40 complex in MOLM-13. This higher H2BK120ub level aligns with the elevated activity of DOT1L in MOLM-13 cells, as H2BK120ub is known to enhance DOT1L's methyltransferase activity. Thus, these results suggest that H2BK120ub facilitates DOT1L's localization to the MOLM-13 genome, potentially leading to increased H3K79me2 methylation compared to K562. It's important to note that H2BK120ub turnover is rapid, indicating active removal by deubiquitination enzymes like USP22 (Figure 32). However, I have not examined the levels of USP22 in MOLM-13 and K562 cells. Understanding USP22 levels

could provide insights into the regulation of H2BK120ub dynamics and its impact on DOT1L-mediated H3K79me2 methylation in these cell lines.

4.4 Canonical and variant histone H3

My research studies have shown that levels of H3 canonical (H3.1 and H3.2) and variant H3.3 are similar in K562 and MOLM-13 cells. However, ChIP-Seq studies would be needed to determine the genomic location of H3.3. It is expected that H3.3 will be located in the expressed regions of the genome. H3.3 is considered a replacement histone, and it can be used to rebuild nucleosomes that are displaced by the elongation machinery, transcription factors, and/or chromatin remodelers. Thus, I predict that H3.3 will be present throughout the *HOXA* H3K79me2 domain in MOLM-13 cells but not in this region in K562 cells. Moreover, H3.1, H3.2, and H3.3 have K79me2, with the levels of this PTM being greater in MOLM-13 than in K562 cells. This result suggests that expressed regions in MOLM-13 cells, such as the *HOXA* cluster, will have nucleosomes with several possible combinations. For example, one nucleosome may likely have a combination of one of the canonical H3 variants (H3.1 or H3.2) and one H3.3 variant.

More importantly, I observed that H3.3 had more K79me2 than H3.1 or H3.2 which revealed that the histone variant H3.3 is preferentially dimethylated at lysine 79 (K79). Methylation at K79 of histone H3, particularly dimethylation, is associated with active transcription (elongation) and plays a role in regulating gene expression. The dimethylation of H3.3 at K79 could enhance the transcriptional activity of genes in regions where H3.3 is incorporated, thereby promoting gene expression necessary for leukemic cell functions. This modification could contribute to the transcriptional activation of oncogenes or other genes involved in cell proliferation and survival, driving leukemogenesis. Considering the usable chromatin structure and high transcriptional activity at the *HOXA9* gene in MOLM-13, it is likely that H3.3 is incorporated more in that region. This could facilitate nucleosome turnover and chromatin instability, further promoting *HOXA9* gene expression. More information is needed to confirm these findings, and a ChIP-Seq experiment to map H3.3 distribution along the *HOXA9* gene could be crucial in understanding H3.3's role in *HOXA9* expression in MOLM-13 cells.

I also demonstrated that there is a preference for the K79me2 antibody binding to the H3.1K79me2 peptide over the H3.3K79me2 peptide. This suggests that the K79me2 antibody has a higher

affinity for the H3.1K79me2 modification. Consequently, the levels of H3.3K79me2 might be higher than observed in my study.

4.5 Bortezomib

Treatment of MOLM-13 cells with Bortezomib, a proteasome inhibitor, results in the rapid deubiquitination of the histones. My results showed the rapid loss of H2BK120ub in Bortezomib-treated cells. I reason that the activity of the deubiquitinases (DUBs) to remove ubiquitin from H2BK120ub and the lack of nuclear ubiquitin for RNF20/40 to put ubiquitin back into H2BK120 resulted in the loss of H2BK120ub. I speculate that the loss of H2BK120ub may cripple elongation, resulting in the decline of *HOXA9* transcripts. This idea is consistent with my observations that there is a decline in *HOXA9* transcripts in the Bortezomib-treated MOLM-13 cells.

I observed a decline in the H3K79me2 level in the Bortezomib-treated MOLM-13 cells. The loss of H2BK120ub which attracts and enhances the activity of the DOT1L enzyme, is the likely explanation for the decline in H3K79me2 levels. The decline in H3K79me2 is slower than that of H2BK120ub because of the low activity of the H3K79me2 erasers or other events that result in the removal of nucleosomes with H3K79me2. Both H2BK120ub and H3K79me2 are marks of elongation, and the loss of these PTMs could result in the decline of the transcriptional activity of expressed genes. Moreover, H2BK120ub and H3K79me2 both are marks of elongation, and the loss of these PTMs could result in the decline of transcriptional activity of expressed genes like *HOXA9*.

4.6 Significance of study

Developing effective treatments with lower side effects for mixed lineage leukemia remains a formidable challenge despite substantial research efforts. This leukemia subtype, characterized by the KMT2A-MLLT3 fusion protein, presents a complex pathogenesis contributing to its poor prognosis. Novel therapeutic strategies are urgently needed to address the unique molecular features and treatment resistance mechanisms associated with MLL harboring KMT2A-MLLT3, aiming to significantly improve outcomes for affected patients. We know that MLL patients with KMT2A-MLLT3 exhibit heightened transcriptional activity, largely driven by the overexpression of *HOXA9*. Transcriptional elongation control is a crucial regulatory step in *HOXA9* gene expression. Therefore, targeting and disrupting the transcriptional machinery presents a novel

approach to tackling the elevated gene expression in MLL. This is why I chose to use proteasome inhibitors like bortezomib to manipulate key transcriptional elongation markers such as H2BK120ub and H3K79me2. By disrupting these markers, we aim to diminish *HOXA9* expression, offering a promising strategy to combat MLL. My study delves into the fundamental mechanisms of mixed lineage leukemia using the MOLM-13 cell line, a model that accurately mimics the disease in a controlled laboratory setting. Utilizing cell lines instead of patient samples makes the research more cost-effective and manageable, allowing for detailed mechanistic insights. However, future investigations with patient samples are essential to validate these findings and understand their real-world applicability, ensuring that our research translates effectively to patient care.

I discovered that bortezomib, an FDA-approved drug for treating multiple myeloma, effectively reduces HOXA9 gene expression and lowers the H3K79me2 level in MOLM-13 cells at clinically relevant concentrations (5 nM). This efficacy is promising for clinical application, as it may minimize side effects due to the lower concentration required. Our findings suggest that exploring bortezomib further could lead to novel treatment approaches for mixed lineage leukemia. By uncovering these insights, my study aims to contribute to the development of targeted therapies that could significantly improve the management and outcomes for patients with mixed lineage leukemia.

DOT1L inhibitors like EPZ5676 have shown promise in early trials but faced challenges due to off-target side effects and toxicity concerns. There is still a critical need for effective DOT1L inhibitors that can advance through clinical trials successfully. Other approaches can also be considered to mitigate the effects of histone post-translational modifications. One such strategy involves using inhibitors that block the 'readers' of specific histone modifications. These readers are proteins that recognize and bind to specific histone PTMs, thereby influencing gene expression and other chromatin-related processes. For example, Menin, a protein that acts as a reader of H3K79me2, can be targeted with specific inhibitors. By blocking Menin's ability to recognize and bind to H3K79me2 and KMT2A, it is possible to disrupt the downstream effects mediated by fusion protein and H3K79me2. This approach can be particularly useful in the context of diseases like mixed lineage leukemia, where Menin can bind to the KMT2A and can be recruited to the *HOXA* gene. Moreover, targeting the fusion protein itself presents a promising therapeutic strategy. In mixed lineage leukemia, the fusion protein aberrantly targets CpG islands within the

HOXA cluster, which might lead to the formation of macromolecular condensates. These condensates facilitate the recruitment of various epigenetic modifiers, such as DOT1L, which catalyzes the methylation of H3K79, thereby promoting gene expression and contributing to leukemogenesis (Figure 32). By inhibiting the binding of the fusion protein to CpG islands or by misdirecting the fusion protein away from these critical regions, it may be possible to disrupt the formation of these macromolecular condensates. This, in turn, could reduce the recruitment and activity of DOT1L at the *HOXA* cluster, diminishing the aberrant gene expression that drives MLL. Another option is using combination therapy for leukemia. Several studies have shown that combining different inhibitors can achieve better outcomes than using a single inhibitor alone. For example, combining bortezomib with HDAC inhibitors and Menin inhibitors could be a promising approach to tackling MLL.

References:

Adam, S., Dabin, J., Chevallier, O., Leroy, O., Baldeyron, C., Corpet, A., Lomonte, P., Renaud, O., Almouzni, G., & Polo, S. E. (2016). Real-Time Tracking of Parental Histones Reveals Their Contribution to Chromatin Integrity Following DNA Damage. *Mol Cell*, *64*(1), 65-78. https://doi.org/10.1016/j.molcel.2016.08.019

Adamaki, M., Lambrou, G. I., Athanasiadou, A., Vlahopoulos, S., Papavassiliou, A. G., & Moschovi, M. (2015). HOXA9 and MEIS1 gene overexpression in the diagnosis of childhood acute leukemias: Significant correlation with relapse and overall survival. *Leukemia research*, *39*(8), 874-882.

Adams, J. (2002). Preclinical and clinical evaluation of proteasome inhibitor PS-341 for the treatment of cancer. *Curr Opin Chem Biol*, *6*(4), 493-500. https://doi.org/10.1016/s1367-5931(02)00343-5

Ahmad, K., & Henikoff, S. (2002). The histone variant H3.3 marks active chromatin by replication-independent nucleosome assembly. *Mol Cell*, *9*(6), 1191-1200. https://doi.org/10.1016/s1097-2765(02)00542-7

Ai, H., Sun, M., Liu, A., Sun, Z., Liu, T., Cao, L., Liang, L., Qu, Q., Li, Z., Deng, Z., Tong, Z., Chu, G., Tian, X., Deng, H., Zhao, S., Li, J. B., Lou, Z., & Liu, L. (2022). H2B Lys34 Ubiquitination Induces Nucleosome Distortion to Stimulate Dot1L Activity. *Nat Chem Biol*, *18*(9), 972-980. https://doi.org/10.1038/s41589-022-01067-7

Amin, A. D., Vishnoi, N., & Prochasson, P. (2013). A global requirement for the HIR complex in the assembly of chromatin. *Biochim Biophys Acta*, *1819*(3-4), 264-276. https://doi.org/10.1016/j.bbagrm.2011.07.008

Arnold, O., Barbosa, K., Deshpande, A. J., & Zhu, N. (2022). The Role of DOT1L in Normal and Malignant Hematopoiesis. *Front Cell Dev Biol*, *10*, 917125. https://doi.org/10.3389/fcell.2022.917125

Batta, K., Zhang, Z., Yen, K., Goffman, D. B., & Pugh, B. F. (2011). Genome-wide function of H2B ubiquitylation in promoter and genic regions. *Genes Dev*, *25*(21), 2254-2265. https://doi.org/10.1101/gad.177238.111

Bedford, M. T., & Clarke, S. G. (2009). Protein arginine methylation in mammals: who, what, and why. *Mol Cell*, *33*(1), 1-13. https://doi.org/10.1016/j.molcel.2008.12.013

Belotserkovskaya, R., Oh, S., Bondarenko, V. A., Orphanides, G., Studitsky, V. M., & Reinberg, D. (2003). FACT facilitates transcription-dependent nucleosome alteration. *Science*, *301*(5636), 1090-1093. https://doi.org/10.1126/science.1085703

Bhattacharya, S., Levy, M. J., Zhang, N., Li, H., Florens, L., Washburn, M. P., & Workman, J. L. (2021). The methyltransferase SETD2 couples transcription and splicing by engaging mRNA processing factors through its SHI domain. *Nat Commun*, *12*(1), 1443. https://doi.org/10.1038/s41467-021-21663-w

Bilokapic, S., & Halic, M. (2019). Nucleosome and ubiquitin position Set2 to methylate H3K36. *Nature Communications*, *10*(1), 3795. https://doi.org/10.1038/s41467-019-11726-4

Bilokapic, S., & Halic, M. (2019). Nucleosome and ubiquitin position Set2 to methylate H3K36. *Nat Commun*, *10*(1), 3795. https://doi.org/10.1038/s41467-019-11726-4

Britten, O., Ragusa, D., Tosi, S., & Mostafa Kamel, Y. (2019). MLL-Rearranged Acute Leukemia with t (4; 11)(q21; q23)—Current Treatment Options. Is There a Role for CAR-T Cell Therapy? *Cells*, *8*(11), 1341.

Brown, M. A., Sims, R. J., 3rd, Gottlieb, P. D., & Tucker, P. W. (2006). Identification and characterization of Smyd2: a split SET/MYND domain-containing histone H3 lysine 36-specific methyltransferase that interacts with the Sin3 histone deacetylase complex. *Mol Cancer*, *5*, 26. https://doi.org/10.1186/1476-4598-5-26

Campos, E. I., & Reinberg, D. (2009). Histones: annotating chromatin. *Annu Rev Genet*, *43*, 559-599. https://doi.org/10.1146/annurev.genet.032608.103928

Cao, R., Wang, L., Wang, H., Xia, L., Erdjument-Bromage, H., Tempst, P., Jones, R. S., & Zhang, Y. (2002). Role of histone H3 lysine 27 methylation in Polycomb-group silencing. *Science*, *298*(5595), 1039-1043. https://doi.org/10.1126/science.1076997

Castiglioni, S., Di Fede, E., Bernardelli, C., Lettieri, A., Parodi, C., Grazioli, P., Colombo, E. A., Ancona, S., Milani, D., & Ottaviano, E. (2022). KMT2A: Umbrella gene for multiple diseases. *Genes*, *13*(3), 514.

Cheon, Y., Kim, H., Park, K., Kim, M., & Lee, D. (2020). Dynamic modules of the coactivator SAGA in eukaryotic transcription. *Experimental & Molecular Medicine*, *52*(7), 991-1003. https://doi.org/10.1038/s12276-020-0463-4

Davie, J. R., & Murphy, L. C. (1990). Level of ubiquitinated histone H2B in chromatin is coupled to ongoing transcription. *Biochemistry*, *29*(20), 4752-4757. https://doi.org/10.1021/bi00472a002

Devoucoux, M., Roques, C., Lachance, C., Lashgari, A., Joly-Beauparlant, C., Jacquet, K., Alerasool, N., Prudente, A., Taipale, M., Droit, A., Lambert, J. P., Hussein, S. M. I., & Côté, J. (2022). MRG Proteins Are Shared by Multiple Protein Complexes With Distinct Functions. *Mol Cell Proteomics*, *21*(7), 100253. https://doi.org/10.1016/j.mcpro.2022.100253

Edmunds, J. W., Mahadevan, L. C., & Clayton, A. L. (2008). Dynamic histone H3 methylation during gene induction: HYPB/Setd2 mediates all H3K36 trimethylation. *Embo j*, *27*(2), 406-420. https://doi.org/10.1038/sj.emboj.7601967

Eom, G. H., Kim, K. B., Kim, J. H., Kim, J. Y., Kim, J. R., Kee, H. J., Kim, D. W., Choe, N., Park, H. J., Son, H. J., Choi, S. Y., Kook, H., & Seo, S. B. (2011). Histone methyltransferase SETD3 regulates muscle differentiation. *J Biol Chem*, *286*(40), 34733-34742. https://doi.org/10.1074/jbc.M110.203307

Feng, Q., Wang, H., Ng, H. H., Erdjument-Bromage, H., Tempst, P., Struhl, K., & Zhang, Y. (2002). Methylation of H3-lysine 79 is mediated by a new family of HMTases without a SET domain. *Curr Biol*, *12*(12), 1052-1058. https://doi.org/10.1016/s0960-9822(02)00901-6

Fischle, W., Tseng, B. S., Dormann, H. L., Ueberheide, B. M., Garcia, B. A., Shabanowitz, J., Hunt, D. F., Funabiki, H., & Allis, C. D. (2005). Regulation of HP1-chromatin binding by histone H3 methylation and phosphorylation. *Nature*, *438*(7071), 1116-1122. https://doi.org/10.1038/nature04219

Fodor, B. D., Kubicek, S., Yonezawa, M., O'Sullivan, R. J., Sengupta, R., Perez-Burgos, L., Opravil, S., Mechtler, K., Schotta, G., & Jenuwein, T. (2006). Jmjd2b antagonizes H3K9 trimethylation at pericentric heterochromatin in mammalian cells. *Genes Dev*, *20*(12), 1557-1562. https://doi.org/10.1101/gad.388206

Früh, K., Gossen, M., Wang, K., Bujard, H., Peterson, P. A., & Yang, Y. (1994). Displacement of housekeeping proteasome subunits by MHC-encoded LMPs: a newly discovered mechanism for modulating the multicatalytic proteinase complex. *Embo j*, *13*(14), 3236-3244. https://doi.org/10.1002/j.1460-2075.1994.tb06625.x

Fu, J., Liao, L., Balaji, K. S., Wei, C., Kim, J., & Peng, J. (2021). Epigenetic modification and a role for the E3 ligase RNF40 in cancer development and metastasis. *Oncogene*, *40*(3), 465-474. https://doi.org/10.1038/s41388-020-01556-w

Fuchs, G., & Oren, M. (2014). Writing and reading H2B monoubiquitylation. *Biochim Biophys Acta*, *1839*(8), 694-701. https://doi.org/10.1016/j.bbagrm.2014.01.002

Gal, C., Moore, K. M., Paszkiewicz, K., Kent, N. A., & Whitehall, S. K. (2015). The impact of the HIRA histone chaperone upon global nucleosome architecture. *Cell Cycle*, *14*(1), 123-134. https://doi.org/10.4161/15384101.2014.967123

Gillette, T. G., & Hill, J. A. (2015). Readers, writers, and erasers: chromatin as the whiteboard of heart disease. *Circ Res*, *116*(7), 1245-1253. https://doi.org/10.1161/circresaha.116.303630

Goldberg, A. D., Banaszynski, L. A., Noh, K. M., Lewis, P. W., Elsaesser, S. J., Stadler, S., Dewell, S., Law, M., Guo, X., Li, X., Wen, D., Chapgier, A., DeKelver, R. C., Miller, J. C., Lee, Y. L., Boydston, E. A., Holmes, M. C., Gregory, P. D., Greally, J. M., . . . Allis, C. D. (2010). Distinct factors control histone variant H3.3 localization at specific genomic regions. *Cell*, *140*(5), 678-691. https://doi.org/10.1016/j.cell.2010.01.003

Heard, E., Rougeulle, C., Arnaud, D., Avner, P., Allis, C. D., & Spector, D. L. (2001). Methylation of histone H3 at Lys-9 is an early mark on the X chromosome during X inactivation. *Cell*, *107*(6), 727-738. https://doi.org/10.1016/s0092-8674(01)00598-0

Henikoff, S., & Smith, M. M. (2015). Histone variants and epigenetics. *Cold Spring Harb Perspect Biol*, *7*(1), a019364. https://doi.org/10.1101/cshperspect.a019364

Hershko, A., & Ciechanover, A. (1998). The ubiquitin system. *Annual review of biochemistry*, *67*(1), 425-479.

Hideshima, T., Richardson, P., Chauhan, D., Palombella, V. J., Elliott, P. J., Adams, J., & Anderson, K. C. (2001). The proteasome inhibitor PS-341 inhibits growth, induces apoptosis, and overcomes drug resistance in human multiple myeloma cells. *Cancer Res*, *61*(7), 3071-3076.

Huisinga, K. L., Brower-Toland, B., & Elgin, S. C. (2006). The contradictory definitions of heterochromatin: transcription and silencing. *Chromosoma*, *115*, 110-122.

Jagannath, S., Durie, B. G., Wolf, J., Camacho, E., Irwin, D., Lutzky, J., McKinley, M., Gabayan, E., Mazumder, A., Schenkein, D., & Crowley, J. (2005). Bortezomib therapy alone and in combination with dexamethasone for previously untreated symptomatic multiple myeloma. *Br J Haematol*, *129*(6), 776-783. https://doi.org/10.1111/j.1365-2141.2005.05540.x

Jeusset, L. M., & McManus, K. J. (2017). Ubiquitin Specific Peptidase 22 Regulates Histone H2B Mono-Ubiquitination and Exhibits Both Oncogenic and Tumor Suppressor Roles in Cancer. *Cancers (Basel)*, *9*(12). https://doi.org/10.3390/cancers9120167

Jones, B., Su, H., Bhat, A., Lei, H., Bajko, J., Hevi, S., Baltus, G. A., Kadam, S., Zhai, H., Valdez, R., Gonzalo, S., Zhang, Y., Li, E., & Chen, T. (2008). The histone H3K79 methyltransferase Dot1L is essential for mammalian development and heterochromatin structure. *PLoS Genet*, *4*(9), e1000190. https://doi.org/10.1371/journal.pgen.1000190

Joo, H. Y., Jones, A., Yang, C., Zhai, L., Smith, A. D. t., Zhang, Z., Chandrasekharan, M. B., Sun, Z. W., Renfrow, M. B., Wang, Y., Chang, C., & Wang, H. (2011). Regulation of histone H2A and H2B deubiquitination and Xenopus development by USP12 and USP46. *J Biol Chem*, *286*(9), 7190-7201. https://doi.org/10.1074/jbc.M110.158311

Kamens, J. L., Nance, S., Koss, C., Xu, B., Cotton, A., Lam, J. W., Garfinkle, E. A., Nallagatla, P., Smith, A. M., & Mitchell, S. (2023). Proteasome inhibition targets the KMT2A transcriptional complex in acute lymphoblastic leukemia. *Nature Communications*, *14*(1), 809.

Kamens, J. L., Nance, S., Koss, C., Xu, B., Cotton, A., Lam, J. W., Garfinkle, E. A. R., Nallagatla, P., Smith, A. M. R., Mitchell, S., Ma, J., Currier, D., Wright, W. C., Kavdia, K., Pagala, V. R., Kim, W., Wallace, L. M., Cho, J. H., Fan, Y., . . . Gruber, T. A. (2023). Proteasome inhibition targets the KMT2A transcriptional complex in acute lymphoblastic leukemia. *Nat Commun*, *14*(1), 809. https://doi.org/10.1038/s41467-023-36370-x

Kang, J. Y., Kim, J. Y., Kim, K. B., Park, J. W., Cho, H., Hahm, J. Y., Chae, Y. C., Kim, D., Kook, H., Rhee, S., Ha, N. C., & Seo, S. B. (2018). KDM2B is a histone H3K79 demethylase and induces transcriptional repression via sirtuin-1-mediated chromatin silencing. *Faseb j*, *32*(10), 5737-5750. https://doi.org/10.1096/fj.201800242R

Kari, V., Shchebet, A., Neumann, H., & Johnsen, S. A. (2011). The H2B ubiquitin ligase RNF40 cooperates with SUPT16H to induce dynamic changes in chromatin structure during DNA double-strand break repair. *Cell Cycle*, *10*(20), 3495-3504. https://doi.org/10.4161/cc.10.20.17769

Kemble, D. J., McCullough, L. L., Whitby, F. G., Formosa, T., & Hill, C. P. (2015). FACT Disrupts Nucleosome Structure by Binding H2A-H2B with Conserved Peptide Motifs. *Mol Cell*, *60*(2), 294-306. https://doi.org/10.1016/j.molcel.2015.09.008

Kim, S. K., Jung, I., Lee, H., Kang, K., Kim, M., Jeong, K., Kwon, C. S., Han, Y. M., Kim, Y. S., Kim, D., & Lee, D. (2012). Human histone H3K79 methyltransferase DOT1L protein

[corrected] binds actively transcribing RNA polymerase II to regulate gene expression. *J Biol Chem*, *287*(47), 39698-39709. https://doi.org/10.1074/jbc.M112.384057

Kizer, K. O., Phatnani, H. P., Shibata, Y., Hall, H., Greenleaf, A. L., & Strahl, B. D. (2005). A novel domain in Set2 mediates RNA polymerase II interaction and couples histone H3 K36 methylation with transcript elongation. *Molecular and cellular biology*, *25*(8), 3305-3316.

Klein, R. H., & Knoepfler, P. S. (2023). Knockout tales: the versatile roles of histone H3.3 in development and disease. *Epigenetics Chromatin*, *16*(1), 38. https://doi.org/10.1186/s13072-023-00512-8

Kondagunta, G. V., Drucker, B., Schwartz, L., Bacik, J., Marion, S., Russo, P., Mazumdar, M., & Motzer, R. J. (2004). Phase II trial of bortezomib for patients with advanced renal cell carcinoma. *J Clin Oncol*, *22*(18), 3720-3725. https://doi.org/10.1200/jco.2004.10.155

Latham, J. A., Chosed, R. J., Wang, S., & Dent, S. Y. (2011). Chromatin signaling to kinetochores: transregulation of Dam1 methylation by histone H2B ubiquitination. *Cell*, *146*(5), 709-719. https://doi.org/10.1016/j.cell.2011.07.025

Lee, K. K., & Workman, J. L. (2007). Histone acetyltransferase complexes: one size doesn't fit all. *Nature reviews Molecular cell biology*, *8*(4), 284-295.

Lee, S., Oh, S., Jeong, K., Jo, H., Choi, Y., Seo, H. D., Kim, M., Choe, J., Kwon, C. S., & Lee, D. (2018). Dot1 regulates nucleosome dynamics by its inherent histone chaperone activity in yeast. *Nature Communications*, *9*(1), 240. https://doi.org/10.1038/s41467-017-02759-8

Lee, S. H., Oshige, M., Durant, S. T., Rasila, K. K., Williamson, E. A., Ramsey, H., Kwan, L., Nickoloff, J. A., & Hromas, R. (2005). The SET domain protein Metnase mediates foreign DNA integration and links integration to nonhomologous end-joining repair. *Proc Natl Acad Sci U S A*, *102*(50), 18075-18080. https://doi.org/10.1073/pnas.0503676102

Lempiäinen, J. K., & Garcia, B. A. (2023). Characterizing crosstalk in epigenetic signaling to understand disease physiology. *Biochem J*, *480*(1), 57-85. https://doi.org/10.1042/bcj20220550

Li, B., Carey, M., & Workman, J. L. (2007). The role of chromatin during transcription. *Cell*, *128*(4), 707-719. https://doi.org/10.1016/j.cell.2007.01.015

Li, F., Mao, G., Tong, D., Huang, J., Gu, L., Yang, W., & Li, G. M. (2013). The histone mark H3K36me3 regulates human DNA mismatch repair through its interaction with MutSα. *Cell*, *153*(3), 590-600. https://doi.org/10.1016/j.cell.2013.03.025

Li, Y., Trojer, P., Xu, C. F., Cheung, P., Kuo, A., Drury, W. J., 3rd, Qiao, Q., Neubert, T. A., Xu, R. M., Gozani, O., & Reinberg, D. (2009). The target of the NSD family of histone lysine methyltransferases depends on the nature of the substrate. *J Biol Chem*, *284*(49), 34283-34295. https://doi.org/10.1074/jbc.M109.034462

Li, Y., Wen, H., Xi, Y., Tanaka, K., Wang, H., Peng, D., Ren, Y., Jin, Q., Dent, S. Y., Li, W., Li, H., & Shi, X. (2014). AF9 YEATS domain links histone acetylation to DOT1L-mediated H3K79 methylation. *Cell*, *159*(3), 558-571. https://doi.org/10.1016/j.cell.2014.09.049

Lim, P. S., Shannon, M. F., & Hardy, K. (2010). Epigenetic control of inducible gene expression in the immune system. *Epigenomics*, *2*(6), 775-795. https://doi.org/10.2217/epi.10.55

Luger, K., Mäder, A. W., Richmond, R. K., Sargent, D. F., & Richmond, T. J. (1997). Crystal structure of the nucleosome core particle at 2.8 A resolution. *Nature*, *389*(6648), 251-260. https://doi.org/10.1038/38444

Malik, H. S., & Henikoff, S. (2003). Phylogenomics of the nucleosome. *Nat Struct Biol*, *10*(11), 882-891. https://doi.org/10.1038/nsb996

Malinczak, C. A., Rasky, A. J., Fonseca, W., Schaller, M. A., Allen, R. M., Ptaschinski, C., Morris, S., & Lukacs, N. W. (2020). Upregulation of H3K27 Demethylase KDM6 During Respiratory Syncytial Virus Infection Enhances Proinflammatory Responses and Immunopathology. *J Immunol*, *204*(1), 159-168. https://doi.org/10.4049/jimmunol.1900741

Marschalek, R. (2016). Systematic classification of mixed-lineage leukemia fusion partners predicts additional cancer pathways. *Annals of laboratory medicine*, *36*(2), 85.

Martire, S., & Banaszynski, L. A. (2020). The roles of histone variants in fine-tuning chromatin organization and function. *Nat Rev Mol Cell Biol*, *21*(9), 522-541. https://doi.org/10.1038/s41580-020-0262-8

Martire, S., Gogate, A. A., Whitmill, A., Tafessu, A., Nguyen, J., Teng, Y. C., Tastemel, M., & Banaszynski, L. A. (2019). Phosphorylation of histone H3.3 at serine 31 promotes p300 activity and enhancer acetylation. *Nat Genet*, *51*(6), 941-946. https://doi.org/10.1038/s41588-019-0428-5

Marzluff, W. F., Gongidi, P., Woods, K. R., Jin, J., & Maltais, L. J. (2002). The human and mouse replication-dependent histone genes. *Genomics*, *80*(5), 487-498.

McGrath, J., & Solter, D. (1984). Completion of mouse embryogenesis requires both the maternal and paternal genomes. *Cell*, *37*(1), 179-183.

McKittrick, E., Gafken, P. R., Ahmad, K., & Henikoff, S. (2004). Histone H3.3 is enriched in covalent modifications associated with active chromatin. *Proc Natl Acad Sci U S A*, *101*(6), 1525-1530. https://doi.org/10.1073/pnas.0308092100

Minard, M. E., Jain, A. K., & Barton, M. C. (2009). Analysis of epigenetic alterations to chromatin during development. *Genesis*, *47*(8), 559-572. https://doi.org/10.1002/dvg.20534

Mohan, M., Herz, H. M., Takahashi, Y. H., Lin, C., Lai, K. C., Zhang, Y., Washburn, M. P., Florens, L., & Shilatifard, A. (2010). Linking H3K79 trimethylation to Wnt signaling through a novel Dot1-containing complex (DotCom). *Genes Dev*, *24*(6), 574-589. https://doi.org/10.1101/gad.1898410

Morris, S. A., Shibata, Y., Noma, K.-i., Tsukamoto, Y., Warren, E., Temple, B., Grewal, S. I., & Strahl, B. D. (2005). Histone H3 K36 methylation is associated with transcription elongation in Schizosaccharomyces pombe. *Eukaryotic cell*, *4*(8), 1446-1454.

Muhire, B. M., Booker, M. A., & Tolstorukov, M. Y. (2019). Non-neutral evolution of H3.3-encoding genes occurs without alterations in protein sequence. *Sci Rep*, *9*(1), 8472. https://doi.org/10.1038/s41598-019-44800-4

Newell-Price, J., Clark, A. J., & King, P. (2000). DNA methylation and silencing of gene expression. *Trends in Endocrinology & Metabolism*, *11*(4), 142-148.

Nicassio, F., Corrado, N., Vissers, J. H., Areces, L. B., Bergink, S., Marteijn, J. A., Geverts, B., Houtsmuller, A. B., Vermeulen, W., Di Fiore, P. P., & Citterio, E. (2007). Human USP3 is a chromatin modifier required for S phase progression and genome stability. *Curr Biol*, *17*(22), 1972-1977. https://doi.org/10.1016/j.cub.2007.10.034

Nilsen, T. W., & Graveley, B. R. (2010). Expansion of the eukaryotic proteome by alternative splicing. *Nature*, *463*(7280), 457-463. https://doi.org/10.1038/nature08909

Orphanides, G., LeRoy, G., Chang, C.-H., Luse, D. S., & Reinberg, D. (1998). FACT, a factor that facilitates transcript elongation through nucleosomes. *Cell*, *92*(1), 105-116.

Outchkourov, N. S., Muiño, J. M., Kaufmann, K., van Ijcken, W. F., Groot Koerkamp, M. J., van Leenen, D., de Graaf, P., Holstege, F. C., Grosveld, F. G., & Timmers, H. T. (2013). Balancing of histone H3K4 methylation states by the Kdm5c/SMCX histone demethylase

modulates promoter and enhancer function. *Cell Rep*, *3*(4), 1071-1079. https://doi.org/10.1016/j.celrep.2013.02.030

Papandreou, C. N., Daliani, D. D., Nix, D., Yang, H., Madden, T., Wang, X., Pien, C. S., Millikan, R. E., Tu, S. M., Pagliaro, L., Kim, J., Adams, J., Elliott, P., Esseltine, D., Petrusich, A., Dieringer, P., Perez, C., & Logothetis, C. J. (2004). Phase I trial of the proteasome inhibitor bortezomib in patients with advanced solid tumors with observations in androgen-independent prostate cancer. *J Clin Oncol*, *22*(11), 2108-2121. https://doi.org/10.1200/jco.2004.02.106

Rahman, S., Sowa, M. E., Ottinger, M., Smith, J. A., Shi, Y., Harper, J. W., & Howley, P. M. (2011). The Brd4 extraterminal domain confers transcription activation independent of pTEFb by recruiting multiple proteins, including NSD3. *Mol Cell Biol*, *31*(13), 2641-2652. https://doi.org/10.1128/mcb.01341-10

Rayasam, G. V., Wendling, O., Angrand, P. O., Mark, M., Niederreither, K., Song, L., Lerouge, T., Hager, G. L., Chambon, P., & Losson, R. (2003). NSD1 is essential for early post-implantation development and has a catalytically active SET domain. *Embo j*, *22*(12), 3153-3163. https://doi.org/10.1093/emboj/cdg288

Richardson, P. G., Sonneveld, P., Schuster, M. W., Irwin, D., Stadtmauer, E. A., Facon, T., Harousseau, J. L., Ben-Yehuda, D., Lonial, S., Goldschmidt, H., Reece, D., San-Miguel, J. F., Bladé, J., Boccadoro, M., Cavenagh, J., Dalton, W. S., Boral, A. L., Esseltine, D. L., Porter, J. B., . . . Anderson, K. C. (2005). Bortezomib or high-dose dexamethasone for relapsed multiple myeloma. *N Engl J Med*, *352*(24), 2487-2498. https://doi.org/10.1056/NEJMoa043445

Riggs, A. D. (1975). X inactivation, differentiation, and DNA methylation. *Cytogenetic and Genome Research*, *14*(1), 9-25.

Santos-Rosa, H., Schneider, R., Bannister, A. J., Sherriff, J., Bernstein, B. E., Emre, N. C., Schreiber, S. L., Mellor, J., & Kouzarides, T. (2002). Active genes are tri-methylated at K4 of histone H3. *Nature*, *419*(6905), 407-411. https://doi.org/10.1038/nature01080

Schübeler, D., MacAlpine, D. M., Scalzo, D., Wirbelauer, C., Kooperberg, C., van Leeuwen, F., Gottschling, D. E., O'Neill, L. P., Turner, B. M., Delrow, J., Bell, S. P., & Groudine, M. (2004). The histone modification pattern of active genes revealed through genome-wide chromatin analysis of a higher eukaryote. *Genes Dev*, *18*(11), 1263-1271. https://doi.org/10.1101/gad.1198204

Schwartz, R., & Davidson, T. (2004). Pharmacology, pharmacokinetics, and practical applications of bortezomib. *Oncology (Williston Park)*, *18*(14 Suppl 11), 14-21.

Shah, S. A., Potter, M. W., McDade, T. P., Ricciardi, R., Perugini, R. A., Elliott, P. J., Adams, J., & Callery, M. P. (2001). 26S proteasome inhibition induces apoptosis and limits growth of human pancreatic cancer. *J Cell Biochem*, *82*(1), 110-122. https://doi.org/10.1002/jcb.1150

Sharma, P., Sattarifard, H., Fatemiyan, N., Lakowski, T. M., & Davie, J. R. (2022). Bioinformatic Analyses of Broad H3K79me2 Domains in Different Leukemia Cell Line Data Sets. *Cells*, *11*(18), 2830. https://www.mdpi.com/2073-4409/11/18/2830

Shilatifard, A. (2008). Molecular implementation and physiological roles for histone H3 lysine 4 (H3K4) methylation. *Curr Opin Cell Biol*, *20*(3), 341-348. https://doi.org/10.1016/j.ceb.2008.03.019

Skucha, A., Ebner, J., Schmöllerl, J., Roth, M., Eder, T., César-Razquin, A., Stukalov, A., Vittori, S., Muhar, M., & Lu, B. (2018). MLL-fusion-driven leukemia requires SETD2 to safeguard genomic integrity. *Nature Communications*, *9*(1), 1983.

Song, Y. H., & Ahn, S. H. (2010). A Bre1-associated protein, large 1 (Lge1), promotes H2B ubiquitylation during the early stages of transcription elongation. *J Biol Chem*, *285*(4), 2361-2367. https://doi.org/10.1074/jbc.M109.039255

Strahl, B. D., & Allis, C. D. (2000). The language of covalent histone modifications. *Nature*, *403*(6765), 41-45. https://doi.org/10.1038/47412

Sun, Z., Zhang, Y., Jia, J., Fang, Y., Tang, Y., Wu, H., & Fang, D. (2020). H3K36me3, message from chromatin to DNA damage repair. *Cell & Bioscience*, *10*(1), 9. https://doi.org/10.1186/s13578-020-0374-z

Swigut, T., & Wysocka, J. (2007). H3K27 demethylases, at long last. *Cell*, *131*(1), 29-32. https://doi.org/10.1016/j.cell.2007.09.026

Tafessu, A., O'Hara, R., Martire, S., Dube, A. L., Saha, P., Gant, V. U., & Banaszynski, L. A. (2023). H3.3 contributes to chromatin accessibility and transcription factor binding at promoter-proximal regulatory elements in embryonic stem cells. *Genome Biology*, *24*(1), 25. https://doi.org/10.1186/s13059-023-02867-3

Tagami, H., Ray-Gallet, D., Almouzni, G., & Nakatani, Y. (2004). Histone H3.1 and H3.3 complexes mediate nucleosome assembly pathways dependent or independent of DNA synthesis. *Cell*, *116*(1), 51-61. https://doi.org/10.1016/s0092-8674(03)01064-x

Tamaru, H. (2010). Confining euchromatin/heterochromatin territory: jumonji crosses the line. *Genes Dev*, *24*(14), 1465-1478. https://doi.org/10.1101/gad.1941010

Tamburri, S., Lavarone, E., Fernández-Pérez, D., Conway, E., Zanotti, M., Manganaro, D., & Pasini, D. (2020). Histone H2AK119 Mono-Ubiquitination Is Essential for Polycomb-Mediated Transcriptional Repression. *Mol Cell*, *77*(4), 840-856.e845. https://doi.org/10.1016/j.molcel.2019.11.021

Tanaka, K. (1998). Molecular biology of the proteasome. *Biochem Biophys Res Commun*, *247*(3), 537-541. https://doi.org/10.1006/bbrc.1998.8617

Tanaka, Y., Katagiri, Z., Kawahashi, K., Kioussis, D., & Kitajima, S. (2007). Trithorax-group protein ASH1 methylates histone H3 lysine 36. *Gene*, *397*(1-2), 161-168. https://doi.org/10.1016/j.gene.2007.04.027

Torné, J., Ray-Gallet, D., Boyarchuk, E., Garnier, M., Le Baccon, P., Coulon, A., Orsi, G. A., & Almouzni, G. (2020). Two HIRA-dependent pathways mediate H3.3 de novo deposition and recycling during transcription. *Nat Struct Mol Biol*, *27*(11), 1057-1068. https://doi.org/10.1038/s41594-020-0492-7

Trujillo, K. M., & Osley, M. A. (2012). A role for H2B ubiquitylation in DNA replication. *Mol Cell*, *48*(5), 734-746. https://doi.org/10.1016/j.molcel.2012.09.019

Udugama, M., Vinod, B., Chan, F. L., Hii, L., Garvie, A., Collas, P., Kalitsis, P., Steer, D., Das, P. P., Tripathi, P., Mann, J. R., Voon, H. P. J., & Wong, L. H. (2022). Histone H3.3 phosphorylation promotes heterochromatin formation by inhibiting H3K9/K36 histone demethylase. *Nucleic Acids Res*, *50*(8), 4500-4514. https://doi.org/10.1093/nar/gkac259

van der Knaap, J. A., Kumar, B. R., Moshkin, Y. M., Langenberg, K., Krijgsveld, J., Heck, A. J., Karch, F., & Verrijzer, C. P. (2005). GMP synthetase stimulates histone H2B deubiquitylation by the epigenetic silencer USP7. *Mol Cell*, *17*(5), 695-707. https://doi.org/10.1016/j.molcel.2005.02.013

van Leeuwen, F., Gafken, P. R., & Gottschling, D. E. (2002). Dot1p modulates silencing in yeast by methylation of the nucleosome core. *Cell*, *109*(6), 745-756. https://doi.org/10.1016/s0092-8674(02)00759-6

Venkatesh, S., & Workman, J. L. (2013). Set2 mediated H3 lysine 36 methylation: regulation of transcription elongation and implications in organismal development. *Wiley Interdiscip Rev Dev Biol*, *2*(5), 685-700. https://doi.org/10.1002/wdev.109

Verbrugge, S. E., Scheper, R. J., Lems, W. F., de Gruijl, T. D., & Jansen, G. (2015). Proteasome inhibitors as experimental therapeutics of autoimmune diseases. *Arthritis Res Ther*, *17*(1), 17. https://doi.org/10.1186/s13075-015-0529-1

Verrier, L., Vandromme, M., & Trouche, D. (2011). Histone demethylases in chromatin cross-talks. *Biol Cell*, *103*(8), 381-401. https://doi.org/10.1042/bc20110028

Vlaming, H., van Welsem, T., de Graaf, E. L., Ontoso, D., Altelaar, A. F., San-Segundo, P. A., Heck, A. J., & van Leeuwen, F. (2014). Flexibility in crosstalk between H2B ubiquitination and H3 methylation in vivo. *EMBO Rep*, *15*(10), 1077-1084. https://doi.org/10.15252/embr.201438793

Waddington, C. H. (1942). The epigenotype. *Endeavour*, *1*, 18-20.

Wagner, E. J., & Carpenter, P. B. (2012). Understanding the language of Lys36 methylation at histone H3. *Nat Rev Mol Cell Biol*, *13*(2), 115-126. https://doi.org/10.1038/nrm3274

Wang, Z. F., Sirotkin, A. M., Buchold, G. M., Skoultchi, A. I., & Marzluff, W. F. (1997). The mouse histone H1 genes: gene organization and differential regulation. *J Mol Biol*, *271*(1), 124-138. https://doi.org/10.1006/jmbi.1997.1166

Weinberg, D. N., Papillon-Cavanagh, S., Chen, H., Yue, Y., Chen, X., Rajagopalan, K. N., Horth, C., McGuire, J. T., Xu, X., Nikbakht, H., Lemiesz, A. E., Marchione, D. M., Marunde, M.

R., Meiners, M. J., Cheek, M. A., Keogh, M. C., Bareke, E., Djedid, A., Harutyunyan, A. S., . . . Lu, C. (2019). The histone mark H3K36me2 recruits DNMT3A and shapes the intergenic DNA methylation landscape. *Nature*, *573*(7773), 281-286. https://doi.org/10.1038/s41586-019-1534-3

Wille, C. K., & Sridharan, R. (2022a). Connecting the DOTs on Cell Identity. *Front Cell Dev Biol*, *10*, 906713. https://doi.org/10.3389/fcell.2022.906713

Wille, C. K., & Sridharan, R. (2022b). DOT1L inhibition enhances pluripotency beyond acquisition of epithelial identity and without immediate suppression of the somatic transcriptome. *Stem Cell Reports*, *17*(2), 384-396. https://doi.org/10.1016/j.stemcr.2021.12.004

Wong, L. H., Ren, H., Williams, E., McGhie, J., Ahn, S., Sim, M., Tam, A., Earle, E., Anderson, M. A., Mann, J., & Choo, K. H. (2009). Histone H3.3 incorporation provides a unique and functionally essential telomeric chromatin in embryonic stem cells. *Genome Res*, *19*(3), 404-414. https://doi.org/10.1101/gr.084947.108

Wood, A., Krogan, N. J., Dover, J., Schneider, J., Heidt, J., Boateng, M. A., Dean, K., Golshani, A., Zhang, Y., & Greenblatt, J. F. (2003). Bre1, an E3 ubiquitin ligase required for recruitment and substrate selection of Rad6 at a promoter. *Molecular cell*, *11*(1), 267-274.

Worden, E. J., Hoffmann, N. A., Hicks, C. W., & Wolberger, C. (2019). Mechanism of Cross-talk between H2B Ubiquitination and H3 Methylation by Dot1L. *Cell*, *176*(6), 1490-1501.e1412. https://doi.org/10.1016/j.cell.2019.02.002

Yang, D., He, Y., Li, R., Huang, Z., Zhou, Y., Shi, Y., Deng, Z., Wu, J., & Gao, Y. (2023). Histone H3K79 methylation by DOT1L promotes Aurora B localization at centromeres in mitosis. *Cell Rep*, *42*(8), 112885. https://doi.org/10.1016/j.celrep.2023.112885

Yoh, S. M., Lucas, J. S., & Jones, K. A. (2008). The Iws1:Spt6:CTD complex controls cotranscriptional mRNA biosynthesis and HYPB/Setd2-mediated histone H3K36 methylation. *Genes Dev*, *22*(24), 3422-3434. https://doi.org/10.1101/gad.1720008

Yokoyama, A. (2021). Leukemogenesis via aberrant self-renewal by the MLL/AEP-mediated transcriptional activation system. *Cancer Science*, *112*(10), 3935-3944.

Youdell, M. L., Kizer, K. O., Kisseleva-Romanova, E., Fuchs, S. M., Duro, E., Strahl, B. D., & Mellor, J. (2008). Roles for Ctk1 and Spt6 in regulating the different methylation states of histone H3 lysine 36. *Mol Cell Biol*, *28*(16), 4915-4926. https://doi.org/10.1128/mcb.00001-08

Yun, M., Wu, J., Workman, J. L., & Li, B. (2011). Readers of histone modifications. *Cell Res*, *21*(4), 564-578. https://doi.org/10.1038/cr.2011.42

Zhang, H., Zhou, B., Qin, S., Xu, J., Harding, R., Tempel, W., Nayak, V., Li, Y., Loppnau, P., Dou, Y., & Min, J. (2018). Structural and functional analysis of the DOT1L-AF10 complex reveals mechanistic insights into MLL-AF10-associated leukemogenesis. *Genes Dev*, *32*(5-6), 341-346. https://doi.org/10.1101/gad.311639.118

Zhang, X. Y., Varthi, M., Sykes, S. M., Phillips, C., Warzecha, C., Zhu, W., Wyce, A., Thorne, A. W., Berger, S. L., & McMahon, S. B. (2008). The putative cancer stem cell marker USP22 is a subunit of the human SAGA complex required for activated transcription and cell-cycle progression. *Mol Cell*, *29*(1), 102-111. https://doi.org/10.1016/j.molcel.2007.12.015

Adam, S., Dabin, J., Chevallier, O., Leroy, O., Baldeyron, C., Corpet, A., Lomonte, P., Renaud, O., Almouzni, G., & Polo, S. E. (2016). Real-Time Tracking of Parental Histones Reveals

Their Contribution to Chromatin Integrity Following DNA Damage. *Mol Cell*, *64*(1), 65-78. https://doi.org/10.1016/j.molcel.2016.08.019

Adamaki, M., Lambrou, G. I., Athanasiadou, A., Vlahopoulos, S., Papavassiliou, A. G., & Moschovi, M. (2015). HOXA9 and MEIS1 gene overexpression in the diagnosis of childhood acute leukemias: Significant correlation with relapse and overall survival. *Leukemia research*, *39*(8), 874-882.

Adams, J. (2002). Preclinical and clinical evaluation of proteasome inhibitor PS-341 for the treatment of cancer. *Curr Opin Chem Biol*, *6*(4), 493-500. https://doi.org/10.1016/s1367-5931(02)00343-5

Ahmad, K., & Henikoff, S. (2002). The histone variant H3.3 marks active chromatin by replication-independent nucleosome assembly. *Mol Cell*, *9*(6), 1191-1200. https://doi.org/10.1016/s1097-2765(02)00542-7

Ai, H., Sun, M., Liu, A., Sun, Z., Liu, T., Cao, L., Liang, L., Qu, Q., Li, Z., Deng, Z., Tong, Z., Chu, G., Tian, X., Deng, H., Zhao, S., Li, J. B., Lou, Z., & Liu, L. (2022). H2B Lys34 Ubiquitination Induces Nucleosome Distortion to Stimulate Dot1L Activity. *Nat Chem Biol*, *18*(9), 972-980. https://doi.org/10.1038/s41589-022-01067-7

Amin, A. D., Vishnoi, N., & Prochasson, P. (2013). A global requirement for the HIR complex in the assembly of chromatin. *Biochim Biophys Acta*, *1819*(3-4), 264-276. https://doi.org/10.1016/j.bbagrm.2011.07.008

Arnold, O., Barbosa, K., Deshpande, A. J., & Zhu, N. (2022). The Role of DOT1L in Normal and Malignant Hematopoiesis. *Front Cell Dev Biol*, *10*, 917125. https://doi.org/10.3389/fcell.2022.917125

Batta, K., Zhang, Z., Yen, K., Goffman, D. B., & Pugh, B. F. (2011). Genome-wide function of H2B ubiquitylation in promoter and genic regions. *Genes Dev*, *25*(21), 2254-2265. https://doi.org/10.1101/gad.177238.111

Bedford, M. T., & Clarke, S. G. (2009). Protein arginine methylation in mammals: who, what, and why. *Mol Cell*, *33*(1), 1-13. https://doi.org/10.1016/j.molcel.2008.12.013

Belotserkovskaya, R., Oh, S., Bondarenko, V. A., Orphanides, G., Studitsky, V. M., & Reinberg, D. (2003). FACT facilitates transcription-dependent nucleosome alteration. *Science*, *301*(5636), 1090-1093. https://doi.org/10.1126/science.1085703

Bhattacharya, S., Levy, M. J., Zhang, N., Li, H., Florens, L., Washburn, M. P., & Workman, J. L. (2021). The methyltransferase SETD2 couples transcription and splicing by engaging mRNA processing factors through its SHI domain. *Nat Commun*, *12*(1), 1443. https://doi.org/10.1038/s41467-021-21663-w

Bilokapic, S., & Halic, M. (2019). Nucleosome and ubiquitin position Set2 to methylate H3K36. *Nat Commun*, *10*(1), 3795. https://doi.org/10.1038/s41467-019-11726-4

Bilokapic, S., & Halic, M. (2019). Nucleosome and ubiquitin position Set2 to methylate H3K36. *Nature Communications*, *10*(1), 3795. https://doi.org/10.1038/s41467-019-11726-4

Britten, O., Ragusa, D., Tosi, S., & Mostafa Kamel, Y. (2019). MLL-Rearranged Acute Leukemia with t (4; 11)(q21; q23)—Current Treatment Options. Is There a Role for CAR-T Cell Therapy? *Cells*, *8*(11), 1341.

Brown, M. A., Sims, R. J., 3rd, Gottlieb, P. D., & Tucker, P. W. (2006). Identification and characterization of Smyd2: a split SET/MYND domain-containing histone H3 lysine 36-specific methyltransferase that interacts with the Sin3 histone deacetylase complex. *Mol Cancer*, *5*, 26. https://doi.org/10.1186/1476-4598-5-26

Brzezinka, K., Nevedomskaya, E., Lesche, R., Haegebarth, A., Ter Laak, A., Fernández-Montalván, A. E., Eberspaecher, U., Werbeck, N. D., Moenning, U., Siegel, S., Haendler, B., Eheim, A. L., & Stresemann, C. (2020). Characterization of the Menin-MLL Interaction as Therapeutic Cancer Target. *Cancers (Basel)*, *12*(1). https://doi.org/10.3390/cancers12010201

Campos, E. I., & Reinberg, D. (2009). Histones: annotating chromatin. *Annu Rev Genet*, *43*, 559-599. https://doi.org/10.1146/annurev.genet.032608.103928

Cao, K., Ugarenko, M., Ozark, P. A., Wang, J., Marshall, S. A., Rendleman, E. J., Liang, K., Wang, L., Zou, L., Smith, E. R., Yue, F., & Shilatifard, A. (2020). DOT1L-controlled cell-fate determination and transcription elongation are independent of H3K79 methylation. *Proceedings of the National Academy of Sciences*, *117*(44), 27365-27373. https://doi.org/doi:10.1073/pnas.2001075117

Cao, R., Wang, L., Wang, H., Xia, L., Erdjument-Bromage, H., Tempst, P., Jones, R. S., & Zhang, Y. (2002). Role of histone H3 lysine 27 methylation in Polycomb-group silencing. *Science*, *298*(5595), 1039-1043. https://doi.org/10.1126/science.1076997

Castiglioni, S., Di Fede, E., Bernardelli, C., Lettieri, A., Parodi, C., Grazioli, P., Colombo, E. A., Ancona, S., Milani, D., & Ottaviano, E. (2022). KMT2A: Umbrella gene for multiple diseases. *Genes*, *13*(3), 514.

Cheon, Y., Kim, H., Park, K., Kim, M., & Lee, D. (2020). Dynamic modules of the coactivator SAGA in eukaryotic transcription. *Experimental & Molecular Medicine*, *52*(7), 991-1003. https://doi.org/10.1038/s12276-020-0463-4

Davie, J. R., & Murphy, L. C. (1990). Level of ubiquitinated histone H2B in chromatin is coupled to ongoing transcription. *Biochemistry*, *29*(20), 4752-4757. https://doi.org/10.1021/bi00472a002

Delcuve, G. P., & Davie, J. R. (1992). Western blotting and immunochemical detection of histones electrophoretically resolved on acid-urea-triton-and sodium dodecyl sulfate-polyacrylamide gels. *Analytical biochemistry*, *200*(2), 339-341.

Devoucoux, M., Roques, C., Lachance, C., Lashgari, A., Joly-Beauparlant, C., Jacquet, K., Alerasool, N., Prudente, A., Taipale, M., Droit, A., Lambert, J. P., Hussein, S. M. I., & Côté, J. (2022). MRG Proteins Are Shared by Multiple Protein Complexes With Distinct Functions. *Mol Cell Proteomics*, *21*(7), 100253. https://doi.org/10.1016/j.mcpro.2022.100253

Edmunds, J. W., Mahadevan, L. C., & Clayton, A. L. (2008). Dynamic histone H3 methylation during gene induction: HYPB/Setd2 mediates all H3K36 trimethylation. *Embo j*, *27*(2), 406-420. https://doi.org/10.1038/sj.emboj.7601967

Eom, G. H., Kim, K. B., Kim, J. H., Kim, J. Y., Kim, J. R., Kee, H. J., Kim, D. W., Choe, N., Park, H. J., Son, H. J., Choi, S. Y., Kook, H., & Seo, S. B. (2011). Histone methyltransferase SETD3 regulates muscle differentiation. *J Biol Chem*, *286*(40), 34733-34742. https://doi.org/10.1074/jbc.M110.203307

Feng, Q., Wang, H., Ng, H. H., Erdjument-Bromage, H., Tempst, P., Struhl, K., & Zhang, Y. (2002). Methylation of H3-lysine 79 is mediated by a new family of HMTases without a SET domain. *Curr Biol*, *12*(12), 1052-1058. https://doi.org/10.1016/s0960-9822(02)00901-6

Fischle, W., Tseng, B. S., Dormann, H. L., Ueberheide, B. M., Garcia, B. A., Shabanowitz, J., Hunt, D. F., Funabiki, H., & Allis, C. D. (2005). Regulation of HP1-chromatin binding by

histone H3 methylation and phosphorylation. *Nature*, *438*(7071), 1116-1122. https://doi.org/10.1038/nature04219

Fodor, B. D., Kubicek, S., Yonezawa, M., O'Sullivan, R. J., Sengupta, R., Perez-Burgos, L., Opravil, S., Mechtler, K., Schotta, G., & Jenuwein, T. (2006). Jmjd2b antagonizes H3K9 trimethylation at pericentric heterochromatin in mammalian cells. *Genes Dev*, *20*(12), 1557-1562. https://doi.org/10.1101/gad.388206

Früh, K., Gossen, M., Wang, K., Bujard, H., Peterson, P. A., & Yang, Y. (1994). Displacement of housekeeping proteasome subunits by MHC-encoded LMPs: a newly discovered mechanism for modulating the multicatalytic proteinase complex. *Embo j*, *13*(14), 3236-3244. https://doi.org/10.1002/j.1460-2075.1994.tb06625.x

Fu, J., Liao, L., Balaji, K. S., Wei, C., Kim, J., & Peng, J. (2021). Epigenetic modification and a role for the E3 ligase RNF40 in cancer development and metastasis. *Oncogene*, *40*(3), 465-474. https://doi.org/10.1038/s41388-020-01556-w

Fuchs, G., & Oren, M. (2014). Writing and reading H2B monoubiquitylation. *Biochim Biophys Acta*, *1839*(8), 694-701. https://doi.org/10.1016/j.bbagrm.2014.01.002

Gal, C., Moore, K. M., Paszkiewicz, K., Kent, N. A., & Whitehall, S. K. (2015). The impact of the HIRA histone chaperone upon global nucleosome architecture. *Cell Cycle*, *14*(1), 123-134. https://doi.org/10.4161/15384101.2014.967123

Gillette, T. G., & Hill, J. A. (2015). Readers, writers, and erasers: chromatin as the whiteboard of heart disease. *Circ Res*, *116*(7), 1245-1253. https://doi.org/10.1161/circresaha.116.303630

Goldberg, A. D., Banaszynski, L. A., Noh, K. M., Lewis, P. W., Elsaesser, S. J., Stadler, S., Dewell, S., Law, M., Guo, X., Li, X., Wen, D., Chapgier, A., DeKelver, R. C., Miller, J. C., Lee, Y. L., Boydston, E. A., Holmes, M. C., Gregory, P. D., Greally, J. M., . . . Allis, C. D. (2010).

Distinct factors control histone variant H3.3 localization at specific genomic regions. *Cell*, *140*(5), 678-691. https://doi.org/10.1016/j.cell.2010.01.003

Heard, E., Rougeulle, C., Arnaud, D., Avner, P., Allis, C. D., & Spector, D. L. (2001). Methylation of histone H3 at Lys-9 is an early mark on the X chromosome during X inactivation. *Cell*, *107*(6), 727-738. https://doi.org/10.1016/s0092-8674(01)00598-0

Henikoff, S., & Smith, M. M. (2015). Histone variants and epigenetics. *Cold Spring Harb Perspect Biol*, *7*(1), a019364. https://doi.org/10.1101/cshperspect.a019364

Hershko, A., & Ciechanover, A. (1998). The ubiquitin system. *Annual review of biochemistry*, *67*(1), 425-479.

Hideshima, T., Richardson, P., Chauhan, D., Palombella, V. J., Elliott, P. J., Adams, J., & Anderson, K. C. (2001). The proteasome inhibitor PS-341 inhibits growth, induces apoptosis, and overcomes drug resistance in human multiple myeloma cells. *Cancer Res*, *61*(7), 3071-3076.

Huisinga, K. L., Brower-Toland, B., & Elgin, S. C. (2006). The contradictory definitions of heterochromatin: transcription and silencing. *Chromosoma*, *115*, 110-122.

Jagannath, S., Durie, B. G., Wolf, J., Camacho, E., Irwin, D., Lutzky, J., McKinley, M., Gabayan, E., Mazumder, A., Schenkein, D., & Crowley, J. (2005). Bortezomib therapy alone and in combination with dexamethasone for previously untreated symptomatic multiple myeloma. *Br J Haematol*, *129*(6), 776-783. https://doi.org/10.1111/j.1365-2141.2005.05540.x

Jang, S., Kang, C., Yang, H. S., Jung, T., Hebert, H., Chung, K. Y., Kim, S. J., Hohng, S., & Song, J. J. (2019). Structural basis of recognition and destabilization of the histone H2B

ubiquitinated nucleosome by the DOT1L histone H3 Lys79 methyltransferase. *Genes Dev*, *33*(11-12), 620-625. https://doi.org/10.1101/gad.323790.118

Jeusset, L. M., & McManus, K. J. (2017). Ubiquitin Specific Peptidase 22 Regulates Histone H2B Mono-Ubiquitination and Exhibits Both Oncogenic and Tumor Suppressor Roles in Cancer. *Cancers (Basel)*, *9*(12). https://doi.org/10.3390/cancers9120167

Jones, B., Su, H., Bhat, A., Lei, H., Bajko, J., Hevi, S., Baltus, G. A., Kadam, S., Zhai, H., Valdez, R., Gonzalo, S., Zhang, Y., Li, E., & Chen, T. (2008). The histone H3K79 methyltransferase Dot1L is essential for mammalian development and heterochromatin structure. *PLoS Genet*, *4*(9), e1000190. https://doi.org/10.1371/journal.pgen.1000190

Joo, H. Y., Jones, A., Yang, C., Zhai, L., Smith, A. D. t., Zhang, Z., Chandrasekharan, M. B., Sun, Z. W., Renfrow, M. B., Wang, Y., Chang, C., & Wang, H. (2011). Regulation of histone H2A and H2B deubiquitination and Xenopus development by USP12 and USP46. *J Biol Chem*, *286*(9), 7190-7201. https://doi.org/10.1074/jbc.M110.158311

Kamens, J. L., Nance, S., Koss, C., Xu, B., Cotton, A., Lam, J. W., Garfinkle, E. A., Nallagatla, P., Smith, A. M., & Mitchell, S. (2023). Proteasome inhibition targets the KMT2A transcriptional complex in acute lymphoblastic leukemia. *Nature Communications*, *14*(1), 809.

Kamens, J. L., Nance, S., Koss, C., Xu, B., Cotton, A., Lam, J. W., Garfinkle, E. A. R., Nallagatla, P., Smith, A. M. R., Mitchell, S., Ma, J., Currier, D., Wright, W. C., Kavdia, K., Pagala, V. R., Kim, W., Wallace, L. M., Cho, J. H., Fan, Y., . . . Gruber, T. A. (2023). Proteasome inhibition targets the KMT2A transcriptional complex in acute lymphoblastic leukemia. *Nat Commun*, *14*(1), 809. https://doi.org/10.1038/s41467-023-36370-x

Kang, J. Y., Kim, J. Y., Kim, K. B., Park, J. W., Cho, H., Hahm, J. Y., Chae, Y. C., Kim, D., Kook, H., Rhee, S., Ha, N. C., & Seo, S. B. (2018). KDM2B is a histone H3K79 demethylase and induces transcriptional repression via sirtuin-1-mediated chromatin silencing. *Faseb j*, *32*(10), 5737-5750. https://doi.org/10.1096/fj.201800242R

Kari, V., Shchebet, A., Neumann, H., & Johnsen, S. A. (2011). The H2B ubiquitin ligase RNF40 cooperates with SUPT16H to induce dynamic changes in chromatin structure during DNA double-strand break repair. *Cell Cycle*, *10*(20), 3495-3504. https://doi.org/10.4161/cc.10.20.17769

Kemble, D. J., McCullough, L. L., Whitby, F. G., Formosa, T., & Hill, C. P. (2015). FACT Disrupts Nucleosome Structure by Binding H2A-H2B with Conserved Peptide Motifs. *Mol Cell*, *60*(2), 294-306. https://doi.org/10.1016/j.molcel.2015.09.008

Khan, D. H., Healy, S., He, S., Lichtensztejn, D., Klewes, L., Sharma, K. L., Lau, V., Mai, S., Delcuve, G. P., & Davie, J. R. (2017). Mitogen-induced distinct epialleles are phosphorylated at either H3S10 or H3S28, depending on H3K27 acetylation. *Mol Biol Cell*, *28*(6), 817-824. https://doi.org/10.1091/mbc.E16-08-0618

Kim, S. K., Jung, I., Lee, H., Kang, K., Kim, M., Jeong, K., Kwon, C. S., Han, Y. M., Kim, Y. S., Kim, D., & Lee, D. (2012). Human histone H3K79 methyltransferase DOT1L protein [corrected] binds actively transcribing RNA polymerase II to regulate gene expression. *J Biol Chem*, *287*(47), 39698-39709. https://doi.org/10.1074/jbc.M112.384057

Kizer, K. O., Phatnani, H. P., Shibata, Y., Hall, H., Greenleaf, A. L., & Strahl, B. D. (2005). A novel domain in Set2 mediates RNA polymerase II interaction and couples histone H3 K36 methylation with transcript elongation. *Molecular and cellular biology*, *25*(8), 3305-3316.

Klein, R. H., & Knoepfler, P. S. (2023). Knockout tales: the versatile roles of histone H3.3 in development and disease. *Epigenetics Chromatin*, *16*(1), 38. https://doi.org/10.1186/s13072-023-00512-8

Kondagunta, G. V., Drucker, B., Schwartz, L., Bacik, J., Marion, S., Russo, P., Mazumdar, M., & Motzer, R. J. (2004). Phase II trial of bortezomib for patients with advanced renal cell carcinoma. *J Clin Oncol*, *22*(18), 3720-3725. https://doi.org/10.1200/jco.2004.10.155

Laemmli, U. K. (1970). Cleavage of Structural Proteins during the Assembly of the Head of Bacteriophage T4. *Nature*, *227*(5259), 680-685. https://doi.org/10.1038/227680a0

Latham, J. A., Chosed, R. J., Wang, S., & Dent, S. Y. (2011). Chromatin signaling to kinetochores: transregulation of Dam1 methylation by histone H2B ubiquitination. *Cell*, *146*(5), 709-719. https://doi.org/10.1016/j.cell.2011.07.025

Lee, K. K., & Workman, J. L. (2007). Histone acetyltransferase complexes: one size doesn't fit all. *Nature reviews Molecular cell biology*, *8*(4), 284-295.

Lee, S., Oh, S., Jeong, K., Jo, H., Choi, Y., Seo, H. D., Kim, M., Choe, J., Kwon, C. S., & Lee, D. (2018). Dot1 regulates nucleosome dynamics by its inherent histone chaperone activity in yeast. *Nature Communications*, *9*(1), 240. https://doi.org/10.1038/s41467-017-02759-8

Lee, S. H., Oshige, M., Durant, S. T., Rasila, K. K., Williamson, E. A., Ramsey, H., Kwan, L., Nickoloff, J. A., & Hromas, R. (2005). The SET domain protein Metnase mediates foreign DNA integration and links integration to nonhomologous end-joining repair. *Proc Natl Acad Sci U S A*, *102*(50), 18075-18080. https://doi.org/10.1073/pnas.0503676102

Lempiäinen, J. K., & Garcia, B. A. (2023). Characterizing crosstalk in epigenetic signaling to understand disease physiology. *Biochem J*, *480*(1), 57-85. https://doi.org/10.1042/bcj20220550

Li, B., Carey, M., & Workman, J. L. (2007). The role of chromatin during transcription. *Cell*, *128*(4), 707-719. https://doi.org/10.1016/j.cell.2007.01.015

Li, F., Mao, G., Tong, D., Huang, J., Gu, L., Yang, W., & Li, G. M. (2013). The histone mark H3K36me3 regulates human DNA mismatch repair through its interaction with MutSα. *Cell*, *153*(3), 590-600. https://doi.org/10.1016/j.cell.2013.03.025

Li, Y., Trojer, P., Xu, C. F., Cheung, P., Kuo, A., Drury, W. J., 3rd, Qiao, Q., Neubert, T. A., Xu, R. M., Gozani, O., & Reinberg, D. (2009). The target of the NSD family of histone lysine methyltransferases depends on the nature of the substrate. *J Biol Chem*, *284*(49), 34283-34295. https://doi.org/10.1074/jbc.M109.034462

Li, Y., Wen, H., Xi, Y., Tanaka, K., Wang, H., Peng, D., Ren, Y., Jin, Q., Dent, S. Y., Li, W., Li, H., & Shi, X. (2014). AF9 YEATS domain links histone acetylation to DOT1L-mediated H3K79 methylation. *Cell*, *159*(3), 558-571. https://doi.org/10.1016/j.cell.2014.09.049

Lim, P. S., Shannon, M. F., & Hardy, K. (2010). Epigenetic control of inducible gene expression in the immune system. *Epigenomics*, *2*(6), 775-795. https://doi.org/10.2217/epi.10.55

Lin, J., Wu, Y., Tian, G., Yu, D., Yang, E., Lam, W. H., Liu, Z., Jing, Y., Dang, S., Bao, X., Wong, J. W. H., Zhai, Y., & Li, X. D. (2023). Menin "reads" H3K79me2 mark in a nucleosomal context. *Science*, *379*(6633), 717-723. https://doi.org/10.1126/science.adc9318

Luger, K., Mäder, A. W., Richmond, R. K., Sargent, D. F., & Richmond, T. J. (1997). Crystal structure of the nucleosome core particle at 2.8 A resolution. *Nature*, *389*(6648), 251-260. https://doi.org/10.1038/38444

Malik, H. S., & Henikoff, S. (2003). Phylogenomics of the nucleosome. *Nat Struct Biol*, *10*(11), 882-891. https://doi.org/10.1038/nsb996

Malinczak, C. A., Rasky, A. J., Fonseca, W., Schaller, M. A., Allen, R. M., Ptaschinski, C., Morris, S., & Lukacs, N. W. (2020). Upregulation of H3K27 Demethylase KDM6 During Respiratory Syncytial Virus Infection Enhances Proinflammatory Responses and Immunopathology. *J Immunol*, *204*(1), 159-168. https://doi.org/10.4049/jimmunol.1900741

Marschalek, R. (2016). Systematic classification of mixed-lineage leukemia fusion partners predicts additional cancer pathways. *Annals of laboratory medicine*, *36*(2), 85.

Martire, S., & Banaszynski, L. A. (2020). The roles of histone variants in fine-tuning chromatin organization and function. *Nat Rev Mol Cell Biol*, *21*(9), 522-541. https://doi.org/10.1038/s41580-020-0262-8

Martire, S., Gogate, A. A., Whitmill, A., Tafessu, A., Nguyen, J., Teng, Y. C., Tastemel, M., & Banaszynski, L. A. (2019). Phosphorylation of histone H3.3 at serine 31 promotes p300 activity and enhancer acetylation. *Nat Genet*, *51*(6), 941-946. https://doi.org/10.1038/s41588-019-0428-5

Marzluff, W. F., Gongidi, P., Woods, K. R., Jin, J., & Maltais, L. J. (2002). The human and mouse replication-dependent histone genes. *Genomics*, *80*(5), 487-498.

McGrath, J., & Solter, D. (1984). Completion of mouse embryogenesis requires both the maternal and paternal genomes. *Cell*, *37*(1), 179-183.

McKittrick, E., Gafken, P. R., Ahmad, K., & Henikoff, S. (2004). Histone H3.3 is enriched in covalent modifications associated with active chromatin. *Proc Natl Acad Sci U S A*, *101*(6), 1525-1530. https://doi.org/10.1073/pnas.0308092100

Milne, T. A. (2017). Mouse models of MLL leukemia: recapitulating the human disease. *Blood*, *129*(16), 2217-2223. https://doi.org/10.1182/blood-2016-10-691428

Minard, M. E., Jain, A. K., & Barton, M. C. (2009). Analysis of epigenetic alterations to chromatin during development. *Genesis*, *47*(8), 559-572. https://doi.org/10.1002/dvg.20534

Mohan, M., Herz, H. M., Takahashi, Y. H., Lin, C., Lai, K. C., Zhang, Y., Washburn, M. P., Florens, L., & Shilatifard, A. (2010). Linking H3K79 trimethylation to Wnt signaling through a novel Dot1-containing complex (DotCom). *Genes Dev*, *24*(6), 574-589. https://doi.org/10.1101/gad.1898410

Morris, S. A., Shibata, Y., Noma, K.-i., Tsukamoto, Y., Warren, E., Temple, B., Grewal, S. I., & Strahl, B. D. (2005). Histone H3 K36 methylation is associated with transcription elongation in Schizosaccharomyces pombe. *Eukaryotic cell*, *4*(8), 1446-1454.

Muhire, B. M., Booker, M. A., & Tolstorukov, M. Y. (2019). Non-neutral evolution of H3.3-encoding genes occurs without alterations in protein sequence. *Sci Rep*, *9*(1), 8472. https://doi.org/10.1038/s41598-019-44800-4

Newell-Price, J., Clark, A. J., & King, P. (2000). DNA methylation and silencing of gene expression. *Trends in Endocrinology & Metabolism*, *11*(4), 142-148.

Nicassio, F., Corrado, N., Vissers, J. H., Areces, L. B., Bergink, S., Marteijn, J. A., Geverts, B., Houtsmuller, A. B., Vermeulen, W., Di Fiore, P. P., & Citterio, E. (2007). Human USP3 is a chromatin modifier required for S phase progression and genome stability. *Curr Biol*, *17*(22), 1972-1977. https://doi.org/10.1016/j.cub.2007.10.034

Nilsen, T. W., & Graveley, B. R. (2010). Expansion of the eukaryotic proteome by alternative splicing. *Nature*, *463*(7280), 457-463. https://doi.org/10.1038/nature08909

Orphanides, G., LeRoy, G., Chang, C.-H., Luse, D. S., & Reinberg, D. (1998). FACT, a factor that facilitates transcript elongation through nucleosomes. *Cell*, *92*(1), 105-116.

Outchkourov, N. S., Muiño, J. M., Kaufmann, K., van Ijcken, W. F., Groot Koerkamp, M. J., van Leenen, D., de Graaf, P., Holstege, F. C., Grosveld, F. G., & Timmers, H. T. (2013). Balancing of histone H3K4 methylation states by the Kdm5c/SMCX histone demethylase modulates promoter and enhancer function. *Cell Rep*, *3*(4), 1071-1079. https://doi.org/10.1016/j.celrep.2013.02.030

Papandreou, C. N., Daliani, D. D., Nix, D., Yang, H., Madden, T., Wang, X., Pien, C. S., Millikan, R. E., Tu, S. M., Pagliaro, L., Kim, J., Adams, J., Elliott, P., Esseltine, D., Petrusich, A., Dieringer, P., Perez, C., & Logothetis, C. J. (2004). Phase I trial of the proteasome inhibitor bortezomib in patients with advanced solid tumors with observations in androgen-independent prostate cancer. *J Clin Oncol*, *22*(11), 2108-2121. https://doi.org/10.1200/jco.2004.02.106

Rahman, S., Sowa, M. E., Ottinger, M., Smith, J. A., Shi, Y., Harper, J. W., & Howley, P. M. (2011). The Brd4 extraterminal domain confers transcription activation independent of pTEFb by recruiting multiple proteins, including NSD3. *Mol Cell Biol*, *31*(13), 2641-2652. https://doi.org/10.1128/mcb.01341-10

Rayasam, G. V., Wendling, O., Angrand, P. O., Mark, M., Niederreither, K., Song, L., Lerouge, T., Hager, G. L., Chambon, P., & Losson, R. (2003). NSD1 is essential for early post-implantation development and has a catalytically active SET domain. *Embo j*, *22*(12), 3153-3163. https://doi.org/10.1093/emboj/cdg288

Richardson, P. G., Sonneveld, P., Schuster, M. W., Irwin, D., Stadtmauer, E. A., Facon, T., Harousseau, J. L., Ben-Yehuda, D., Lonial, S., Goldschmidt, H., Reece, D., San-Miguel, J. F., Bladé, J., Boccadoro, M., Cavenagh, J., Dalton, W. S., Boral, A. L., Esseltine, D. L., Porter, J. B., . . . Anderson, K. C. (2005). Bortezomib or high-dose dexamethasone for

relapsed multiple myeloma. *N Engl J Med*, *352*(24), 2487-2498. https://doi.org/10.1056/NEJMoa043445

Riggs, A. D. (1975). X inactivation, differentiation, and DNA methylation. *Cytogenetic and Genome Research*, *14*(1), 9-25.

Santos-Rosa, H., Schneider, R., Bannister, A. J., Sherriff, J., Bernstein, B. E., Emre, N. C., Schreiber, S. L., Mellor, J., & Kouzarides, T. (2002). Active genes are tri-methylated at K4 of histone H3. *Nature*, *419*(6905), 407-411. https://doi.org/10.1038/nature01080

Schübeler, D., MacAlpine, D. M., Scalzo, D., Wirbelauer, C., Kooperberg, C., van Leeuwen, F., Gottschling, D. E., O'Neill, L. P., Turner, B. M., Delrow, J., Bell, S. P., & Groudine, M. (2004). The histone modification pattern of active genes revealed through genome-wide chromatin analysis of a higher eukaryote. *Genes Dev*, *18*(11), 1263-1271. https://doi.org/10.1101/gad.1198204

Schwartz, R., & Davidson, T. (2004). Pharmacology, pharmacokinetics, and practical applications of bortezomib. *Oncology (Williston Park)*, *18*(14 Suppl 11), 14-21.

Shah, S. A., Potter, M. W., McDade, T. P., Ricciardi, R., Perugini, R. A., Elliott, P. J., Adams, J., & Callery, M. P. (2001). 26S proteasome inhibition induces apoptosis and limits growth of human pancreatic cancer. *J Cell Biochem*, *82*(1), 110-122. https://doi.org/10.1002/jcb.1150

Sharda, A., & Humphrey, T. C. (2022). The role of histone H3K36me3 writers, readers and erasers in maintaining genome stability. *DNA Repair (Amst)*, *119*, 103407. https://doi.org/10.1016/j.dnarep.2022.103407

Sharma, P., Sattarifard, H., Fatemiyan, N., Lakowski, T. M., & Davie, J. R. (2022). Bioinformatic Analyses of Broad H3K79me2 Domains in Different Leukemia Cell Line Data Sets. *Cells*, *11*(18), 2830. https://www.mdpi.com/2073-4409/11/18/2830

Shilatifard, A. (2008). Molecular implementation and physiological roles for histone H3 lysine 4 (H3K4) methylation. *Curr Opin Cell Biol*, *20*(3), 341-348. https://doi.org/10.1016/j.ceb.2008.03.019

Skucha, A., Ebner, J., Schmöllerl, J., Roth, M., Eder, T., César-Razquin, A., Stukalov, A., Vittori, S., Muhar, M., & Lu, B. (2018). MLL-fusion-driven leukemia requires SETD2 to safeguard genomic integrity. *Nature Communications*, *9*(1), 1983.

Skucha, A., Ebner, J., Schmöllerl, J., Roth, M., Eder, T., César-Razquin, A., Stukalov, A., Vittori, S., Muhar, M., Lu, B., Aichinger, M., Jude, J., Müller, A. C., Győrffy, B., Vakoc, C. R., Valent, P., Bennett, K. L., Zuber, J., Superti-Furga, G., & Grebien, F. (2018). MLL-fusion-driven leukemia requires SETD2 to safeguard genomic integrity. *Nat Commun*, *9*(1), 1983. https://doi.org/10.1038/s41467-018-04329-y

Song, Y. H., & Ahn, S. H. (2010). A Bre1-associated protein, large 1 (Lge1), promotes H2B ubiquitylation during the early stages of transcription elongation. *J Biol Chem*, *285*(4), 2361-2367. https://doi.org/10.1074/jbc.M109.039255

Strahl, B. D., & Allis, C. D. (2000). The language of covalent histone modifications. *Nature*, *403*(6765), 41-45. https://doi.org/10.1038/47412

Sun, Z., Zhang, Y., Jia, J., Fang, Y., Tang, Y., Wu, H., & Fang, D. (2020). H3K36me3, message from chromatin to DNA damage repair. *Cell & Bioscience*, *10*(1), 9. https://doi.org/10.1186/s13578-020-0374-z

Swigut, T., & Wysocka, J. (2007). H3K27 demethylases, at long last. *Cell*, *131*(1), 29-32. https://doi.org/10.1016/j.cell.2007.09.026

Tafessu, A., O'Hara, R., Martire, S., Dube, A. L., Saha, P., Gant, V. U., & Banaszynski, L. A. (2023). H3.3 contributes to chromatin accessibility and transcription factor binding at

promoter-proximal regulatory elements in embryonic stem cells. *Genome Biology*, *24*(1), 25. https://doi.org/10.1186/s13059-023-02867-3

Tagami, H., Ray-Gallet, D., Almouzni, G., & Nakatani, Y. (2004). Histone H3.1 and H3.3 complexes mediate nucleosome assembly pathways dependent or independent of DNA synthesis. *Cell*, *116*(1), 51-61. https://doi.org/10.1016/s0092-8674(03)01064-x

Tamaru, H. (2010). Confining euchromatin/heterochromatin territory: jumonji crosses the line. *Genes Dev*, *24*(14), 1465-1478. https://doi.org/10.1101/gad.1941010

Tamburri, S., Lavarone, E., Fernández-Pérez, D., Conway, E., Zanotti, M., Manganaro, D., & Pasini, D. (2020). Histone H2AK119 Mono-Ubiquitination Is Essential for Polycomb-Mediated Transcriptional Repression. *Mol Cell*, *77*(4), 840-856.e845. https://doi.org/10.1016/j.molcel.2019.11.021

Tanaka, K. (1998). Molecular biology of the proteasome. *Biochem Biophys Res Commun*, *247*(3), 537-541. https://doi.org/10.1006/bbrc.1998.8617

Tanaka, Y., Katagiri, Z., Kawahashi, K., Kioussis, D., & Kitajima, S. (2007). Trithorax-group protein ASH1 methylates histone H3 lysine 36. *Gene*, *397*(1-2), 161-168. https://doi.org/10.1016/j.gene.2007.04.027

Torné, J., Ray-Gallet, D., Boyarchuk, E., Garnier, M., Le Baccon, P., Coulon, A., Orsi, G. A., & Almouzni, G. (2020). Two HIRA-dependent pathways mediate H3.3 de novo deposition and recycling during transcription. *Nat Struct Mol Biol*, *27*(11), 1057-1068. https://doi.org/10.1038/s41594-020-0492-7

Trujillo, K. M., & Osley, M. A. (2012). A role for H2B ubiquitylation in DNA replication. *Mol Cell*, *48*(5), 734-746. https://doi.org/10.1016/j.molcel.2012.09.019

Udugama, M., Vinod, B., Chan, F. L., Hii, L., Garvie, A., Collas, P., Kalitsis, P., Steer, D., Das, P. P., Tripathi, P., Mann, J. R., Voon, H. P. J., & Wong, L. H. (2022). Histone H3.3 phosphorylation promotes heterochromatin formation by inhibiting H3K9/K36 histone demethylase. *Nucleic Acids Res*, *50*(8), 4500-4514. https://doi.org/10.1093/nar/gkac259

van der Knaap, J. A., Kumar, B. R., Moshkin, Y. M., Langenberg, K., Krijgsveld, J., Heck, A. J., Karch, F., & Verrijzer, C. P. (2005). GMP synthetase stimulates histone H2B deubiquitylation by the epigenetic silencer USP7. *Mol Cell*, *17*(5), 695-707. https://doi.org/10.1016/j.molcel.2005.02.013

van Leeuwen, F., Gafken, P. R., & Gottschling, D. E. (2002). Dot1p modulates silencing in yeast by methylation of the nucleosome core. *Cell*, *109*(6), 745-756. https://doi.org/10.1016/s0092-8674(02)00759-6

Venkatesh, S., & Workman, J. L. (2013). Set2 mediated H3 lysine 36 methylation: regulation of transcription elongation and implications in organismal development. *Wiley Interdiscip Rev Dev Biol*, *2*(5), 685-700. https://doi.org/10.1002/wdev.109

Verbrugge, S. E., Scheper, R. J., Lems, W. F., de Gruijl, T. D., & Jansen, G. (2015). Proteasome inhibitors as experimental therapeutics of autoimmune diseases. *Arthritis Res Ther*, *17*(1), 17. https://doi.org/10.1186/s13075-015-0529-1

Verrier, L., Vandromme, M., & Trouche, D. (2011). Histone demethylases in chromatin cross-talks. *Biol Cell*, *103*(8), 381-401. https://doi.org/10.1042/bc20110028

Vlaming, H., van Welsem, T., de Graaf, E. L., Ontoso, D., Altelaar, A. F., San-Segundo, P. A., Heck, A. J., & van Leeuwen, F. (2014). Flexibility in crosstalk between H2B ubiquitination and H3 methylation in vivo. *EMBO Rep*, *15*(10), 1077-1084. https://doi.org/10.15252/embr.201438793

Waddington, C. H. (1942). The epigenotype. *Endeavour*, *1*, 18-20.

Wagner, E. J., & Carpenter, P. B. (2012). Understanding the language of Lys36 methylation at histone H3. *Nat Rev Mol Cell Biol*, *13*(2), 115-126. https://doi.org/10.1038/nrm3274

Wang, E., Kawaoka, S., Yu, M., Shi, J., Ni, T., Yang, W., Zhu, J., Roeder, R. G., & Vakoc, C. R. (2013). Histone H2B ubiquitin ligase RNF20 is required for MLL-rearranged leukemia. *Proceedings of the National Academy of Sciences*, *110*(10), 3901-3906. https://doi.org/doi:10.1073/pnas.1301045110

Wang, E., Kawaoka, S., Yu, M., Shi, J., Ni, T., Yang, W., Zhu, J., Roeder, R. G., & Vakoc, C. R. (2013). Histone H2B ubiquitin ligase RNF20 is required for MLL-rearranged leukemia. *Proc Natl Acad Sci U S A*, *110*(10), 3901-3906. https://doi.org/10.1073/pnas.1301045110

Wang, Z. F., Sirotkin, A. M., Buchold, G. M., Skoultchi, A. I., & Marzluff, W. F. (1997). The mouse histone H1 genes: gene organization and differential regulation. *J Mol Biol*, *271*(1), 124-138. https://doi.org/10.1006/jmbi.1997.1166

Waterborg, J. H. (2002). Acid-urea-triton polyacrylamide gel electrophoresis of histones. *The protein protocols handbook*, 113-123.

Weinberg, D. N., Papillon-Cavanagh, S., Chen, H., Yue, Y., Chen, X., Rajagopalan, K. N., Horth, C., McGuire, J. T., Xu, X., Nikbakht, H., Lemiesz, A. E., Marchione, D. M., Marunde, M. R., Meiners, M. J., Cheek, M. A., Keogh, M. C., Bareke, E., Djedid, A., Harutyunyan, A. S., . . . Lu, C. (2019). The histone mark H3K36me2 recruits DNMT3A and shapes the intergenic DNA methylation landscape. *Nature*, *573*(7773), 281-286. https://doi.org/10.1038/s41586-019-1534-3

Wille, C. K., & Sridharan, R. (2022a). Connecting the DOTs on Cell Identity. *Front Cell Dev Biol*, *10*, 906713. https://doi.org/10.3389/fcell.2022.906713

Wille, C. K., & Sridharan, R. (2022b). DOT1L inhibition enhances pluripotency beyond acquisition of epithelial identity and without immediate suppression of the somatic transcriptome. *Stem Cell Reports*, *17*(2), 384-396. https://doi.org/10.1016/j.stemcr.2021.12.004

Wong, L. H., Ren, H., Williams, E., McGhie, J., Ahn, S., Sim, M., Tam, A., Earle, E., Anderson, M. A., Mann, J., & Choo, K. H. (2009). Histone H3.3 incorporation provides a unique and functionally essential telomeric chromatin in embryonic stem cells. *Genome Res*, *19*(3), 404-414. https://doi.org/10.1101/gr.084947.108

Wood, A., Krogan, N. J., Dover, J., Schneider, J., Heidt, J., Boateng, M. A., Dean, K., Golshani, A., Zhang, Y., & Greenblatt, J. F. (2003). Bre1, an E3 ubiquitin ligase required for recruitment and substrate selection of Rad6 at a promoter. *Molecular cell*, *11*(1), 267-274.

Worden, E. J., Hoffmann, N. A., Hicks, C. W., & Wolberger, C. (2019). Mechanism of Cross-talk between H2B Ubiquitination and H3 Methylation by Dot1L. *Cell*, *176*(6), 1490-1501.e1412. https://doi.org/10.1016/j.cell.2019.02.002

Yang, D., He, Y., Li, R., Huang, Z., Zhou, Y., Shi, Y., Deng, Z., Wu, J., & Gao, Y. (2023). Histone H3K79 methylation by DOT1L promotes Aurora B localization at centromeres in mitosis. *Cell Rep*, *42*(8), 112885. https://doi.org/10.1016/j.celrep.2023.112885

Yoh, S. M., Lucas, J. S., & Jones, K. A. (2008). The Iws1:Spt6:CTD complex controls cotranscriptional mRNA biosynthesis and HYPB/Setd2-mediated histone H3K36 methylation. *Genes Dev*, *22*(24), 3422-3434. https://doi.org/10.1101/gad.1720008

Yokoyama, A. (2021). Leukemogenesis via aberrant self-renewal by the MLL/AEP-mediated transcriptional activation system. *Cancer Science*, *112*(10), 3935-3944.

Youdell, M. L., Kizer, K. O., Kisseleva-Romanova, E., Fuchs, S. M., Duro, E., Strahl, B. D., & Mellor, J. (2008). Roles for Ctk1 and Spt6 in regulating the different methylation states of histone H3 lysine 36. *Mol Cell Biol*, *28*(16), 4915-4926. https://doi.org/10.1128/mcb.00001-08

Yun, M., Wu, J., Workman, J. L., & Li, B. (2011). Readers of histone modifications. *Cell Res*, *21*(4), 564-578. https://doi.org/10.1038/cr.2011.42

Zhang, H., Zhou, B., Qin, S., Xu, J., Harding, R., Tempel, W., Nayak, V., Li, Y., Loppnau, P., Dou, Y., & Min, J. (2018). Structural and functional analysis of the DOT1L-AF10 complex reveals mechanistic insights into MLL-AF10-associated leukemogenesis. *Genes Dev*, *32*(5-6), 341-346. https://doi.org/10.1101/gad.311639.118

Zhang, X. Y., Varthi, M., Sykes, S. M., Phillips, C., Warzecha, C., Zhu, W., Wyce, A., Thorne, A. W., Berger, S. L., & McMahon, S. B. (2008). The putative cancer stem cell marker USP22 is a subunit of the human SAGA complex required for activated transcription and cell-cycle progression. *Mol Cell*, *29*(1), 102-111. https://doi.org/10.1016/j.molcel.2007.12.015

Adam, S., Dabin, J., Chevallier, O., Leroy, O., Baldeyron, C., Corpet, A., Lomonte, P., Renaud, O., Almouzni, G., & Polo, S. E. (2016). Real-Time Tracking of Parental Histones Reveals Their Contribution to Chromatin Integrity Following DNA Damage. *Mol Cell*, *64*(1), 65-78. https://doi.org/10.1016/j.molcel.2016.08.019

Adamaki, M., Lambrou, G. I., Athanasiadou, A., Vlahopoulos, S., Papavassiliou, A. G., & Moschovi, M. (2015). HOXA9 and MEIS1 gene overexpression in the diagnosis of childhood acute leukemias: Significant correlation with relapse and overall survival. *Leukemia research*, *39*(8), 874-882.

Adams, J. (2002). Preclinical and clinical evaluation of proteasome inhibitor PS-341 for the treatment of cancer. *Curr Opin Chem Biol*, *6*(4), 493-500. https://doi.org/10.1016/s1367-5931(02)00343-5

Ahmad, K., & Henikoff, S. (2002). The histone variant H3.3 marks active chromatin by replication-independent nucleosome assembly. *Mol Cell*, *9*(6), 1191-1200. https://doi.org/10.1016/s1097-2765(02)00542-7

Ai, H., Sun, M., Liu, A., Sun, Z., Liu, T., Cao, L., Liang, L., Qu, Q., Li, Z., Deng, Z., Tong, Z., Chu, G., Tian, X., Deng, H., Zhao, S., Li, J. B., Lou, Z., & Liu, L. (2022). H2B Lys34 Ubiquitination Induces Nucleosome Distortion to Stimulate Dot1L Activity. *Nat Chem Biol*, *18*(9), 972-980. https://doi.org/10.1038/s41589-022-01067-7

Amin, A. D., Vishnoi, N., & Prochasson, P. (2013). A global requirement for the HIR complex in the assembly of chromatin. *Biochim Biophys Acta*, *1819*(3-4), 264-276. https://doi.org/10.1016/j.bbagrm.2011.07.008

Arnold, O., Barbosa, K., Deshpande, A. J., & Zhu, N. (2022). The Role of DOT1L in Normal and Malignant Hematopoiesis. *Front Cell Dev Biol*, *10*, 917125. https://doi.org/10.3389/fcell.2022.917125

Batta, K., Zhang, Z., Yen, K., Goffman, D. B., & Pugh, B. F. (2011). Genome-wide function of H2B ubiquitylation in promoter and genic regions. *Genes Dev*, *25*(21), 2254-2265. https://doi.org/10.1101/gad.177238.111

Bedford, M. T., & Clarke, S. G. (2009). Protein arginine methylation in mammals: who, what, and why. *Mol Cell*, *33*(1), 1-13. https://doi.org/10.1016/j.molcel.2008.12.013

Belotserkovskaya, R., Oh, S., Bondarenko, V. A., Orphanides, G., Studitsky, V. M., & Reinberg, D. (2003). FACT facilitates transcription-dependent nucleosome alteration. *Science*, *301*(5636), 1090-1093. https://doi.org/10.1126/science.1085703

Bhattacharya, S., Levy, M. J., Zhang, N., Li, H., Florens, L., Washburn, M. P., & Workman, J. L. (2021). The methyltransferase SETD2 couples transcription and splicing by engaging mRNA processing factors through its SHI domain. *Nat Commun*, *12*(1), 1443. https://doi.org/10.1038/s41467-021-21663-w

Bilokapic, S., & Halic, M. (2019). Nucleosome and ubiquitin position Set2 to methylate H3K36. *Nature Communications*, *10*(1), 3795. https://doi.org/10.1038/s41467-019-11726-4

Bilokapic, S., & Halic, M. (2019). Nucleosome and ubiquitin position Set2 to methylate H3K36. *Nat Commun*, *10*(1), 3795. https://doi.org/10.1038/s41467-019-11726-4

Britten, O., Ragusa, D., Tosi, S., & Mostafa Kamel, Y. (2019). MLL-Rearranged Acute Leukemia with t (4; 11)(q21; q23)—Current Treatment Options. Is There a Role for CAR-T Cell Therapy? *Cells*, *8*(11), 1341.

Brown, M. A., Sims, R. J., 3rd, Gottlieb, P. D., & Tucker, P. W. (2006). Identification and characterization of Smyd2: a split SET/MYND domain-containing histone H3 lysine 36-specific methyltransferase that interacts with the Sin3 histone deacetylase complex. *Mol Cancer*, *5*, 26. https://doi.org/10.1186/1476-4598-5-26

Brzezinka, K., Nevedomskaya, E., Lesche, R., Haegebarth, A., Ter Laak, A., Fernández-Montalván, A. E., Eberspaecher, U., Werbeck, N. D., Moenning, U., Siegel, S., Haendler, B., Eheim, A. L., & Stresemann, C. (2020). Characterization of the Menin-MLL Interaction as Therapeutic Cancer Target. *Cancers (Basel)*, *12*(1). https://doi.org/10.3390/cancers12010201

Campos, E. I., & Reinberg, D. (2009). Histones: annotating chromatin. *Annu Rev Genet*, *43*, 559-599. https://doi.org/10.1146/annurev.genet.032608.103928

Cao, K., Ugarenko, M., Ozark, P. A., Wang, J., Marshall, S. A., Rendleman, E. J., Liang, K., Wang, L., Zou, L., Smith, E. R., Yue, F., & Shilatifard, A. (2020). DOT1L-controlled cell-fate determination and transcription elongation are independent of H3K79 methylation. *Proceedings of the National Academy of Sciences*, *117*(44), 27365-27373. https://doi.org/doi:10.1073/pnas.2001075117

Cao, R., Wang, L., Wang, H., Xia, L., Erdjument-Bromage, H., Tempst, P., Jones, R. S., & Zhang, Y. (2002). Role of histone H3 lysine 27 methylation in Polycomb-group silencing. *Science*, *298*(5595), 1039-1043. https://doi.org/10.1126/science.1076997

Castiglioni, S., Di Fede, E., Bernardelli, C., Lettieri, A., Parodi, C., Grazioli, P., Colombo, E. A., Ancona, S., Milani, D., & Ottaviano, E. (2022). KMT2A: Umbrella gene for multiple diseases. *Genes*, *13*(3), 514.

Cheon, Y., Kim, H., Park, K., Kim, M., & Lee, D. (2020). Dynamic modules of the coactivator SAGA in eukaryotic transcription. *Experimental & Molecular Medicine*, *52*(7), 991-1003. https://doi.org/10.1038/s12276-020-0463-4

Davie, J. R., & Murphy, L. C. (1990). Level of ubiquitinated histone H2B in chromatin is coupled to ongoing transcription. *Biochemistry*, *29*(20), 4752-4757. https://doi.org/10.1021/bi00472a002

Delcuve, G. P., & Davie, J. R. (1992). Western blotting and immunochemical detection of histones electrophoretically resolved on acid-urea-triton-and sodium dodecyl sulfate-polyacrylamide gels. *Analytical biochemistry*, *200*(2), 339-341.

Devoucoux, M., Roques, C., Lachance, C., Lashgari, A., Joly-Beauparlant, C., Jacquet, K., Alerasool, N., Prudente, A., Taipale, M., Droit, A., Lambert, J. P., Hussein, S. M. I., & Côté, J. (2022). MRG Proteins Are Shared by Multiple Protein Complexes With Distinct Functions. *Mol Cell Proteomics*, *21*(7), 100253. https://doi.org/10.1016/j.mcpro.2022.100253

Edmunds, J. W., Mahadevan, L. C., & Clayton, A. L. (2008). Dynamic histone H3 methylation during gene induction: HYPB/Setd2 mediates all H3K36 trimethylation. *Embo j*, *27*(2), 406-420. https://doi.org/10.1038/sj.emboj.7601967

Eom, G. H., Kim, K. B., Kim, J. H., Kim, J. Y., Kim, J. R., Kee, H. J., Kim, D. W., Choe, N., Park, H. J., Son, H. J., Choi, S. Y., Kook, H., & Seo, S. B. (2011). Histone methyltransferase SETD3 regulates muscle differentiation. *J Biol Chem*, *286*(40), 34733-34742. https://doi.org/10.1074/jbc.M110.203307

Feng, Q., Wang, H., Ng, H. H., Erdjument-Bromage, H., Tempst, P., Struhl, K., & Zhang, Y. (2002). Methylation of H3-lysine 79 is mediated by a new family of HMTases without a SET domain. *Curr Biol*, *12*(12), 1052-1058. https://doi.org/10.1016/s0960-9822(02)00901-6

Fierz, B., Chatterjee, C., McGinty, R. K., Bar-Dagan, M., Raleigh, D. P., & Muir, T. W. (2011). Histone H2B ubiquitylation disrupts local and higher-order chromatin compaction. *Nat Chem Biol*, *7*(2), 113-119. https://doi.org/10.1038/nchembio.501

Fischle, W., Tseng, B. S., Dormann, H. L., Ueberheide, B. M., Garcia, B. A., Shabanowitz, J., Hunt, D. F., Funabiki, H., & Allis, C. D. (2005). Regulation of HP1-chromatin binding by histone H3 methylation and phosphorylation. *Nature*, *438*(7071), 1116-1122. https://doi.org/10.1038/nature04219

Fodor, B. D., Kubicek, S., Yonezawa, M., O'Sullivan, R. J., Sengupta, R., Perez-Burgos, L., Opravil, S., Mechtler, K., Schotta, G., & Jenuwein, T. (2006). Jmjd2b antagonizes H3K9 trimethylation at pericentric heterochromatin in mammalian cells. *Genes Dev*, *20*(12), 1557-1562. https://doi.org/10.1101/gad.388206

Früh, K., Gossen, M., Wang, K., Bujard, H., Peterson, P. A., & Yang, Y. (1994). Displacement of housekeeping proteasome subunits by MHC-encoded LMPs: a newly discovered mechanism for modulating the multicatalytic proteinase complex. *Embo j*, *13*(14), 3236-3244. https://doi.org/10.1002/j.1460-2075.1994.tb06625.x

Fu, J., Liao, L., Balaji, K. S., Wei, C., Kim, J., & Peng, J. (2021). Epigenetic modification and a role for the E3 ligase RNF40 in cancer development and metastasis. *Oncogene*, *40*(3), 465-474. https://doi.org/10.1038/s41388-020-01556-w

Fuchs, G., & Oren, M. (2014). Writing and reading H2B monoubiquitylation. *Biochim Biophys Acta*, *1839*(8), 694-701. https://doi.org/10.1016/j.bbagrm.2014.01.002

Gal, C., Moore, K. M., Paszkiewicz, K., Kent, N. A., & Whitehall, S. K. (2015). The impact of the HIRA histone chaperone upon global nucleosome architecture. *Cell Cycle*, *14*(1), 123-134. https://doi.org/10.4161/15384101.2014.967123

Gillette, T. G., & Hill, J. A. (2015). Readers, writers, and erasers: chromatin as the whiteboard of heart disease. *Circ Res*, *116*(7), 1245-1253. https://doi.org/10.1161/circresaha.116.303630

Goldberg, A. D., Banaszynski, L. A., Noh, K. M., Lewis, P. W., Elsaesser, S. J., Stadler, S., Dewell, S., Law, M., Guo, X., Li, X., Wen, D., Chapgier, A., DeKelver, R. C., Miller, J. C., Lee, Y. L., Boydston, E. A., Holmes, M. C., Gregory, P. D., Greally, J. M., . . . Allis, C. D. (2010). Distinct factors control histone variant H3.3 localization at specific genomic regions. *Cell*, *140*(5), 678-691. https://doi.org/10.1016/j.cell.2010.01.003

Heard, E., Rougeulle, C., Arnaud, D., Avner, P., Allis, C. D., & Spector, D. L. (2001). Methylation of histone H3 at Lys-9 is an early mark on the X chromosome during X inactivation. *Cell*, *107*(6), 727-738. https://doi.org/10.1016/s0092-8674(01)00598-0

Henikoff, S., & Smith, M. M. (2015). Histone variants and epigenetics. *Cold Spring Harb Perspect Biol*, *7*(1), a019364. https://doi.org/10.1101/cshperspect.a019364

Hershko, A., & Ciechanover, A. (1998). The ubiquitin system. *Annual review of biochemistry*, *67*(1), 425-479.

Hideshima, T., Richardson, P., Chauhan, D., Palombella, V. J., Elliott, P. J., Adams, J., & Anderson, K. C. (2001). The proteasome inhibitor PS-341 inhibits growth, induces apoptosis, and overcomes drug resistance in human multiple myeloma cells. *Cancer Res*, *61*(7), 3071-3076.

Huisinga, K. L., Brower-Toland, B., & Elgin, S. C. (2006). The contradictory definitions of heterochromatin: transcription and silencing. *Chromosoma*, *115*, 110-122.

Jagannath, S., Durie, B. G., Wolf, J., Camacho, E., Irwin, D., Lutzky, J., McKinley, M., Gabayan, E., Mazumder, A., Schenkein, D., & Crowley, J. (2005). Bortezomib therapy alone and in combination with dexamethasone for previously untreated symptomatic multiple myeloma. *Br J Haematol*, *129*(6), 776-783. https://doi.org/10.1111/j.1365-2141.2005.05540.x

Jang, S., Kang, C., Yang, H. S., Jung, T., Hebert, H., Chung, K. Y., Kim, S. J., Hohng, S., & Song, J. J. (2019). Structural basis of recognition and destabilization of the histone H2B ubiquitinated nucleosome by the DOT1L histone H3 Lys79 methyltransferase. *Genes Dev*, *33*(11-12), 620-625. https://doi.org/10.1101/gad.323790.118

Jeusset, L. M., & McManus, K. J. (2017). Ubiquitin Specific Peptidase 22 Regulates Histone H2B Mono-Ubiquitination and Exhibits Both Oncogenic and Tumor Suppressor Roles in Cancer. *Cancers (Basel)*, *9*(12). https://doi.org/10.3390/cancers9120167

Jones, B., Su, H., Bhat, A., Lei, H., Bajko, J., Hevi, S., Baltus, G. A., Kadam, S., Zhai, H., Valdez, R., Gonzalo, S., Zhang, Y., Li, E., & Chen, T. (2008). The histone H3K79 methyltransferase Dot1L is essential for mammalian development and heterochromatin structure. *PLoS Genet*, *4*(9), e1000190. https://doi.org/10.1371/journal.pgen.1000190

Joo, H. Y., Jones, A., Yang, C., Zhai, L., Smith, A. D. t., Zhang, Z., Chandrasekharan, M. B., Sun, Z. W., Renfrow, M. B., Wang, Y., Chang, C., & Wang, H. (2011). Regulation of histone H2A and H2B deubiquitination and Xenopus development by USP12 and USP46. *J Biol Chem*, *286*(9), 7190-7201. https://doi.org/10.1074/jbc.M110.158311

Kamens, J. L., Nance, S., Koss, C., Xu, B., Cotton, A., Lam, J. W., Garfinkle, E. A., Nallagatla, P., Smith, A. M., & Mitchell, S. (2023). Proteasome inhibition targets the KMT2A transcriptional complex in acute lymphoblastic leukemia. *Nature Communications*, *14*(1), 809.

Kamens, J. L., Nance, S., Koss, C., Xu, B., Cotton, A., Lam, J. W., Garfinkle, E. A. R., Nallagatla, P., Smith, A. M. R., Mitchell, S., Ma, J., Currier, D., Wright, W. C., Kavdia, K., Pagala, V. R., Kim, W., Wallace, L. M., Cho, J. H., Fan, Y., . . . Gruber, T. A. (2023). Proteasome inhibition targets the KMT2A transcriptional complex in acute lymphoblastic leukemia. *Nat Commun*, *14*(1), 809. https://doi.org/10.1038/s41467-023-36370-x

Kang, J. Y., Kim, J. Y., Kim, K. B., Park, J. W., Cho, H., Hahm, J. Y., Chae, Y. C., Kim, D., Kook, H., Rhee, S., Ha, N. C., & Seo, S. B. (2018). KDM2B is a histone H3K79 demethylase and

induces transcriptional repression via sirtuin-1-mediated chromatin silencing. *Faseb j*, *32*(10), 5737-5750. https://doi.org/10.1096/fj.201800242R

Kari, V., Shchebet, A., Neumann, H., & Johnsen, S. A. (2011). The H2B ubiquitin ligase RNF40 cooperates with SUPT16H to induce dynamic changes in chromatin structure during DNA double-strand break repair. *Cell Cycle*, *10*(20), 3495-3504. https://doi.org/10.4161/cc.10.20.17769

Kemble, D. J., McCullough, L. L., Whitby, F. G., Formosa, T., & Hill, C. P. (2015). FACT Disrupts Nucleosome Structure by Binding H2A-H2B with Conserved Peptide Motifs. *Mol Cell*, *60*(2), 294-306. https://doi.org/10.1016/j.molcel.2015.09.008

Khan, D. H., Healy, S., He, S., Lichtensztejn, D., Klewes, L., Sharma, K. L., Lau, V., Mai, S., Delcuve, G. P., & Davie, J. R. (2017). Mitogen-induced distinct epialleles are phosphorylated at either H3S10 or H3S28, depending on H3K27 acetylation. *Mol Biol Cell*, *28*(6), 817-824. https://doi.org/10.1091/mbc.E16-08-0618

Kim, S. K., Jung, I., Lee, H., Kang, K., Kim, M., Jeong, K., Kwon, C. S., Han, Y. M., Kim, Y. S., Kim, D., & Lee, D. (2012). Human histone H3K79 methyltransferase DOT1L protein [corrected] binds actively transcribing RNA polymerase II to regulate gene expression. *J Biol Chem*, *287*(47), 39698-39709. https://doi.org/10.1074/jbc.M112.384057

Kizer, K. O., Phatnani, H. P., Shibata, Y., Hall, H., Greenleaf, A. L., & Strahl, B. D. (2005). A novel domain in Set2 mediates RNA polymerase II interaction and couples histone H3 K36 methylation with transcript elongation. *Molecular and cellular biology*, *25*(8), 3305-3316.

Klein, R. H., & Knoepfler, P. S. (2023). Knockout tales: the versatile roles of histone H3.3 in development and disease. *Epigenetics Chromatin*, *16*(1), 38. https://doi.org/10.1186/s13072-023-00512-8

Kondagunta, G. V., Drucker, B., Schwartz, L., Bacik, J., Marion, S., Russo, P., Mazumdar, M., & Motzer, R. J. (2004). Phase II trial of bortezomib for patients with advanced renal cell carcinoma. *J Clin Oncol*, *22*(18), 3720-3725. https://doi.org/10.1200/jco.2004.10.155

Laemmli, U. K. (1970). Cleavage of Structural Proteins during the Assembly of the Head of Bacteriophage T4. *Nature*, *227*(5259), 680-685. https://doi.org/10.1038/227680a0

Latham, J. A., Chosed, R. J., Wang, S., & Dent, S. Y. (2011). Chromatin signaling to kinetochores: transregulation of Dam1 methylation by histone H2B ubiquitination. *Cell*, *146*(5), 709-719. https://doi.org/10.1016/j.cell.2011.07.025

Lee, K. K., & Workman, J. L. (2007). Histone acetyltransferase complexes: one size doesn't fit all. *Nature reviews Molecular cell biology*, *8*(4), 284-295.

Lee, S., Oh, S., Jeong, K., Jo, H., Choi, Y., Seo, H. D., Kim, M., Choe, J., Kwon, C. S., & Lee, D. (2018). Dot1 regulates nucleosome dynamics by its inherent histone chaperone activity in yeast. *Nature Communications*, *9*(1), 240. https://doi.org/10.1038/s41467-017-02759-8

Lee, S. H., Oshige, M., Durant, S. T., Rasila, K. K., Williamson, E. A., Ramsey, H., Kwan, L., Nickoloff, J. A., & Hromas, R. (2005). The SET domain protein Metnase mediates foreign DNA integration and links integration to nonhomologous end-joining repair. *Proc Natl Acad Sci U S A*, *102*(50), 18075-18080. https://doi.org/10.1073/pnas.0503676102

Lempiäinen, J. K., & Garcia, B. A. (2023). Characterizing crosstalk in epigenetic signaling to understand disease physiology. *Biochem J*, *480*(1), 57-85. https://doi.org/10.1042/bcj20220550

Li, B., Carey, M., & Workman, J. L. (2007). The role of chromatin during transcription. *Cell*, *128*(4), 707-719. https://doi.org/10.1016/j.cell.2007.01.015

Li, F., Mao, G., Tong, D., Huang, J., Gu, L., Yang, W., & Li, G. M. (2013). The histone mark H3K36me3 regulates human DNA mismatch repair through its interaction with MutSα. *Cell*, *153*(3), 590-600. https://doi.org/10.1016/j.cell.2013.03.025

Li, Y., Trojer, P., Xu, C. F., Cheung, P., Kuo, A., Drury, W. J., 3rd, Qiao, Q., Neubert, T. A., Xu, R. M., Gozani, O., & Reinberg, D. (2009). The target of the NSD family of histone lysine methyltransferases depends on the nature of the substrate. *J Biol Chem*, *284*(49), 34283-34295. https://doi.org/10.1074/jbc.M109.034462

Li, Y., Wen, H., Xi, Y., Tanaka, K., Wang, H., Peng, D., Ren, Y., Jin, Q., Dent, S. Y., Li, W., Li, H., & Shi, X. (2014). AF9 YEATS domain links histone acetylation to DOT1L-mediated H3K79 methylation. *Cell*, *159*(3), 558-571. https://doi.org/10.1016/j.cell.2014.09.049

Lim, P. S., Shannon, M. F., & Hardy, K. (2010). Epigenetic control of inducible gene expression in the immune system. *Epigenomics*, *2*(6), 775-795. https://doi.org/10.2217/epi.10.55

Lin, J., Wu, Y., Tian, G., Yu, D., Yang, E., Lam, W. H., Liu, Z., Jing, Y., Dang, S., Bao, X., Wong, J. W. H., Zhai, Y., & Li, X. D. (2023). Menin "reads" H3K79me2 mark in a nucleosomal context. *Science*, *379*(6633), 717-723. https://doi.org/10.1126/science.adc9318

Luger, K., Mäder, A. W., Richmond, R. K., Sargent, D. F., & Richmond, T. J. (1997). Crystal structure of the nucleosome core particle at 2.8 A resolution. *Nature*, *389*(6648), 251-260. https://doi.org/10.1038/38444

Malik, H. S., & Henikoff, S. (2003). Phylogenomics of the nucleosome. *Nat Struct Biol*, *10*(11), 882-891. https://doi.org/10.1038/nsb996

Malinczak, C. A., Rasky, A. J., Fonseca, W., Schaller, M. A., Allen, R. M., Ptaschinski, C., Morris, S., & Lukacs, N. W. (2020). Upregulation of H3K27 Demethylase KDM6 During Respiratory Syncytial Virus Infection Enhances Proinflammatory Responses and

Immunopathology. *J Immunol*, *204*(1), 159-168. https://doi.org/10.4049/jimmunol.1900741

Marschalek, R. (2016). Systematic classification of mixed-lineage leukemia fusion partners predicts additional cancer pathways. *Annals of laboratory medicine*, *36*(2), 85.

Martire, S., & Banaszynski, L. A. (2020). The roles of histone variants in fine-tuning chromatin organization and function. *Nat Rev Mol Cell Biol*, *21*(9), 522-541. https://doi.org/10.1038/s41580-020-0262-8

Martire, S., Gogate, A. A., Whitmill, A., Tafessu, A., Nguyen, J., Teng, Y. C., Tastemel, M., & Banaszynski, L. A. (2019). Phosphorylation of histone H3.3 at serine 31 promotes p300 activity and enhancer acetylation. *Nat Genet*, *51*(6), 941-946. https://doi.org/10.1038/s41588-019-0428-5

Marzluff, W. F., Gongidi, P., Woods, K. R., Jin, J., & Maltais, L. J. (2002). The human and mouse replication-dependent histone genes. *Genomics*, *80*(5), 487-498.

McGrath, J., & Solter, D. (1984). Completion of mouse embryogenesis requires both the maternal and paternal genomes. *Cell*, *37*(1), 179-183.

McKittrick, E., Gafken, P. R., Ahmad, K., & Henikoff, S. (2004). Histone H3.3 is enriched in covalent modifications associated with active chromatin. *Proc Natl Acad Sci U S A*, *101*(6), 1525-1530. https://doi.org/10.1073/pnas.0308092100

Milne, T. A. (2017). Mouse models of MLL leukemia: recapitulating the human disease. *Blood*, *129*(16), 2217-2223. https://doi.org/10.1182/blood-2016-10-691428

Minard, M. E., Jain, A. K., & Barton, M. C. (2009). Analysis of epigenetic alterations to chromatin during development. *Genesis*, *47*(8), 559-572. https://doi.org/10.1002/dvg.20534

Mohan, M., Herz, H. M., Takahashi, Y. H., Lin, C., Lai, K. C., Zhang, Y., Washburn, M. P., Florens, L., & Shilatifard, A. (2010). Linking H3K79 trimethylation to Wnt signaling through a novel Dot1-containing complex (DotCom). *Genes Dev*, *24*(6), 574-589. https://doi.org/10.1101/gad.1898410

Morris, S. A., Shibata, Y., Noma, K.-i., Tsukamoto, Y., Warren, E., Temple, B., Grewal, S. I., & Strahl, B. D. (2005). Histone H3 K36 methylation is associated with transcription elongation in Schizosaccharomyces pombe. *Eukaryotic cell*, *4*(8), 1446-1454.

Muhire, B. M., Booker, M. A., & Tolstorukov, M. Y. (2019). Non-neutral evolution of H3.3-encoding genes occurs without alterations in protein sequence. *Sci Rep*, *9*(1), 8472. https://doi.org/10.1038/s41598-019-44800-4

Newell-Price, J., Clark, A. J., & King, P. (2000). DNA methylation and silencing of gene expression. *Trends in Endocrinology & Metabolism*, *11*(4), 142-148.

Nicassio, F., Corrado, N., Vissers, J. H., Areces, L. B., Bergink, S., Marteijn, J. A., Geverts, B., Houtsmuller, A. B., Vermeulen, W., Di Fiore, P. P., & Citterio, E. (2007). Human USP3 is a chromatin modifier required for S phase progression and genome stability. *Curr Biol*, *17*(22), 1972-1977. https://doi.org/10.1016/j.cub.2007.10.034

Nilsen, T. W., & Graveley, B. R. (2010). Expansion of the eukaryotic proteome by alternative splicing. *Nature*, *463*(7280), 457-463. https://doi.org/10.1038/nature08909

Orphanides, G., LeRoy, G., Chang, C.-H., Luse, D. S., & Reinberg, D. (1998). FACT, a factor that facilitates transcript elongation through nucleosomes. *Cell*, *92*(1), 105-116.

Outchkourov, N. S., Muiño, J. M., Kaufmann, K., van Ijcken, W. F., Groot Koerkamp, M. J., van Leenen, D., de Graaf, P., Holstege, F. C., Grosveld, F. G., & Timmers, H. T. (2013). Balancing of histone H3K4 methylation states by the Kdm5c/SMCX histone demethylase

modulates promoter and enhancer function. *Cell Rep*, *3*(4), 1071-1079. https://doi.org/10.1016/j.celrep.2013.02.030

Papandreou, C. N., Daliani, D. D., Nix, D., Yang, H., Madden, T., Wang, X., Pien, C. S., Millikan, R. E., Tu, S. M., Pagliaro, L., Kim, J., Adams, J., Elliott, P., Esseltine, D., Petrusich, A., Dieringer, P., Perez, C., & Logothetis, C. J. (2004). Phase I trial of the proteasome inhibitor bortezomib in patients with advanced solid tumors with observations in androgen-independent prostate cancer. *J Clin Oncol*, *22*(11), 2108-2121. https://doi.org/10.1200/jco.2004.02.106

Rahman, S., Sowa, M. E., Ottinger, M., Smith, J. A., Shi, Y., Harper, J. W., & Howley, P. M. (2011). The Brd4 extraterminal domain confers transcription activation independent of pTEFb by recruiting multiple proteins, including NSD3. *Mol Cell Biol*, *31*(13), 2641-2652. https://doi.org/10.1128/mcb.01341-10

Rayasam, G. V., Wendling, O., Angrand, P. O., Mark, M., Niederreither, K., Song, L., Lerouge, T., Hager, G. L., Chambon, P., & Losson, R. (2003). NSD1 is essential for early post-implantation development and has a catalytically active SET domain. *Embo j*, *22*(12), 3153-3163. https://doi.org/10.1093/emboj/cdg288

Richardson, P. G., Sonneveld, P., Schuster, M. W., Irwin, D., Stadtmauer, E. A., Facon, T., Harousseau, J. L., Ben-Yehuda, D., Lonial, S., Goldschmidt, H., Reece, D., San-Miguel, J. F., Bladé, J., Boccadoro, M., Cavenagh, J., Dalton, W. S., Boral, A. L., Esseltine, D. L., Porter, J. B., . . . Anderson, K. C. (2005). Bortezomib or high-dose dexamethasone for relapsed multiple myeloma. *N Engl J Med*, *352*(24), 2487-2498. https://doi.org/10.1056/NEJMoa043445

Riggs, A. D. (1975). X inactivation, differentiation, and DNA methylation. *Cytogenetic and Genome Research*, *14*(1), 9-25.

Santos-Rosa, H., Schneider, R., Bannister, A. J., Sherriff, J., Bernstein, B. E., Emre, N. C., Schreiber, S. L., Mellor, J., & Kouzarides, T. (2002). Active genes are tri-methylated at K4 of histone H3. *Nature*, *419*(6905), 407-411. https://doi.org/10.1038/nature01080

Schübeler, D., MacAlpine, D. M., Scalzo, D., Wirbelauer, C., Kooperberg, C., van Leeuwen, F., Gottschling, D. E., O'Neill, L. P., Turner, B. M., Delrow, J., Bell, S. P., & Groudine, M. (2004). The histone modification pattern of active genes revealed through genome-wide chromatin analysis of a higher eukaryote. *Genes Dev*, *18*(11), 1263-1271. https://doi.org/10.1101/gad.1198204

Schwartz, R., & Davidson, T. (2004). Pharmacology, pharmacokinetics, and practical applications of bortezomib. *Oncology (Williston Park)*, *18*(14 Suppl 11), 14-21.

Shah, S. A., Potter, M. W., McDade, T. P., Ricciardi, R., Perugini, R. A., Elliott, P. J., Adams, J., & Callery, M. P. (2001). 26S proteasome inhibition induces apoptosis and limits growth of human pancreatic cancer. *J Cell Biochem*, *82*(1), 110-122. https://doi.org/10.1002/jcb.1150

Sharda, A., & Humphrey, T. C. (2022). The role of histone H3K36me3 writers, readers and erasers in maintaining genome stability. *DNA Repair (Amst)*, *119*, 103407. https://doi.org/10.1016/j.dnarep.2022.103407

Sharma, P., Sattarifard, H., Fatemiyan, N., Lakowski, T. M., & Davie, J. R. (2022). Bioinformatic Analyses of Broad H3K79me2 Domains in Different Leukemia Cell Line Data Sets. *Cells*, *11*(18), 2830. https://www.mdpi.com/2073-4409/11/18/2830

Shilatifard, A. (2008). Molecular implementation and physiological roles for histone H3 lysine 4 (H3K4) methylation. *Curr Opin Cell Biol*, *20*(3), 341-348. https://doi.org/10.1016/j.ceb.2008.03.019

Skucha, A., Ebner, J., Schmöllerl, J., Roth, M., Eder, T., César-Razquin, A., Stukalov, A., Vittori, S., Muhar, M., & Lu, B. (2018). MLL-fusion-driven leukemia requires SETD2 to safeguard genomic integrity. *Nature Communications*, *9*(1), 1983.

Skucha, A., Ebner, J., Schmöllerl, J., Roth, M., Eder, T., César-Razquin, A., Stukalov, A., Vittori, S., Muhar, M., Lu, B., Aichinger, M., Jude, J., Müller, A. C., Győrffy, B., Vakoc, C. R., Valent, P., Bennett, K. L., Zuber, J., Superti-Furga, G., & Grebien, F. (2018). MLL-fusion-driven leukemia requires SETD2 to safeguard genomic integrity. *Nat Commun*, *9*(1), 1983. https://doi.org/10.1038/s41467-018-04329-y

Song, Y. H., & Ahn, S. H. (2010). A Bre1-associated protein, large 1 (Lge1), promotes H2B ubiquitylation during the early stages of transcription elongation. *J Biol Chem*, *285*(4), 2361-2367. https://doi.org/10.1074/jbc.M109.039255

Strahl, B. D., & Allis, C. D. (2000). The language of covalent histone modifications. *Nature*, *403*(6765), 41-45. https://doi.org/10.1038/47412

Sun, Z., Zhang, Y., Jia, J., Fang, Y., Tang, Y., Wu, H., & Fang, D. (2020). H3K36me3, message from chromatin to DNA damage repair. *Cell & Bioscience*, *10*(1), 9. https://doi.org/10.1186/s13578-020-0374-z

Swigut, T., & Wysocka, J. (2007). H3K27 demethylases, at long last. *Cell*, *131*(1), 29-32. https://doi.org/10.1016/j.cell.2007.09.026

Tafessu, A., O'Hara, R., Martire, S., Dube, A. L., Saha, P., Gant, V. U., & Banaszynski, L. A. (2023). H3.3 contributes to chromatin accessibility and transcription factor binding at

promoter-proximal regulatory elements in embryonic stem cells. *Genome Biology*, *24*(1), 25. https://doi.org/10.1186/s13059-023-02867-3

Tagami, H., Ray-Gallet, D., Almouzni, G., & Nakatani, Y. (2004). Histone H3.1 and H3.3 complexes mediate nucleosome assembly pathways dependent or independent of DNA synthesis. *Cell*, *116*(1), 51-61. https://doi.org/10.1016/s0092-8674(03)01064-x

Tamaru, H. (2010). Confining euchromatin/heterochromatin territory: jumonji crosses the line. *Genes Dev*, *24*(14), 1465-1478. https://doi.org/10.1101/gad.1941010

Tamburri, S., Lavarone, E., Fernández-Pérez, D., Conway, E., Zanotti, M., Manganaro, D., & Pasini, D. (2020). Histone H2AK119 Mono-Ubiquitination Is Essential for Polycomb-Mediated Transcriptional Repression. *Mol Cell*, *77*(4), 840-856.e845. https://doi.org/10.1016/j.molcel.2019.11.021

Tanaka, K. (1998). Molecular biology of the proteasome. *Biochem Biophys Res Commun*, *247*(3), 537-541. https://doi.org/10.1006/bbrc.1998.8617

Tanaka, Y., Katagiri, Z., Kawahashi, K., Kioussis, D., & Kitajima, S. (2007). Trithorax-group protein ASH1 methylates histone H3 lysine 36. *Gene*, *397*(1-2), 161-168. https://doi.org/10.1016/j.gene.2007.04.027

Torné, J., Ray-Gallet, D., Boyarchuk, E., Garnier, M., Le Baccon, P., Coulon, A., Orsi, G. A., & Almouzni, G. (2020). Two HIRA-dependent pathways mediate H3.3 de novo deposition and recycling during transcription. *Nat Struct Mol Biol*, *27*(11), 1057-1068. https://doi.org/10.1038/s41594-020-0492-7

Trujillo, K. M., & Osley, M. A. (2012). A role for H2B ubiquitylation in DNA replication. *Mol Cell*, *48*(5), 734-746. https://doi.org/10.1016/j.molcel.2012.09.019

Udugama, M., Vinod, B., Chan, F. L., Hii, L., Garvie, A., Collas, P., Kalitsis, P., Steer, D., Das, P. P., Tripathi, P., Mann, J. R., Voon, H. P. J., & Wong, L. H. (2022). Histone H3.3 phosphorylation promotes heterochromatin formation by inhibiting H3K9/K36 histone demethylase. *Nucleic Acids Res*, *50*(8), 4500-4514. https://doi.org/10.1093/nar/gkac259

van der Knaap, J. A., Kumar, B. R., Moshkin, Y. M., Langenberg, K., Krijgsveld, J., Heck, A. J., Karch, F., & Verrijzer, C. P. (2005). GMP synthetase stimulates histone H2B deubiquitylation by the epigenetic silencer USP7. *Mol Cell*, *17*(5), 695-707. https://doi.org/10.1016/j.molcel.2005.02.013

van Leeuwen, F., Gafken, P. R., & Gottschling, D. E. (2002). Dot1p modulates silencing in yeast by methylation of the nucleosome core. *Cell*, *109*(6), 745-756. https://doi.org/10.1016/s0092-8674(02)00759-6

Venkatesh, S., & Workman, J. L. (2013). Set2 mediated H3 lysine 36 methylation: regulation of transcription elongation and implications in organismal development. *Wiley Interdiscip Rev Dev Biol*, *2*(5), 685-700. https://doi.org/10.1002/wdev.109

Verbrugge, S. E., Scheper, R. J., Lems, W. F., de Gruijl, T. D., & Jansen, G. (2015). Proteasome inhibitors as experimental therapeutics of autoimmune diseases. *Arthritis Res Ther*, *17*(1), 17. https://doi.org/10.1186/s13075-015-0529-1

Verrier, L., Vandromme, M., & Trouche, D. (2011). Histone demethylases in chromatin cross-talks. *Biol Cell*, *103*(8), 381-401. https://doi.org/10.1042/bc20110028

Vlaming, H., van Welsem, T., de Graaf, E. L., Ontoso, D., Altelaar, A. F., San-Segundo, P. A., Heck, A. J., & van Leeuwen, F. (2014). Flexibility in crosstalk between H2B ubiquitination and H3 methylation in vivo. *EMBO Rep*, *15*(10), 1077-1084. https://doi.org/10.15252/embr.201438793

Waddington, C. H. (1942). The epigenotype. *Endeavour*, *1*, 18-20.

Wagner, E. J., & Carpenter, P. B. (2012). Understanding the language of Lys36 methylation at histone H3. *Nat Rev Mol Cell Biol*, *13*(2), 115-126. https://doi.org/10.1038/nrm3274

Wang, E., Kawaoka, S., Yu, M., Shi, J., Ni, T., Yang, W., Zhu, J., Roeder, R. G., & Vakoc, C. R. (2013). Histone H2B ubiquitin ligase RNF20 is required for MLL-rearranged leukemia. *Proceedings of the National Academy of Sciences*, *110*(10), 3901-3906. https://doi.org/doi:10.1073/pnas.1301045110

Wang, E., Kawaoka, S., Yu, M., Shi, J., Ni, T., Yang, W., Zhu, J., Roeder, R. G., & Vakoc, C. R. (2013). Histone H2B ubiquitin ligase RNF20 is required for MLL-rearranged leukemia. *Proc Natl Acad Sci U S A*, *110*(10), 3901-3906. https://doi.org/10.1073/pnas.1301045110

Wang, Z. F., Sirotkin, A. M., Buchold, G. M., Skoultchi, A. I., & Marzluff, W. F. (1997). The mouse histone H1 genes: gene organization and differential regulation. *J Mol Biol*, *271*(1), 124-138. https://doi.org/10.1006/jmbi.1997.1166

Waterborg, J. H. (2002). Acid-urea-triton polyacrylamide gel electrophoresis of histones. *The protein protocols handbook*, 113-123.

Weinberg, D. N., Papillon-Cavanagh, S., Chen, H., Yue, Y., Chen, X., Rajagopalan, K. N., Horth, C., McGuire, J. T., Xu, X., Nikbakht, H., Lemiesz, A. E., Marchione, D. M., Marunde, M. R., Meiners, M. J., Cheek, M. A., Keogh, M. C., Bareke, E., Djedid, A., Harutyunyan, A. S., . . . Lu, C. (2019). The histone mark H3K36me2 recruits DNMT3A and shapes the intergenic DNA methylation landscape. *Nature*, *573*(7773), 281-286. https://doi.org/10.1038/s41586-019-1534-3

Wille, C. K., & Sridharan, R. (2022a). Connecting the DOTs on Cell Identity. *Front Cell Dev Biol*, *10*, 906713. https://doi.org/10.3389/fcell.2022.906713

Wille, C. K., & Sridharan, R. (2022b). DOT1L inhibition enhances pluripotency beyond acquisition of epithelial identity and without immediate suppression of the somatic transcriptome. *Stem Cell Reports*, *17*(2), 384-396. https://doi.org/10.1016/j.stemcr.2021.12.004

Wong, L. H., Ren, H., Williams, E., McGhie, J., Ahn, S., Sim, M., Tam, A., Earle, E., Anderson, M. A., Mann, J., & Choo, K. H. (2009). Histone H3.3 incorporation provides a unique and functionally essential telomeric chromatin in embryonic stem cells. *Genome Res*, *19*(3), 404-414. https://doi.org/10.1101/gr.084947.108

Wood, A., Krogan, N. J., Dover, J., Schneider, J., Heidt, J., Boateng, M. A., Dean, K., Golshani, A., Zhang, Y., & Greenblatt, J. F. (2003). Bre1, an E3 ubiquitin ligase required for recruitment and substrate selection of Rad6 at a promoter. *Molecular cell*, *11*(1), 267-274.

Worden, E. J., Hoffmann, N. A., Hicks, C. W., & Wolberger, C. (2019). Mechanism of Cross-talk between H2B Ubiquitination and H3 Methylation by Dot1L. *Cell*, *176*(6), 1490-1501.e1412. https://doi.org/10.1016/j.cell.2019.02.002

Yang, D., He, Y., Li, R., Huang, Z., Zhou, Y., Shi, Y., Deng, Z., Wu, J., & Gao, Y. (2023). Histone H3K79 methylation by DOT1L promotes Aurora B localization at centromeres in mitosis. *Cell Rep*, *42*(8), 112885. https://doi.org/10.1016/j.celrep.2023.112885

Yoh, S. M., Lucas, J. S., & Jones, K. A. (2008). The Iws1:Spt6:CTD complex controls cotranscriptional mRNA biosynthesis and HYPB/Setd2-mediated histone H3K36 methylation. *Genes Dev*, *22*(24), 3422-3434. https://doi.org/10.1101/gad.1720008

Yokoyama, A. (2021). Leukemogenesis via aberrant self-renewal by the MLL/AEP-mediated transcriptional activation system. *Cancer Science*, *112*(10), 3935-3944.

Yokoyama, A., Somervaille, T. C., Smith, K. S., Rozenblatt-Rosen, O., Meyerson, M., & Cleary, M. L. (2005). The menin tumor suppressor protein is an essential oncogenic cofactor for MLL-associated leukemogenesis. *Cell*, *123*(2), 207-218. https://doi.org/10.1016/j.cell.2005.09.025

Youdell, M. L., Kizer, K. O., Kisseleva-Romanova, E., Fuchs, S. M., Duro, E., Strahl, B. D., & Mellor, J. (2008). Roles for Ctk1 and Spt6 in regulating the different methylation states of histone H3 lysine 36. *Mol Cell Biol*, *28*(16), 4915-4926. https://doi.org/10.1128/mcb.00001-08

Yun, M., Wu, J., Workman, J. L., & Li, B. (2011). Readers of histone modifications. *Cell Res*, *21*(4), 564-578. https://doi.org/10.1038/cr.2011.42

Zhang, H., Zhou, B., Qin, S., Xu, J., Harding, R., Tempel, W., Nayak, V., Li, Y., Loppnau, P., Dou, Y., & Min, J. (2018). Structural and functional analysis of the DOT1L-AF10 complex reveals mechanistic insights into MLL-AF10-associated leukemogenesis. *Genes Dev*, *32*(5-6), 341-346. https://doi.org/10.1101/gad.311639.118

Zhang, X. Y., Varthi, M., Sykes, S. M., Phillips, C., Warzecha, C., Zhu, W., Wyce, A., Thorne, A. W., Berger, S. L., & McMahon, S. B. (2008). The putative cancer stem cell marker USP22 is a subunit of the human SAGA complex required for activated transcription and cell-cycle progression. *Mol Cell*, *29*(1), 102-111. https://doi.org/10.1016/j.molcel.2007.12.015